

UNIVERSITÉ DE SHERBROOKE

Faculté de génie

Département de génie civil

Performance du béton intégrant les résidus de silice
amorphe et les cendres des boues de désencrage

Performance of Concrete Incorporating Amorphous Silica
Residue and Biomass Fly Ash

Mémoire de maîtrise

Spécialité : génie civil

Majid JERBAN

Jury: Arezki TAGNIT-HAMOU (Directeur)
Ammar YAHIA (Rapporteur)
Radhouane MASMOUDI (Examineur)

Abstract

Cement manufacturing industry is one of the carbon dioxide emitting sources. The global cement industry contributes about 7% of greenhouse gas emission to the earth's atmosphere. In order to address environmental effects associated with cement manufacturing and constantly depleting natural resources, there is necessity to develop alternative binders to make sustainable concrete. Thus, many industrial by-products have been used to partially substitute cement in order to generate more economic and durable concrete. The performance of a cement additive depends on kinetics hydration and synergy between additions and Portland cement. In this project, two industrial by-products are investigated as alternative supplementary cementitious materials (ASCMs), non-toxic amorphous silica residue (AmSR) and wastepaper sludge ash (WSA). AmSR is by-product of production of magnesium from Alliance Magnesium near of Asbestos and Thetford Mines Cities, and wastepaper sludge ash is by-product of combustion of de-inking sludge, bark and residues of woods in fluidized-bed system from Brompton mill located near Sherbrooke, Quebec, Canada. The AmSR is new industrial by-products. Recently, wastepaper sludge ash has been used as cementitious materials. Utilization of these ashes as cementitious material in concrete manufacturing leads to reduce the mechanical properties of concretes. These problems are caused by disruptive hydration products of biomass fly ash once these ashes partially blended with cement in concrete manufacturing. The pre-wetting process of WSA before concrete manufacturing reduced disruptive hydration products and consequently improved concrete mechanical properties. Approaches for investigation of WSA in this project consist on characterizing regular and pre-wetted WSA, the effect of regular and pre-wetted WSA on performance of mortar and concrete. The high content of amorphous silica in AmSR is excellent potential as cementitious material in concrete. In this project, evaluation of AmSR as cementitious materials consists of three steps. Characterizing and determining physical, chemical and mineralogical properties of AmSR. Then, effect of different rates of replacement of cement by AmSR in mortar. Finally, study of effect of AmSR as partial replacement of cement in different concrete types with binary and ternary binder combinations. This study revealed that high performance concrete (HPC) incorporating AmSR showed similar mechanical properties and durability, compared to control mixture. AmSR improved mechanical properties and durability of ordinary concrete. Self-consolidating (SCC) concrete incorporating AmSR was

stable, homogenous and showed good mechanical properties and durability. AmSR had good synergy in ternary binder combination with other supplementary cementitious materials (SCMs). This study showed AmSR can be use as new cementitious materials in concrete.

Keywords: wastepaper sludge ash, amorphous silica residue, alternative supplementary cementitious material, high performance concrete, ordinary concrete, self-consolidating concrete.

Résumé

L'industrie du ciment est l'une des principales sources d'émission de dioxyde de carbone. L'industrie mondiale du ciment contribue à environ 7% des émissions de gaz à effet de serre dans l'atmosphère. Afin d'aborder les effets environnementaux associés à la fabrication de ciment exploitant en permanence les ressources naturelles, il est nécessaire de développer des liants alternatifs pour fabriquer du béton durable. Ainsi, de nombreux sous-produits industriels ont été utilisés pour remplacer partiellement le ciment dans le béton afin de générer plus d'économie et de durabilité. La performance d'un additif de ciment est dans la cinétique d'hydratation et de la synergie entre les additions et de ciment Portland. Dans ce projet, deux sous-produits industriels sont étudiés comme des matériaux cimentaires alternatifs: le résidu de silice amorphe (RSA) et les cendres des boues de désencrage. Le RSA est un sous-produit de la production de magnésium provenant de l'Alliance Magnésium des villes d'Asbestos et Thedford Mines, et les cendres des boues de désencrage est un sous-produit de la combustion des boues de désencrage, l'écorce et les résidus de bois dans le système à lit fluidisé de l'usine de Brompton située près de Sherbrooke, Québec, Canada. Récemment, les cendres des boues de désencrage ont été utilisées comme des matériaux cimentaires alternatifs. L'utilisation de ces cendres comme matériau cimentaire dans la fabrication du béton conduit à réduire la qualité des bétons. Ces problèmes sont causés par des produits d'hydratation perturbateurs des cendres volantes de la biomasse quand ces cendres sont partiellement mélangées avec du ciment dans la fabrication du béton. Le processus de pré-mouillage de la cendre de boue de désencrage avant la fabrication du béton réduit les produits d'hydratation perturbateurs et par conséquent les propriétés mécaniques du béton sont améliorées. Les approches pour étudier la cendre de boue de désencrage dans ce projet sont : 1) caractérisation de cette cendre volante régulière et pré-humidifiée, 2) l'étude de la performance du mortier et du béton incorporant cette cendre volante régulière et pré-humidifiée. Le RSA est un nouveau sous-produit industriel. La haute teneur en silice amorphe en RSA est un excellent potentiel en tant que matériau cimentaire dans le béton. Dans ce projet, l'évaluation des RSA comme matériaux cimentaires alternatifs compose trois étapes. Tout d'abord, la caractérisation par la détermination des propriétés minéralogiques, physiques et chimiques des RSA, ensuite, l'optimisation du taux de remplacement du ciment par le RSA dans le mortier, et enfin l'évaluation du RSA en remplacement partiel du ciment dans différents types de béton dans

le système binaire et ternaire. Cette étude a révélé que le béton de haute performance (BHP) incorporant le RSA a montré des propriétés mécaniques et la durabilité, similaire du contrôle. Le RSA a amélioré les propriétés des mécaniques et la durabilité du béton ordinaire (BO). Le béton autoplaçant (BAP) incorporant le RSA est stable, homogène et a montré de bonnes propriétés mécaniques et la durabilité. Le RSA avait une bonne synergie en combinaison de liant ternaire avec d'autres matériaux cimentaires supplémentaires. Cette étude a montré que le RSA peut être utilisé comme nouveaux matériaux cimentaires dans le béton.

Mots clés: résidu de silice amorphe, cendres des boues de désencrage, matériaux cimentaires alternatif, gaz à effet de serre, béton durable.

ACKNOWLEDGEMENTS

I would like to express my sincere appreciation to my supervisor, Professor Arezki Tagnit-Hamou, for his technical, scientific and financial support during my Master's study. Special thanks to Dr. Ablam Zidol, because this work would never have been accomplished without his kind support. Also, I would like to express my deepest appreciation to jury member professor Yahia, professor Masmoudi and the technician staff, Mr. Rajko Vojnovic, Ms. Josée Bilodeau, and Mr. Claude Faucher.

I would like to thank everyone in concrete group who helped me in any way for doing my research.

My thankfulness is extended to my lovely family for their unlimited love and their support.

TABLE OF CONTENTS

1.	Introduction.....	1
1.1.	Definition and problem statement.....	1
1.2.	Objective of project.....	3
1.3.	Structure of thesis	3
2.	Literature survey	5
2.1.	Supplementary Cementitious Materials (SCMs)	5
2.1.1	Silica Fume (SF).....	7
2.1.2	Ground Granulated Blast furnace Slag (GGBS).....	8
2.1.3	Metakaolin (MK)	9
2.1.4	Fly Ash (FA)	10
2.2.	Alternative supplementary cementitious materials (ASCMs)	12
2.2.1	Glass Powder (GP)	12
2.2.2	Amorphous Silica Residue (AmSR).....	14
2.2.2.1	Residue of Magnesium production (Alliance Magnesium).....	14
2.2.2.2	Studied Amorphous Silica Residue (AmSR)	15
2.2.3	Waste paper sludge ash (WSA).....	16
2.2.3.1	Residues of pulp and paper industries (Kruger power plant).....	16
2.2.3.2	Properties of concrete incorporating WSA.....	20
3.	Experimental program and tests procedures.....	24
3.1.	Methodology	24
3.1.1	Phase 1 - Characterization of AmSR	25
3.1.2	Phase 2 - Effect of pre-wetted and regular WSA on main properties of mortar and concrete ...	25

3.1.3	Phase 3 - Optimization of the AmSR in mortar	26
3.1.4	Phase 4 - Performance of AmSR in different types of concrete made with binary and ternary system	27
3.1.4.1	Binary system	27
3.1.4.2	Ternary system	29
3.2.	Materials.....	30
3.2.1	Cement.....	30
3.2.2	Supplementary cementitious materials	31
3.2.2.1	Physical characteristics	31
3.2.2.1	Chemical characteristics.....	31
3.2.3	Aggregate.....	32
3.2.4	Chemical admixture	32
3.3.	Mixing procedures.....	33
3.3.1	Mortar mixing.....	33
3.3.2	Concrete mixing.....	34
3.4.	Description of test methods	35
3.4.1	Characteristic tests of materials	35
3.4.1.1	Chemical analysis	35
3.4.1.2	Physical analysis	35
3.4.1.3	Mineral analysis (The X-ray diffraction (XRD)).....	36
3.4.1.4	Morphology (Scanning electron microscope)	37
3.4.2	Test method for Mortar	38
3.4.3	Test method for concrete.....	38
3.4.3.1	Fresh properties	38
3.4.3.2	Mechanical properties	41
3.4.3.3	Durability	42

4.	Results and discussions	46
4.1.	Phase 1 - Characterization of Physical and chemical composition of AmSR.....	46
4.2.	Phase 2 - Effect of pre-wetted and regular WSA on main properties of mortar and concrete ...	48
4.2.1	Characterization of pre-wetted and regular WSA.....	48
4.2.2	Mortar incorporating regular and pre-wetted WSA	50
4.2.3	Concrete incorporating regular and pre-wetted WSA	51
4.3.	Phase 3 - Optimization of the AmSR content in mortar	55
4.3.1	Composition and fresh properties	55
4.3.2	Compressive strength.....	56
4.3.3	Strength activity index (SAI)	58
4.3.4	Electrical resistivity.....	59
4.4.	Phase 4 - Performance of AmSR in different type of concrete with binary and ternary system	60
4.4.1	Binary concrete.....	60
4.4.1.1	Ordinary concrete (OC) and High performance concrete (HPC)	60
4.4.1.1.1	Fresh properties	61
4.4.1.1.2	Mechanical properties	66
4.4.1.1.3	Durability	78
4.4.1.2	Self-consolidating concrete (SCC)	95
4.4.1.2.1	Fresh properties	96
4.4.1.2.2	Mechanical properties	98
4.4.1.2.3	Durability	101
4.4.2	Ternary concrete	104
4.4.2.1	Fresh properties	105
4.4.2.2	Mechanical properties	107
4.4.2.3	Durability	109
5.	Conclusions and recommendations.....	113

5.1.	Conclusions.....	113
5.2.	Recommendations for future research	122
6.	Reference.....	123

LIST OF FIGURES

Figure 2-1: Supplementary cementitious materials: From left to right, fly ash (Class C), metakaolin (calcined clay), silica fume, fly ash (Class F), slag, and calcined shale (Kosmatka et al.,2002).....	6
Figure 2-2: $\text{CaO}-\text{Al}_2\text{O}_3-\text{SiO}_2$ ternary diagram of cementitious materials (Barbara et al, 2011).	7
Figure 2-3: Spherical particles of fly ash type F	12
Figure 2-4: Glass powdre as ASCMs.....	14
Figure 2-5 : Amourphous silica residue (AmSR) as ASCMs	16
Figure 2-6 : Wastepaper sludge ash (WSA) as ASCMs	17
Figure 2-7: XRD results of five WSA samples: Q= Quartz, CaO= Lime, A=Anhydrite,CC=Calcite,C= Graphite, An=Anorthite, C3A= Calcium aluminate, C2S=Calcium silicate, Cr= Cristobalite, E=Ettringite,Y= Yeelimite G= Gehlenite, P= Portlandite, (Davidenko et al., 2012)	19
Figure 2-8: Slump of concrete incorporating with waste paper sludge ash w/b=0.45 (Ahmad et al., 2013)	21
Figure 2-9: Setting times of concrete incorporating 20% WSA, w/cm= 0.4 (Roby 2011).....	22
Figure 2-10: Compressive strength of concrete incorporating 20% WSA, w/cm=0.40 (Roby, 2011)	23
Figure 3-1: Organigram of the experimental phases.....	24
Figure 3-2: Principal of SEM	37
Figure 3-3: Types of slump shape (Concrete Society 2010).	38
Figure 3-4 : Schema of V-Funnel (Khayat, 1999).....	40
Figure 4-1: Particle size distribution of AmSR and Portland cement GU.....	47
Figure 4-2: The XRD analysis of the AmSR	47
Figure 4-3: Particle size distribution of pre-wetted and regular WSA.....	48
Figure 4-4: X-ray diffraction analysis of pre-wetted and regular WSA.....	49
Figure 4-5: Compressive strength of mortar incorporating 20% pre-wetted and regular WSA	51

Figure 4-6: Required dosage of chemical admixtures for control, concrete incorporating 20 % pre-wetted and regular WSA	53
Figure 4-7: Slump of concrete incorporating 20% pre-wetted WSA, 20% regular WSA and control	53
Figure 4-8: The initial and final setting time of control, concrete incorporating 20% pre-wetted and regular WSA.....	54
Figure 4-9: The compressive strength of control and concrete incorporating 20% pre-wetted and regular WSA.....	55
Figure 4-10: The compressive strength of mortar mixtures incorporating AmSR (w/b = 0.485)	57
Figure 4-11: The compressive strength of mortar mixtures incorporating AmSR (w/b = 0.40)	57
Figure 4-12: Electrical resistivity of mortar mixtures incorporating AmSR (w/b = 0.485)	59
Figure 4-13: Electrical resistivity of mortar mixtures incorporating AmSR (w/b = 0.40)	59
Figure 4-14: The comparison of required quantities of chemical admixtures of HPC and OC mixtures incorporating 20% AmSR and control mixtures	63
Figure 4-15: Measured slump and slump loss of HPC and OC mixtures incorporating 20% AmSR and control mixtures	64
Figure 4-16: Fresh air content of HPC and OC mixtures incorporating 20% AmSR and control mixtures	65
Figure 4-17: The initial and final settings of OC and HPC mixtures incorporating 20% AmSR and control mixtures	66
Figure 4-18: Compressive strength of HPC incorporating 20% AmSR and control mixture (w/b=0.35) ..	67
Figure 4-19: Compressive strength of OC incorporating 20% AmSR and control mixture (w/b=0.40) ...	67
Figure 4-20: Compressive strength of OC incorporating 20% AmSR and control mixture (w/b=0.45) ...	68
Figure 4-21: Compressive strength of OC incorporating 20% AmSR and control mixture (w/b=0.50) ...	68
Figure 4-22: Compressive strength of OC incorporating 20% AmSR and control mixture (w/b=0.55) ...	69
Figure 4-23: Compressive strength of OC incorporating 20% AmSR and control mixture (w/b=0.65) ...	69
Figure 4-24: Compressive strength of OC incorporating 20% AmSR and control mixture (w/b=0.70) ...	70
Figure 4-25: Different of compressive strength of 20% AmSR concrete with their control at 91 days.....	70

Figure 4-26: Tensile splitting strength of HPC incorporating 20% AmSR and control mixture (w/b=0.35)	72
Figure 4-27: Tensile splitting strength of OC incorporating 20% AmSR and control mixture (w/b=0.40)	72
Figure 4-28: Tensile splitting strength of OC incorporating 20% AmSR and control mixture (w/b=0.45)	73
Figure 4-29: Tensile splitting strength of OC incorporating 20% AmSR and control mixture (w/b=0.50)	73
Figure 4-30: Tensile splitting strength of OC incorporating 20% AmSR and control mixture (w/b=0.55)	74
Figure 4-31: Tensile splitting strength of OC incorporating 20% AmSR and control mixture (w/b=0.65)	74
Figure 4-32: Tensile splitting strength of OC incorporating 20% AmSR and control mixture (w/b=0.70)	75
Figure 4-33: Flexural strength of HPC incorporating 20% AmSR and control mixture (w/b= 0.35)	76
Figure 4-34: Flexural strength of OC incorporating 20% AmSR and control mixture (w/b= 0.40)	76
Figure 4-35: Flexural strength of OC incorporating 20% AmSR and control mixture (w/b= 0.45)	76
Figure 4-36: Modulus of elasticity of HPC incorporating 20% AmSR and control mixture (w/b=0.35)	77
Figure 4-37: Modulus of elasticity of OC incorporating 20% AmSR and control mixture (w/b=0.40)	78
Figure 4-38: Modulus of elasticity of OC incorporating 20% AmSR and control mixture (w/b=0.45)	78
Figure 4-39: Electrical resistivity of HPC incorporating 20% AmSR and control mixture (w/b=0.35)	79
Figure 4-40: Electrical resistivity of OC incorporating 20% AmSR and control mixture (w/b=0.40)	80
Figure 4-41: Electrical resistivity of OC incorporating 20% AmSR and control mixture (w/b=0.45)	80
Figure 4-42: Electrical resistivity of OC incorporating 20% AmSR and control mixture (w/b=0.50)	81
Figure 4-43: Electrical resistivity of OC incorporating 20% AmSR and control mixture (w/b=0.55)	81
Figure 4-44: Electrical resistivity of OC incorporating 20% AmSR and control mixture (w/b=0.65)	82
Figure 4-45: Electrical resistivity of OC incorporating 20% AmSR and control mixture (w/b=0.70)	82

Figure 4-46: Chloride-ions penetration of HPC incorporating 20% AmSR and control mixture (w/b = 0.35).....	83
Figure 4-47: Chloride-ions penetration of OC incorporating 20% AmSR and control mixture (w/b = 0.40).....	84
Figure 4-48: Chloride-ions penetration of OC incorporating 20% AmSR and control mixture (w/b = 0.45).....	84
Figure 4-49: Chloride-ions penetration of OC incorporating 20% AmSR and control mixture (w/b= 0.50).....	85
Figure 4-50: Chloride-ions penetration of OC incorporating 20% AmSR and control mixture (w/b= 0.70).....	85
Figure 4-51: The autogenous shrinkage of HPC incorporating 20% AmR and control mixture (w/b=0.35).....	86
Figure 4-52: The variation of temperature of HPC incorporating 20% AmSR and control mixture (w/b=0.35).....	87
Figure 4-53 : The drying shrinkage of HPC incorporating 20% AmSR and control mixture (w/b= 0.35) .	87
Figure 4-54: The drying shrinkage of OC incorporating 20% AmSR and control mixture (w/b= 0.40)....	88
Figure 4-55: The drying shrinkage of OC incorporating 20% AmSR and control mixture (w/b= 0.45)....	89
Figure 4-56: The drying shrinkage of OC incorporating 20% AmSR and control mixture (w/b= 0.50)....	89
Figure 4-57: The drying shrinkage of OC incorporating 20% AmSR and control mixture (w/b= 0.55)....	90
Figure 4-58: The drying shrinkage of OC incorporating 20% AmSR and control mixture (w/b= 0.65)....	90
Figure 4-59: The drying shrinkage of OC incorporating 20% AmSR and control mixture (w/b= 0.70)....	91
Figure 4-60: The de-icing scaling of HPC incorporating 20% AmSR and control mixture (w/b=0.35).....	92
Figure 4-61: The de-icing scaling of OC incorporating 20% AmSR and control mixture (w/b= 0.40).....	92
Figure 4-62: The de-icing scaling of OC incorporating 20% AmSR and control mixture (w/b=0.45).....	93
Figure 4-63: The de-icing scaling of OC incorporating 20% AmSR and control mixture (w/b=0.50).....	93
Figure 4-64: The de-icing scaling of OC incorporating 20% AmSR and control mixture (w/b=0.55).....	94
Figure 4-65: Comparison of dosage of SP and slump flow of SCC mixtures (w/b= 0.42)	96

Figure 4-66 : Comparison of V-funnel, T50 and slump flow of SCC mixtures ($w/b = 0.42$)	97
Figure 4-67: The yield stress and plastic viscosity of SCC mixture (0.42)	98
Figure 4-68: The compressive strength of SCC incorporating AmSR and control mixture ($w/b = 0.42$) .	99
Figure 4-69: The tensile strength of SCC incorporating AmSR and control mixture ($w/b = 0.42$)	99
Figure 4-70: The flexural strength of SCC incorporating AmSR and control mixture ($w/b = 0.42$).....	100
Figure 4-71: The modulus of elasticity of SCC incorporating AmSR and control mixture ($w/b = 0.42$)	101
Figure 4-72: The electrical resistivity of SCC mixtures incorporating AmSR and control ($w/b = 0.42$) .	101
Figure 4-73: The chloride-ions penetration of SCC incorporating AmSR and control ($w/b = 0.42$)	102
Figure 4-74: Drying shrinkage of SCC incorporating AmSR and control ($w/b = 0.42$).....	103
Figure 4-75: The required chemical admixtures for studied ternary concrete ($w/b = 0.40$).....	105
Figure 4-76: The slump and slump loss of ternary concretes ($w/b = 0.40$).....	106
Figure 4-77: The fresh air content of ternary concretes ($w/b = 0.40$)	106
Figure 4-78: The initial and final setting time of ternary concretes ($w/b = 0.40$)	107
Figure 4-79: The compressive strength of ternary concretes ($w/b = 0.40$).....	108
Figure 4-80: The tensile splitting strength of ternary concretes ($w/b = 0.40$)	108
Figure 4-81: The electrical resistivity of ternary concretes ($w/b = 0.40$).....	109
Figure 4-82: The chloride-ions penetration of ternary concretes ($w/b = 0.40$)	110
Figure 4-83: The drying shrinkage of ternary concretes ($w/b = 0.40$)	111
Figure 4-84: The de-icing scaling of ternary concretes ($w/b = 0.40$)	112

LIST OF TABLES

Table 2-1: The chemical composition of waste paper sludge ashes founded in literature.....	18
Table 3-1: Test methods and apparatuses for characterize of materials (WSA and AmSR)	25
Table 3-2: Tests on mortar and concrete incorporating regular and Pre-wetted WSA	26
Table 3-3: Tests on mortar incorporating AmSR	27
Table 3-4: The w/b and rate of replacement of AmSR in ordinary and high performance concrete	27
Table 3-5: Fresh properties tests for conventional and high performance concrete (HPC)	27
Table 3-6: Hardened properties tests for conventional and high performance concrete (HPC)	28
Table 3-7: Self consolidating concrete.....	28
Table 3-8: Fresh properties tests for self consolidating concrete (SCC)	28
Table 3-9: Hardened concrete tests for self consolidating concrete (SCC)	29
Table 3-10: Ternary concrete combinations	29
Table 3-11: Fresh properties tests for ternary concrete	29
Table 3-12: Hardened properties test for ternary concrete	30
Table 3-13: The physical-chemical analysis of three type of cement where used	30
Table 3-14: Physical properties of used SCMs.....	32
Table 3-15: Chemical analysis of used SCMs	32
Table 3-16: The physical properties of natural sand and coarse aggregates used.....	32
Table 3-17: Different classes of penetration of chloride ions (Whiting 1988)	43
Table 3-18: Durability classes with the indicative limit of the electrical resistivity (AFGC, 2004)	43
Table 3-19: The visual observation criterion of scaling (BNQ 2621-900).....	44
Table 4-1: The chemical composition of AmSR	46
Table 4-2: The physical properties of AmSR	46

Table 4-3: The chemical compositions of pre-wetted and regular WSA	48
Table 4-4: The physical properties of pre-wetted and regular WSA	49
Table 4-5: Composition and fresh properties of mortars	50
Table 4-6: Results of SAI of mortar cubes incorporating regular and pre-wetted WSA	51
Table 4-7: The composition of control mix, concrete incorporating 20% regular and pre-wetted WSA	52
Table 4-8: Fresh properties of control mixture, concrete incorporating 20% regular and pre-wetted WSA	52
Table 4-9: Composition and fresh properties of mortars with 0.485 of w/b	56
Table 4-10: Composition and fresh properties of mortars with 0.40 of w/b	56
Table 4-11: Results of SAI of mortar cubes incorporating AmSR, w/b = 0.485	58
Table 4-12: Results of SAI of mortar cubes incorporating AmSR, w/b = 0.40	58
Table 4-13: Composition of OC and HPC mixtures	61
Table 4-14: Composition of OC residential mixtures	61
Table 4-15: Fresh properties of OC and HPC mixtures	62
Table 4-16: Fresh properties of residential OC mixtures	62
Table 4-17: The results of freezing thawing resistance	94
Table 4-18: Composition of SCC mixtures	95
Table 4-19: Fresh properties of SCC mixtures	95
Table 4-20: The durability coefficient of SCC	103
Table 4-21 : The compositions of ternary studied ternary concretes	104
Table 4-22 : The fresh properties and required dosage of chemical admixtures of ternary concrete..	105
Table 4-23: The durability coefficient of ternary concretes	112

LIST OF ABBREVIATIONS

AEA: Air-Entrainment Agent

ACMS: Alternative supplementary Cementitious materials

AmSR: Amorphous silica residue

DEF: Delay Ettringite Formation

FBC: Fluidized-Bed Combustion

GHG: Greenhouse Gas

GGBS: Ground Granulated Blast Furnace Slag

KFA: Kruger Fly Ash

LOI: Loss on Ignition

MK: Metakaolin

SF: Silica Fume

GP: Glass powder

FA: Fly ash

PKFA: Pre-wetted Kruger Fly ash

SCMs: Supplementary Cementitious Materials

SP: Superplasticizer

SEM: Scanning Electron Microscope

WSA: Waste paper sludge ash

XRD: X-ray Diffraction

w/cm: Water-to-Cementitious ratio

w/b: Water-to-Binder ratio

1. Introduction

1.1. Definition and problem statement

Nowadays, there are two significant challenges to achieve sustainable development, reducing greenhouse gas (GHG) emission and reducing or specifically recycling of waste materials. High quantities of cement are necessary to develop constructions and maintenance of structures. The cement industries are one of major producer of CO₂ emission which in turn has significantly contributed to global warming. Almost 7% of global CO₂ emissions are caused by cement plants. It is reported that 900 kg CO₂ is emitted to the atmosphere due to the production of one ton of cement (Benhelal et al, 2013). However, in the last years this figure was reduced up to 5% in the worldwide considering the last improvements in energy efficiency, or alternative fuels and materials (Aranda et al, 2013). Utilization of supplementary cementitious materials (SCMs) such as fly ash, silica fume, blast furnace slag, and natural pozzolan in concrete is a feasible approach, resulting in the reduction of cement content and consequently CO₂ emission in concrete manufacturing. Furthermore, some of the SCMs have a certain property called pozzolanicity and hydraulic, which has beneficial effect in improving concrete properties. Significant CO₂ emission of cement production leads to more incentive to use alternative supplementary materials in concrete manufacturing. These alternative materials consist of industrial by-products or waste industrial materials. In this research project two industrial by-products are investigated as ASCMs in concrete, non-toxic amorphous silica residue (AmSR) and Wastepaper Sludge Ash (WSA). Utilization of WSA and AmSR in concrete manufacturing has environmental and economical standpoints. Economics dimension corresponds to decrease cost of concrete manufacturing. The WSA and AmSR are recycled product and cheaper than cement. Also using these materials in concrete leads to reduce cost of landfills. Environmental dimension corresponds to decrease the CO₂ emissions during the cement production and also decrease landfill pollution. Thus, the valorization of WSA and AmSR as alternative supplementary cementitious materials (ASCMs) presents a great interest.

AmSR is by-product of production of magnesium from Alliance Magnesium near of Asbestos and Thetford Mines Cities, Quebec, Canada. Alliance Magnesium is a privately-owned Canadian company which has developed a technology for the production of magnesium metal from waste arising from the asbestos industry. These residues consist mainly of serpentine (silicate magnesium) containing 40% magnesium oxide and 50% silica. Near the towns of Asbestos and Thetford Mines, there are about 800 million tons of tailings ready to be processed. Production of magnesium from this waste asbestos industry generates amorphous silica residue (AmSR) (Alliance magnesium Inc, 2015). High content of amorphous silica and small particle size of AmSR have excellent potential as alternative cementitious material in concrete. Adding fine ASCMs brings millions of very small particles to concrete mixture. They contribute in filling the spaces between cement particles. This phenomenon is frequently referred to as particle packing or micro-filling. Because of its very high amorphous silicon dioxide content, AmSR can be a very reactive pozzolanic material in concrete. As the portland cement in concrete begins to react chemically, it releases calcium hydroxide. AmSR reacts with this calcium hydroxide to form additional binder material called calcium silicate hydrate (CSH). The mentioned parameters in AmSR present great potential of utilization of AmSR as ASCMs in concrete.

The paper industry generates a significant amount of waste which has to be dumped in landfill. To reduce the environmental impact and cost of land-filling, some pulp and paper plants use fluidized bed combustion (FBC) to generate their required energy by using its own sludge as a raw fuel (Davidenko et al, 2012). However, the combustion of biomass residues generates another type of wastes as wastepaper sludge ash. Indeed, a significant amount of wastepaper sludge ash (WSA) is generated and must be dumped to landfill. The burned biomass is generally composed of the sludge from water treatment process, the de-inking sludge, and the wood residues from construction and demolition. Brompton mill de-inking plant, which belongs to Kruger Company, is located in the municipality of Brompton, near to the city of Sherbrooke in Quebec. Brompton mill consists of pulp and paper mill, including a de-inking facility, hydraulic power plant and biomass cogeneration operation. Kruger paper mill uses barks, residues of wood, and sorting wastes (de-inking and waste water-treatment sludge) during the recycling process to generate electricity. Therefore, all the ingredients are disposed by thermal means in a fluidized-bed combustion (FBC) boiler at about 850°C to generate electricity. All these

combusted recycle materials produce WSA. According to the literature survey, WSA can potentially be used in concrete applications (Xie, 2009). Blending WSA as alternative supplementary cementitious materials in concrete matrixes leads to some problems such as reduction in mechanical properties. The variation in chemical composition of this biomass fly ash, especially the content of CaO, Al (metallic aluminum), SO₂, carbon contents and SO₃ contents influences the quality and properties of concrete made of biomass fly ashes (Aubert et al, 2004; Bai et al, 2003; Cheah et al, 2011; Segui et al, 2012). Mentioned problem will restrict increasing rates of replacement of biomass fly ash as supplementary cementitious materials in concrete. Pre-wetting process of WSA before concrete manufacturing may enable to reduce significantly some of these problems and improve concrete mechanical properties.

1.2. Objective of project

There are two principal objectives for this project. The first objective is to improve the performance of concrete incorporating WSA. The second objective is to valorize AmSR as cementitious materials. The specific objectives of this study are:

- a) Improving the performance of concrete incorporating WSA**
 - ✓ Characterization of chemical, physical and mineralogical properties of WSA
 - ✓ Evaluation of the effect of pre-wetting of WSA on mortar and concrete properties
- b) Valorizing AmSR in cementitious system**
 - ✓ Characterization of chemical, physical and mineralogical properties of AmSR
 - ✓ Study the performance of mortar incorporating AmSR
 - ✓ Evaluation the fresh, mechanical, and durability of various concrete types incorporating AmSR in binary and ternary systems

1.3. Structure of thesis

This master thesis mainly consists of five chapters:

Chapter 1: In this chapter the definition of project, problem statement, and objective of this study are presented (Introduction).

Chapter 2: The second chapter is an overview on the utilization of different supplementary cementitious materials (SCMs) and alternative supplementary cementitious materials (ASCMS) in cementitious in concrete (literature survey).

Chapter 3: This chapter covered the experimental program developed in order to achieve the objectives of project. The characteristics of the used materials and the tests procedures are described (Methodology).

Chapter 4: The results obtained throughout the project phases are described and analyzed in this chapter (Results and analysis).

Chapter 5: Conclusions and perspectives. This chapter is a summary of final conclusion of this research project

2. Literature survey

2.1. Supplementary Cementitious Materials (SCMs)

The principal binder in concrete has been Portland cement until latter of the 20th century. According to the requirements of complicated structures over this period as increase the performance of concrete, especially for durable concrete. The utilization of "Pozzolan" as a popular substitution material in concrete increased at the end of the 20th century (Newman et al, 2003). Based on Hewlett, lime-pozzolan composites were used as a cementitious material for construction overall the Roman Empire (Hewlett, 2004). In fact, it was in Italy that the term, "pozzolan" was first used to describe the volcanic ash mined at Pozzuoli, a village near Naples. Firstly, ash was produced by the volcanic eruption. After that, this word "Pozzolan" has been used to the all class of mineral matters which has same properties. Generally, a pozzolan is a natural or artificial material containing amorphous silica. Examples of pozzolanic materials are volcanic ash, fly ash, silica fume, metakaolin.

Volcanic ash acts just like fly ash. The only difference is: fly ash today is produced by the burning of coal. The first reference to the idea of using coal fly ash in modern concrete was reported in 1934 by McMillan and Powers in the United States. Later, Sear showed that fly ash was a possible artificial pozzolan (Sear, 2004). During the same period, the development of coal plants in the UK, especially after World War II, lead to generating numerous quantities of fly ash. Therefore, it increased the application of fly ash. For instance, fly ash was used in concrete of the Lednock and Lubreoch Dams (Newman et al, 2003). Since then, fly ash as one of the primary mineral admixtures has been extensively used in concrete. Recently, in order to producing durable concrete, some other inorganic materials were introduced into the concrete mix. These materials called supplementary cementitious materials (SCMs) or mineral admixtures. Usually SCMs are cheaper than cement and improve various properties in concrete, as fresh and hardened properties and durability of concrete. These materials can be divided into several categories and contain cementitious and/or pozzolan properties. The different SCMs showed in Figure 2-1.



Figure 2-1: Supplementary cementitious materials: From left to right, fly ash (Class C), metakaolin (calcined clay), silica fume, fly ash (Class F), slag, and calcined shale (Kosmatka et al, 2002)

As explained before, pozzolan is natural or industrial by-products that consist of amorphous silica. Amorphous silica reacts at ordinary temperature with the lime produced by the hydration of Alit (C_3S) and Belit (C_2S) to form calcium silicate hydrate (C-S-H) similar to producing by the direct hydration of C_3S and C_2S . Definition of ASTM C 618 for pozzolan is a siliceous or siliceous and aluminous fine material which in itself possesses little or no cementitious value that in the presence of moisture, chemically react with calcium hydroxide (i.e. portlandite) at ordinary temperatures to form cementitious properties. When a pozzolanic reaction starts, the lime produced during hydration of C_3S and C_2S , will transform into calcium silicate hydrate. Therefore, pozzolanic reaction improves the concrete performance. Aitcin presents the pozzolanic reaction schematically as follows (Aitcin, 1998):

- $C_2S/C_3S + H_2O \longrightarrow \text{calcium silicate hydrate (C-S-H)} + \text{lime}$
- $\text{Pozzolan} + \text{lime} + \text{water} \longrightarrow \text{calcium silicate hydrate (C-S-H)}$

At ordinary environment the development of a pozzolanic reaction is slower than the rate of Portland cement hydration. Over time in water curing ambient, concrete that contains a pozzolana will provide more strength and less permeability. The Ca/Si ratio in C-S-H gel varies in a wide range, but normal values are between 0.8 and 2.1. SCMs are still not completely understood. The specific surface and chemical composition of SCMs are known as the key factors. Fresh and mechanical properties and durability of concrete incorporating SCMs depend on chemical composition and specific surface of SCMs. Figure 2-2 shows the $CaO-Al_2O_3-SiO_2$

ternary diagram of cementitious materials. SCMs cause refined pore structure (due particle packing and later formation of C-S-H), improve transition zone properties, reduction in soluble hydration products, like CH, and therefore reduce permeability of concrete. Consequently Pozzolanic SCMs like silica fume, metakaolin and Fly ash, improve mechanical properties in long term and durability of concrete

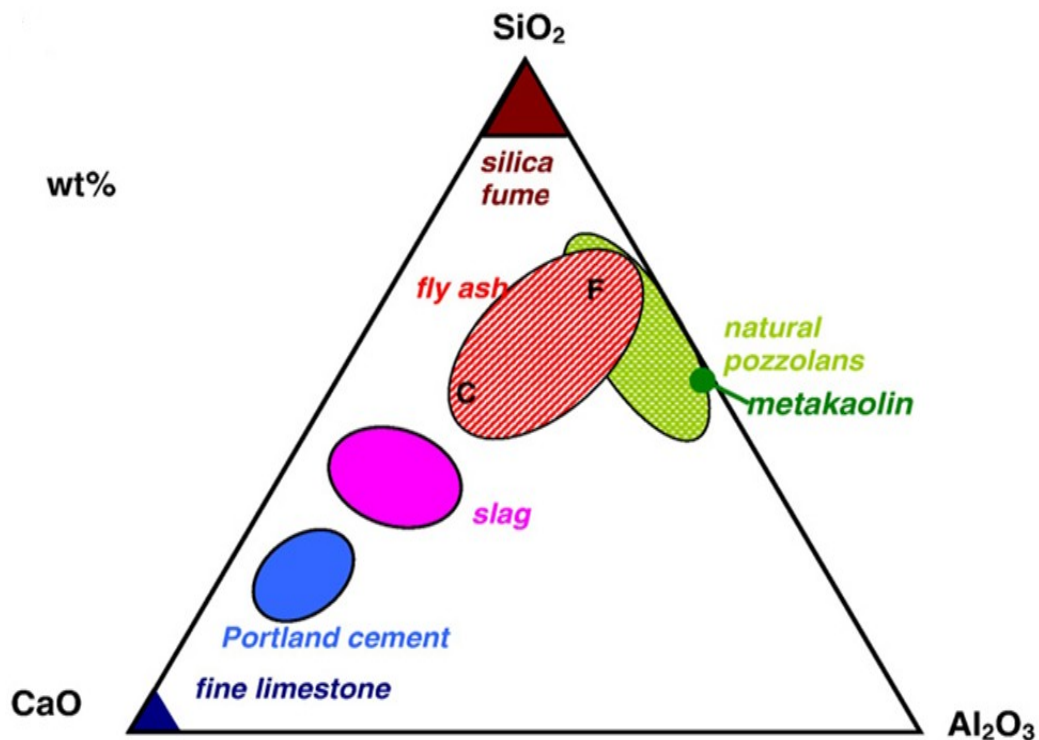


Figure 2-2: $\text{CaO}-\text{Al}_2\text{O}_3-\text{SiO}_2$ ternary diagram of cementitious materials (Barbara et al, 2011)

2.1.1 Silica Fume (SF)

Silica fume (SF) is a by-product from manufacturing silicon and ferrosilicon alloys, by high-purity quartz and coal in a submerged-arc electric furnace (Neville, 1996). The American Concrete Institute (ACI) defines silica fume as “very fine non-crystalline silica produced in electric arc furnaces as a by-product of the production of elemental silicon or alloys containing silicon”. It is usually a gray colored powder, somewhat similar to portland cement or some fly ashes. Silica fume was originally considered as a pozzolan. However, SF action in concrete is not

just as a very reactive pozzolan but also because of fine particles, it has other advantageous properties like filler effect. Depends on silicon and ferrosilicon alloys SF consist of 85% to 98% SiO_2 . The specific gravity of silica fume is generally 2.2, which is the usual specific gravity of amorphous silica. The particles of silica fume are extremely fine, usually a diameter ranging between 0.03 and 0.3 μm , the average diameter is typically less than 0.1 μm . specific surface is the total surface area of a given mass of a material. The specific surface of silica fume is 15,000 to 30,000 (m^2/kg) which is 13 to 20 times more than the specific surface of other pozzolanic materials (Neville, 1996). Because the particles of silica fume are very small, the surface area is very large. We know that water demand increases for sand as the particles become smaller; the same phenomenon happens for silica fume. This fact is why it is necessity to use silica fume in combination with a water-reducing admixture or a super-plasticizer. A specialized test called the “BET method” or “nitrogen adsorption method” must be used to measure the specific surface of silica fume. Specific surface determination based on Blaine analysis or air-permeability testing are meaningless for silica fume. When SF is added to concrete, it decreases the bleeding and improves the microstructure of the hydrated paste matrix. In addition, when silica fume is used, the transition zone around the coarse aggregates is much more compact than that of pure Portland cement. Generally, it is used 5% to 10% by mass of the total cementing material in applications where a high degree of impermeability is needed (Kosmatka et al, 2002). Silica fume is usually categorized as a supplementary cementitious material. This term refers to materials that are used in concrete in addition to portland cement. These materials can exhibit the Pozzolanic and cementitious properties, combination of both properties like some fly ash.

2.1.2 Ground Granulated Blast furnace Slag (GGBS)

Blast furnace slag is an industrial by-product of pig iron from iron ore in blast furnaces. Raw iron is decomposed into molten iron and molten slag when it is melted at a temperature of 1500°C along with limestone in a blast furnace. The slag solidifies in an amorphous form and can then develop cementitious properties if it is properly ground and activated (Aitcin, 1998). Since this amorphous slag involves sufficient silica and alumina, it also shows some hydraulic properties if it is ground to obtain a fine-grained structure. About 300 kg of slag is generated from each ton of pig iron (Neville, 1996). GGBS particles are angular and generally white color. It has 35-45% CaO , 32-38% SiO_2 , and 8-16% Al_2O_3 contents. The granulated material, which is ground to less

than 45 μm , has a specific surface area about 400 to 600 m^2/kg . The relative specific gravity for ground granulated blast furnace slag (GGBS) is within 2.85 to 2.95 (Kosmatka et al, 2002). Slag is a widely available SCM in most parts of North America. Concrete incorporating slag is durable under freezing and thawing conditions. Also, it is resistant to de-ice salt scaling (up to a level of 50% replacement), and it exhibits approximately equivalent shrinkage to that of ordinary Portland cement concrete (Lamond, 2006). Aitcin noted that slag is not just a hydraulic binder or a pozzolanic material (Aitcin, 2007). When slag is mixed with water, it does not harden or combine directly with the lime removed from the C_3S and C_2S to form secondary C-S-H. Slag can be activated by lime, calcium sulphate and alkali, which act as catalysts in the attack of the glass. This kind of chemical attack is called alkaline activation (Aitcin, 2007). When slag is mixed with Portland cement, the latter acts as a good catalyst for slag activation because it contains the three main chemical components (lime, calcium sulphate and alkalis) that activate slag. GGBS reduce heat of hydration and water demand also in long term increase compressive strength and improve durability of concrete.

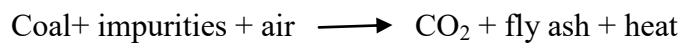
2.1.3 Metakaolin (MK)

Metakaolin (MK), as especial calcined clay, is produced by low-temperature calcinations of high purity kaolin clay to a range of 700-900°C. MK has 55% SiO_2 , and 35-45% Al_2O_3 contents. The particle size of metakaolin is smaller than cement particles, but not as fine as silica fume. Average diameter of MK is about 1 to 2 μm . Replacing portland cement with 8–20% MK produces a concrete mix, which exhibits favorable properties, including: the filler effect, the acceleration of cement hydration, and the pozzolanic reaction. The filler effect is immediate, while the effect of pozzolanic reaction occurs between 3 to 14 days. Researchers have shown a lot of interest in MK as it has been found to possess both pozzolanic and micro-filler characteristics (Poon et al, 2001; Wild et al, 1997). Metakaolin improves concrete performance by reacting with calcium hydroxide to form secondary C-S-H. Because of its white color, metakaolin does not darken concrete as silica fume typically does. It is suitable for color-matching and other architectural applications (Ding et al, 2002). Research shows that mixtures containing highly-reactive metakaolin perform similarly to silica fume mixtures in terms of improve compressive strength and reduced permeability. Reduced shrinkage, due to "particle packing" making concrete denser, therefore improves durability of concrete (Ruben et al, 2012).

2.1.4 Fly Ash (FA)

Coal fly ash is generated from combustion of coal in power plant. During this process, minerals in coal become fluid and then cooled, in this process the mineral matter within the coal may decompose, oxidize or agglomerate. Fly ashes are generally fine-grained material that most of them are spherical, glassy particles as showed in Figure 2-3. There are some ashes also by irregular or angular particles. The chemical properties of fly ash are influenced to a great extent by the properties of the coal being burned and the techniques used for handling and storage. The four types (ranks) of coal are anthracite, bituminous, sub-bituminous, and lignite. In addition to being handled in a dry conditioned or wet form, fly ash is also sometimes classified according to the type of coal from which the ash was derived. The principal components of bituminous coal fly ash are silica, alumina, iron oxide, and calcium, with varying amounts of carbon, as measured by the loss on ignition (LOI). Lignite and sub-bituminous coal fly ash is characterized by higher concentrations of calcium and magnesium oxide and reduced percentages of silica and iron oxide, as well as lower carbon content, compared with bituminous coal fly ash. Very little anthracite coal is burned in utility boilers, so there are only small amounts of anthracite coal fly ash. Lignite and sub-bituminous coal fly ash may have a higher concentration of sulphate compounds than bituminous coal fly ash (Ahmaruzzaman et al, 2010).

A schematic of production fly ash can be written as follows (Nehidim, 1998)



The chemical composition of fly ashes consist of minor and major element in their compositions, generally most constituent are determined by means of X-ray fluorescence (XRF) and spectrometry procedures. It shows the major constituents of most of fly ashes are SiO_2 , Al_2O_3 , FeO_3 and CaO , other elements are Na_2O , MgO , K_2O , SO_3 , MnO , TiO_2 and carbon (Xie, 2009). The weight loss of fly ash burned, which known as loss on ignition (LOI) is needed to be determined. LOI is related to the presence of carbonates and constituent of free carbon in fly ash. This factor is most effective on concrete workability and water demand. The higher content of carbon caused the more water demand on paste or mortar with normal consistency. Generally, traditional coal produced fly ash as a pozzolanic material has been classified into two classes,

according to the American Society for Testing Materials (ASTM C618), the ash containing more than 70 wt% $\text{SiO}_2 + \text{Al}_2\text{O}_3 + \text{Fe}_2\text{O}_3$ and being low in lime (CaO less than 10%) are defined as class F, while those with a $\text{SiO}_2 + \text{Al}_2\text{O}_3 + \text{Fe}_2\text{O}_3$ content between 50 and 70 wt% and high in lime (CaO more than 20%) are defined as class C. Briefly, the high-calcium Class C fly ash is normally produced from the burning of low-rank coals (lignite or sub-bituminous coals) and have cementations properties (self-hardening when reacted with water). On the other hand, the low-calcium Class F fly ash is commonly produced from the burning of higher-rank coals (bituminous coals or anthracites) that are pozzolanic in nature. The chief difference between Class F and Class C fly ash is in the amount of calcium and the silica, alumina, and iron content in the ash. In Class F fly ash, total calcium typically ranges from 1 to 12%, mostly in the form of calcium hydroxide, calcium sulphate, and glassy components, in combination with silica and alumina. In contrast, Class C fly ash may have reported calcium oxide contents as high as 30–40%. Another difference between Class F and Class C is that the amount of alkalis (combined sodium and potassium) and sulphate (SO_4) are generally higher in the Class C fly ash than in the Class F fly ash.

Based on the Canadian standards association (CSA A3001, 2004) ashes are classified as follow:

- Low calcium oxide (Type F, CaO less than 8%)
- Intermediate calcium oxide (Type CI, between 8 to 20%)
- High calcium oxide (Type CH, Cao more than 20%)

Generally fly ashes cause reduction of water demand relative than Portland cement for the constant workability. Because of spherical shape that so-called ‘ball-bearing effect’. Because of electrical charges, the finer particles of fly ashes can be adsorbed on the surface of cement particles. Therefore if the fine particles are enough they can be covered the surface of the cement particles, as a result become deflocculated and so on water demand for a given workability is decreased (Xie, 2009).

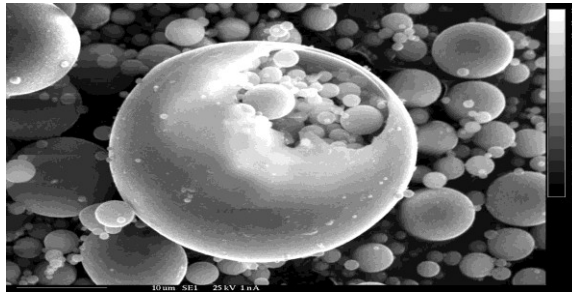


Figure 2-3: Spherical particles of fly ash type F (Tagnit-Hamou 2014)

Most of fly ashes generally increase the setting time of concrete. The effect of fly ash on setting time corresponds on the amount of fly ash used and its characteristics. The fly ashes have pozzolan properties which can be improved the compressive strength of concrete. In addition to pozzolanicity, fly ashes have a physical effect of improving the microstructure of the hydrated cement matrix. The main physical action is the packing effect of fly ash particles at the interface of coarse aggregate particles and cement paste. A number of authors have noted that the concrete incorporating low calcium fly ash as a replacement of cement has no significant effect on concrete strength at early ages. Particles of fly ashes have a very high fineness as a result the specific surface is high that mean's is fly ashes is readily available for reaction with calcium hydroxide (CH). By this property fly ashes exhibit high pozzolanic activity and can be used to produce high strength concrete. Actually the particle size of low calcium fly ash usually is coarser than that of high calcium fly ash. Therefore when low calcium fly ash used in concrete, it showed an exceptionally slow rate in strength development at the young age. Generally the fly ash concrete at young age has high permeability rather than concrete without the fly ash. Over time fly ash concrete acquires a very low permeability.

2.2. Alternative supplementary cementitious materials (ASCMs)

2.2.1 Glass Powder (GP)

The utilization of glass powder produced by grinding waste mixed bottle glass in concrete has attracted much research interest. Non-recycled glass considered as one of the most wastes produced in some countries and sets a major environmental issue. Unlike other waste materials as paper or organic constituents, waste glass bottles will remain stable in landfills. Utilization of

waste material in concrete is still an alternative for its recycling. Since in many part of the world, conventional SCMs which explained before, are not available. For example in Quebec (Canada), fly ash and slag have to be imported from Ontario or United States (Bouzoubaa et al, 2004), inducing additional transportation costs and CO₂ emissions. The development of alternative SCMs such as glass powder has double benefits: economic and ecological advantages. About 90,000 tones of glass were collected by means of various systems in Quebec. Chemical and mineralogical composition of the glass powder can present interesting properties in concrete. Utilization of finely ground glass powder as partial replacement of cement in a cement-based system began in 1970 (Pattengil et al, 1973). Chemical composition revealed that fine glass powder consist of a high level of amorphous silica (SiO₂: 70-75%) that it could possess pozzolanic properties. However, due to the high alkali (10% -15%) content of the glass powder, concrete incorporating glass powder is expected to be easily subject to alkali-silica reaction (ASR). In fact, some phases from siliceous aggregates are unstable in high pH environments react with alkalis and produce an expansive gel causing swelling and cracking of the concrete, therefore reducing the service life of concrete. Recent studies carried out by some researchers (Shayan et al, 2006; Shi et al, 2005) showed that the replacement of cement by glass powder improves compressive strength of concrete and the resistance to alkali-silica reaction at later ages. It depends on the replacement rate, the fineness and particle size of glass powder (Idir et al, 2011; Zidol, 2009). According to Shayan and Xu (Shayan et al, 2004), for concrete containing up to 30% of glass powder, the dissolution of alkali is too small to generate an expansion due to Alkali Silica Reaction. Pattengil (Pattengil et al, 1973) mentioned that to having good pozzolanic properties, particle size of glass powder should be less than 75 µm. Idir et al (Idir et al, 2011) have reported that the pozzolanic activity of glass powder increases with increasing fineness. Glass powder is known to decrease the compressive strength of concrete at early age due to its dilution effect, because reactive cement particles are replaced by glass powder. In general, the great contribution of pozzolanic properties of glass powder is observed after 56 days with compressive strength equal or superior to the control one (without glass powder). Zidol (Zidol et al, 2012) showed that glass powder has the ability to significantly improve the resistance to chloride ions penetration, and increasing concrete durability. Decrease in chloride ions penetration is due to the refining of the pores network, because of the pozzolanic reaction of the glass powder. Figure 2-4 shows glass powder as ASCMs.



Figure 2-4: Glass powder as ASCMs

2.2.2 Amorphous Silica Residue (AmSR)

2.2.2.1 Residue of Magnesium production (Alliance Magnesium)

Alliance Magnesium is a privately-owned Canadian company which has developed a patent-pending technology for the production of magnesium metal from serpentine mineral. Decades of chrysotile-asbestos mining in Canada have produced tailings of serpentine rock with 25% magnesium metal content, a highly valuable opportunity for metal extraction. This new process has the potential to replace the Chinese pidgeon process, one of the main CO₂ and sulfuric pollution emission source in the world due to its massive utilization of coal. Magnesium is a strategic metal for the Automotive and Aerospace industries to reduce average vehicle weight and increase fuel efficiency as well as reduce significantly greenhouse gas emissions from the automotive and transport industry (Alliance Inc). Alliance Magnesium has secured access to more than 400 Million tons of tailings for its future operations. Its proprietary technology is patent-pending for 20 years protection and is an effective hydrometallurgical and electrolysis clean tech process that could bring a global paradigm shift in magnesium production. At present, the production of metallic magnesium (Mg) is mainly concentrated in China, and from an archaic and polluting process. Quebec society Magnesium Alliance (AM) has developed and patented a revolutionary technology for the production of magnesium from waste arising from the asbestos industry which Canada was one of the leading producers in the world in recent decades. Waste of asbestos industry consist mainly of serpentine ($\text{Mg}_3\text{Si}_2\text{O}_5(\text{OH})_4$) containing 40% magnesium oxide and 50% silica. Serpentine is a kind of hydrated magnesium silicate. Near the towns of Asbestos and Thetford Mines, there are about 800 million tons of tailings stored ready to be

processed. Production magnesium from serpentine generates non-toxic amorphous silica residue (AmSR).

2.2.2.2 Studied Amorphous Silica Residue (AmSR)

There are various amorphous silica residues which are by-product of various industries. Amorphous silica residue (AmSR) in this project is by-product of production of magnesium from serpentine. Serpentine, is a kind of hydrated magnesium silicate ($\text{Mg}_3\text{Si}_2\text{O}_5(\text{OH})_4$). Serpentine contained 40% magnesium oxide and 50% silica. Chemical, mineralogical and physical properties of AmSR are principal reasons affect on mortar and concrete properties. AmSR has high content of amorphous silica and it seems has small particle size. As before explained high content of amorphous silica in SCMs is principal reason of pozzolan properties. Because of its very high amorphous silicon dioxide content, AmSR could be a very reactive pozzolanic material in concrete. As the Portland cement in concrete begins to react chemically, it releases calcium hydroxide. AmSR reacts with this calcium hydroxide to form additional binder material called calcium silicate hydrate (CSH). Also adding fine SCMs brings millions of very small particles to a concrete mixture. They fill in the spaces between cement grains. This phenomenon is frequently referred to as particle packing or micro-filling. Mbadike studied on effect of amorphous silica residue in mechanical properties of concrete. This study showed formation of calcium silicate hydrate when AmSR is used in concrete production. The amorphous characteristic (reactive property) makes AmSR to have a very high pozzolanic property and therefore can be used as partial replacement of cement for concrete manufacturing. Amorphous Silica Residue (AmSR) can be used where high mechanical property in concrete is required (Mbadike et al, 2013). Figure 2-5 shows investigated AmSR.



Figure 2-5: Amorphous silica residue (AmSR) as ASCMs

2.2.3 Waste paper sludge ash (WSA)

2.2.3.1 Residues of pulp and paper industries (Kruger power plant)

The paper and pulp industries produced significant wastes which are classified as commercial waste. Generally as most of wastes, these wastes have environmental problems because in 1979 most of this waste (96%) is dumped in landfill (Glenn et al, 1997). The biomass contained in by-products of pulp and paper industries can be extracted during combustion to generate energy that can be further used as heat or power. These managed biomass resources are considered green because they are renewable and don't affect on global warming. Pulp and paper industries generate three main types of biomass waste which are Sludge, wood and rejects. There is significant difference in their chemical and physical properties (Mathumathi, 2000). There are two forms of sludge that produce in pulp and paper industries, wastewater treatment sludge and de-inking sludge. Wastewater treatment sludge depends on the technology of wastewater treatment used at pulp and paper mill, as mechanical-chemical and biological effluent treatment (Gavrile et al, 2008). De-inking sludge is the sludge that ink removed from it for efficiently recycling. The process of removing ink from sludge is called "De-inking operation". Effects of this process relate to non-recoverable paper fibers, clay fillers and other solid. This process consists of mechanical re-pulping of wastepaper and using of detergent/surfactants to remove ink as well as pigments. Generally de-inked paper sludge has high in cellulose and low in toxic components and normally de-inked sludge from different mills has different composition (Mathumathi, 2000). Wood or bark is most residue of the pulp and paper industry that it hasn't pollution content. Rejects consist of residue from different sources in pulp production process as

waste paper treatment or stock production (Gavrilescu et al, 2008). Biomass fly ash will be study in this project is from Brompton mill of kruger inc which is a de-inking plant. Kruger energy built and commissioned a 23-MW biomass cogeneration plant at the Kruger paper mill in Brompton (Sherbrooke), Québec, in 2007. This power plant is located in Brompton, adjacent of sherbrooke city in the eastern of Quebec. This mill is pulp and paper mill that has a de-inking facility, hydraulic power plant and biomass cogeneration operation. In this mill barks, wood residues and waste water-treatment sludge are burned by in a fluidized-bed combustion (FBC) boiler at temperature about 850° C. Waste water-treatment and de-inking have been generated during paper recycling process. For low grad fuels like such wet sludge the FBC boiler is appropriate process. As a result, a steam turbine from the boiler produces electricity and provides the steam needed to dry the sledges. Generated electricity is sold to Hydro-Québec under a 20-year contract. The combustion of this sludge generates approximately 150 tons of wastepaper sludge ash (WSA) per day. This cogeneration process has environmental and economical benefits. Because this process produces green energy, and by combusting of biomass, Greenhouse gas emissions reduced by 83,000 tons annually, this means removing approximately 18000 vehicles from the roads (Kruger Inc, 2003). In addition, combustion of wastepaper sludge, bark, and residues reduce the landfills (about 600 tons per day). This process causes reduction fossil fuel consumption about 30 million liters annually. Also, reduced risk of leaching contamination due to less landfilled barks and finally during long-term it causes to improving the local air quality. Potential of utilization of dry sludge and waste paper sludge ashes as cementitious materials have been studying. Study of researchers showed WSA as partial replacement of cement decrease concrete performance especially mechanical properties. Figure 2-6 shows investigated WSA as ASCMs.



Figure 2-6: Wastepaper sludge ash (WSA) as ASCMs

a) Chemical composition

The WSA is essentially composed of calcium, silicon and aluminum. The amounts of the other major elements were low (less than 2%), except for MgO (Segui et al, 2012). Most of researchers such Davidenko (Davidenko, 2014) have recently studied the effect of five WSA from a pulp and paper plant near Sherbrooke (Quebec, Canada) on the properties of cement pastes. They observed that principal chemical compositions of these ashes are lime (CaO), silica (SiO₂) and alumina (Al₂O₃). The chemical composition of WSA is important parameters that affect on concrete properties. Some components as free lime, sulfur and loss on ignition have significant affect on concrete properties. Based on Davidenko (Davidenko et al, 2012) the range of SO₃ contents was between 1.9 to 7.1% and loss on ignition (LOI) varied from 4% and 13%. The high value of the LOI in some cases indicates presence of unburned carbon (Davidenko et al, 2012). It's mentioned in ASTM C618 that SO₃ and LOI contents of cementitious materials must be limited to 5% for SO₃ and 6% for LOI. Based on the chemical composition and hydraulic properties of these ashes, the WSA can be classified as class C fly ash if the sum of the oxides SiO₂ + Al₂O₃ + Fe₂O₃ is lower than the 50% recommended by ASTM C 618. The chemical composition of waste paper sludge ashes (WSA) that founded in the literature are shown in Table 2-1. The composition approximately is same but there are some slight differences.

Table 2-1: The chemical composition of waste paper sludge ashes founded in literature

Researchers investigated biomass fly ash (quantity is in %)	CaO	SiO ₂	Al ₂ O ₃	MgO	Fe ₂ O ₃	SO ₃	LOI	Free lime	Metallic Aluminum
(Bai et al., 2003; Mozaffari et al., 2009)	43.5	25.7	18.8	5.1	0.8	1.0	1.2	5.0	-
(Segui et al., 2012)	45.5	28.0	13.2	4.0	1.3	1.3	5.7	5.0	0.2-0.3
(Gluth et al.,2014)	44.1	22.2	11.9	2.4	0.5	3.6	13.3	10.3	-
(Davidenko et al., 2012.)									
WSA 1	45.1	24.9	14.1	1.9	1.6	1.9	6.4	11.6	-
WSA 2	35.2	26.6	14.4	2.4	1.8	3.4	12.6	4.7	-
WSA 3	32.9	29.1	14.5	3.0	2.4	4.6	7.5	3.4	-
WSA 4	44.4	20.2	10.2	2.1	1.9	4.3	13.1	6.9	-
WSA 5	50.6	22.0	13.3	2.6	1.6	7.1	3.7	12.6	-

b) Physical properties

The physical properties of WSA are not the same for different power plants, the origin and type of raw material and combustion condition affect the physical properties. Density, specific surface, particle size distribution and morphology of the WSA are some physical properties. The density of WSA which studied by Segui was 2.85 g/cm^3 and the specific Surface area measured with the Blaine apparatus was $3700 \text{ cm}^2/\text{g}$ (Segui et al, 2012). Bai et al studied on WSA which density was 2.520 g/cm^3 and specific area $4100 \text{ cm}^2/\text{g}$ (Bai et al, 2003). The specific surface area is measured by two apparatus Blaine and BET techniques. Generally the specific surface area measured by BET technique is higher than the measurement by Blaine technique. This significant difference is due to the fact that the BET technique measures the totality of voids in the surface of particles. According to Malhotra, two types of Canadian WSA showed the average particle size (D_{50}) was about 15 and 19 μm (Malhotra et al, 1994). The particle size distribution of the WSA of the Segui study showed that WSA is the mean diameter (D_{50}) 27 μm (Segui et al, 2012). Based on some researcher such Segui et al and Mozaffari WSA particles are porous and heterogeneous (Mozaffari et al, 2009; Segui et al, 2012). Mozaffari observed that the particles of WSA were porous and seemed to be agglomerated. They mentioned that incineration process caused the WSA particles agglomerate. The high porosity of the WSA could lead to problems in fresh concrete properties. Especially for workability of cement-based materials as the water used in these materials would be absorbed by the large open porosity of the ash, therefore, generate a serious decreasing of the workability.

c) Mineralogical properties

Mineralogy is the principal characters for understanding and valorization of WSA as ASCMs. The XRD results which did by some researcher on different WSA shows that there are almost same crystalline phases but there are some difference. The XRD results show crystalline phases, the principal crystalline phases presented in the WSA were quicklime, calcite, quartz, tricalciumaluminates, gypsum, anhydrite and portlandite (Xie, 2009). The XRD results that performed by Davidenko (Davidenko et al, 2012) on five Canadians WSA are shown in Figure 2-7. The crystalline phases presented in theses ashes were lime (CaO), anhydrite (CaSO_4), calcite

(CaCO_3), gehlenite ($\text{Ca}_2\text{Al}_2\text{SiO}_7$), calcium aluminate (C_3A), calcium silicate (C_2S), graphite (C) periclase (MgO), portlandite ($\text{Ca}(\text{OH})_2$), quartz (SiO_2), anorthite ($\text{CaAl}_2\text{Si}_2\text{O}_8$) and yeelimite ($\text{Ca}_4\text{Al}_6(\text{SO}_4)\text{O}_{12}$).

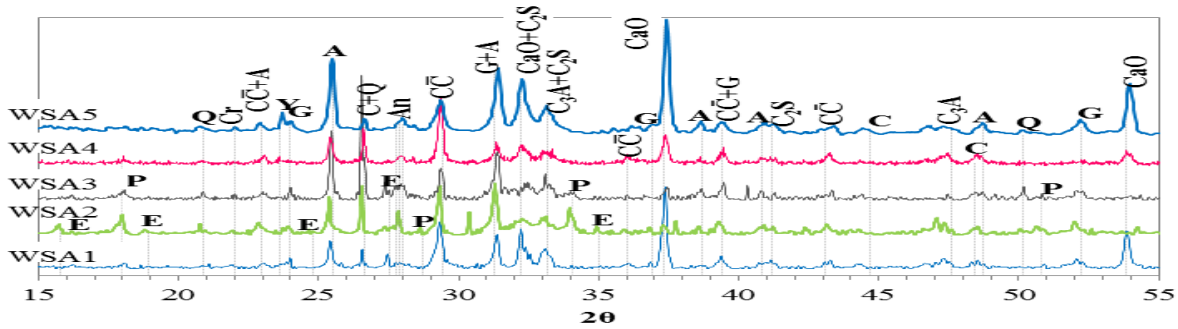


Figure 2-7: XRD results of five WSA samples: Q= Quartz, CaO= Lime, A=Anhydrite, CC=Calcite, C= Graphite, An=Anorthite, C_3A = Calcium aluminate, C_2S =Calcium silicate, Cr= Cristobalite, E=Ettringite, Y= Yeelimite G= Gehlenite, P= Portlandite, (Davidenko et al, 2012)

2.2.3.2 Properties of concrete incorporating WSA

The mortars and concrete properties significantly change when WSA blends partially with cement. The WSA as replacement of cement affect the fresh, mechanical properties and durability of concretes. According to literatures and preliminary results, chemical, mineralogical and physical properties of WSA are principal reasons affect on mortar and concrete properties.

➤ Water demand

Replacement of WSA as cement has significant effect on water demand, workability, air content and setting time of concrete. The fluidity of paste incorporating WSA decreases by increasing time and also with increasing rate of replacement of cement by WSA. Based on Xie study, the WSA paste showed loss of fluidity compare to the control paste. As a result it is emphasized that WSA needs higher water content or more superplasticizer (SP) for acceptable workability when WSA content in the pastes is high quantity (Xie, 2009). Blending WSA as partial replacement of cement increases water demand for the same slump and decrease slump for the same water-to-binder ratio (w/b). Ahmed (Ahmed et al, 2013) studied of concrete involving use of waste paper

sludge ash as partial replacement of cement. They mixed 5, 10, 15 and 20% WSA with cement in concrete. As observed in Figure 2-8, for the same w/b, by increasing the rate of WSA replacement of cement, the slump significantly decreased (Ahmad et al, 2013).

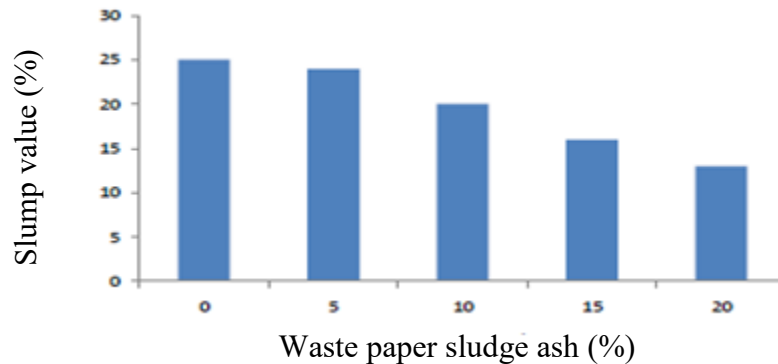


Figure 2-8: Slump of concrete incorporating with WSA, w/b=0.45 (Ahmad et al, 2013)

The WSA particles are very porous, and that could lead to problems of workability and high water demand of cement-based materials containing WSA (Cheah et al, 2011; Segui et al, 2012). In addition, loss on ignition (LOI) that present carbon content in WSA cause absorbed more water and chemical admixtures, such as air entrainer (AE) agents and superplasticizers (SP), resulted the increasing the slump loss, decreasing the air-entraining effect and bleeding (Huang et al, 2013) . Moreover, the presence of free lime in high quantities could explain the principal reason of high water demand (Mozaffari et al, 2009, 2006; Segui et al, 2012).

➤ Setting time

Depends on chemical composition and fineness of WSA, setting time will increase or decrease. Roby showed by increasing WSA content both initial and final setting time increased as shown in Figure 2-9 (Roby, 2011). Sulfur content of WSA could be a reason for increasing setting time. Also somewhere in literature observed rapid setting (Bai et al, 200; Xie, 2009). The hydration mechanism as well as setting time of pastes incorporating WSA appear to be complex and are still being investigated by researchers in the world. Mozaffari reported that when water is added to PC, each particle start hydrating and this continues from the surface of the individual particles and rate of hydration decrease as the layers of reaction products build up. Unlike cement Portland, WSA particles show a wide range of particle size and chemical composition. As a results WSA do not behave in a similar hydration process. Some phases react more rapidly than

others and produce a chemical environment appropriate for other phases to hydrate or possibly contribute to pozzolanic reactions, while some other phases are wholly inert (Bai et al, 2003). According to Wild et al when water adds to WSA two primary phenomena occur. First is dissolution of the free lime available and formation of “slaked” lime, second is dissolution of alumina and silica subsequent to the increase in PH. Hydroxyl ions released from the hydrated lime make the solution alkaline, bredigite begin to hydrate, and subsequently the glassy phases begin dissociating, cause to release more alumina and silica into the system. These phenomenons create an appropriate environment for the calcium ions to bind with Al_2O_3 and SiO_2 in solution to produce more C-S-H gel (Wild et al, 1999). However speed of dissociating of alumina/silica phases; it may be possible to affect the reaction rates and the rate of setting and hardening.

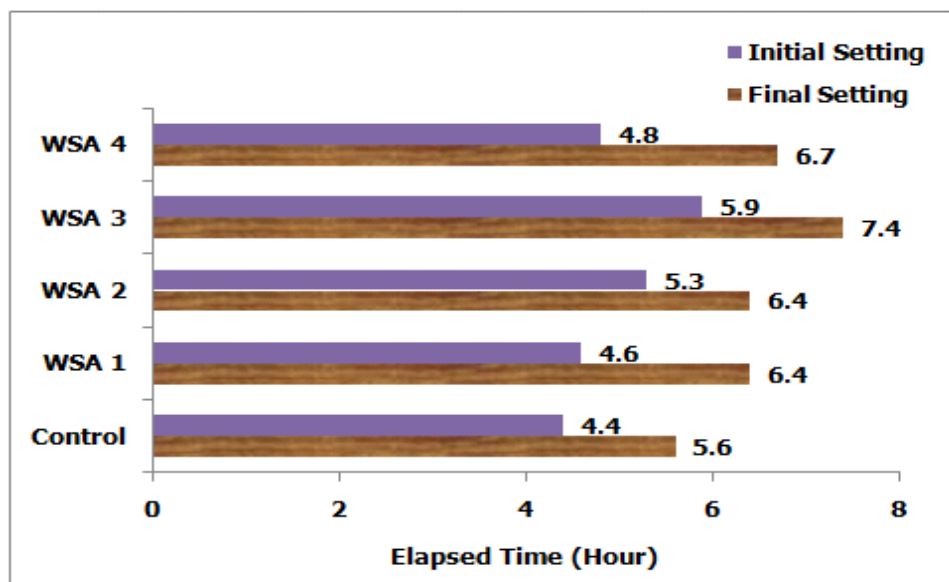


Figure 2-9: Setting times of concrete incorporating 20% WSA, w/b= 0.4 (Roby, 2011)

➤ Hardened properties

The mechanical properties of concrete incorporating WSA significantly affected as well as fresh properties. The results of most of researcher that studied on effect of WSA on mechanical properties have been shown by increasing the rate of replacement of WSA as partial replacement of cement leads to decrease mechanical properties, especially at early age (Yan et al, 2011). As shown in Figure 2-10, compressive strength results of consisted of 20% WSA performed by

Roby in 2011, indicated that compressive strength dramatically reduce by using WSA as partial replacement of cement. Other mechanical properties as tensile and flexural strength are shown same trend of compressive strength (Roby, 2011).

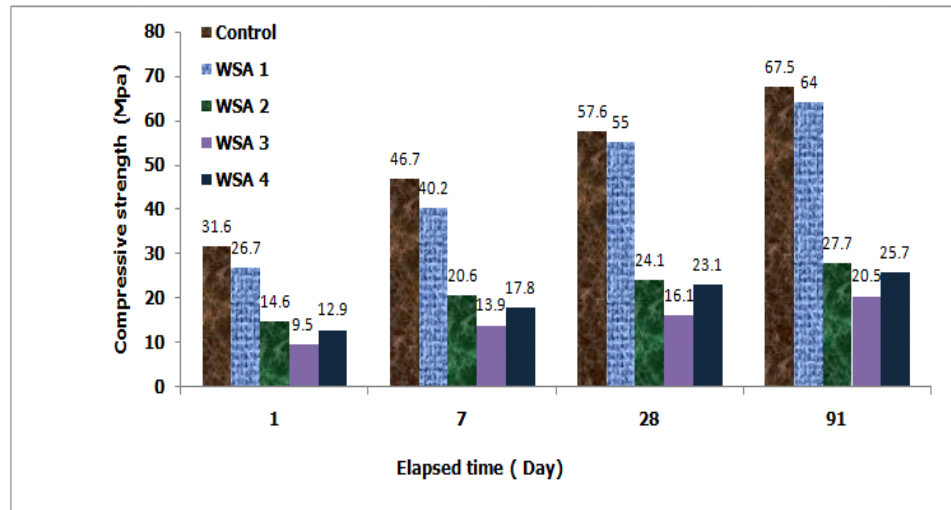


Figure 2-10: Compressive strength of concrete incorporating 20% WSA, w/b=0.40 (Roby, 2011)

As founded in literature survey, generally utilization of WSA reduces the mechanical properties especially compressive strength. Low compressive strength could be related to development of a highly porous paste with a coarse pore structure caused by such unsound matrix, which generate from expansive property of free lime hydration. The main negative aspect is the expansion due to the hydration of CaO to Ca(OH)_2 , which results in unsoundness construction (Bai et al, 2003). Also other chemical composition of WSA such high carbon content and metallic aluminum in WSA and wood ash are reasons of decreasing compressive strength.

3. Experimental program and tests procedures

3.1. Methodology

The experimental program is divided in four different phases:

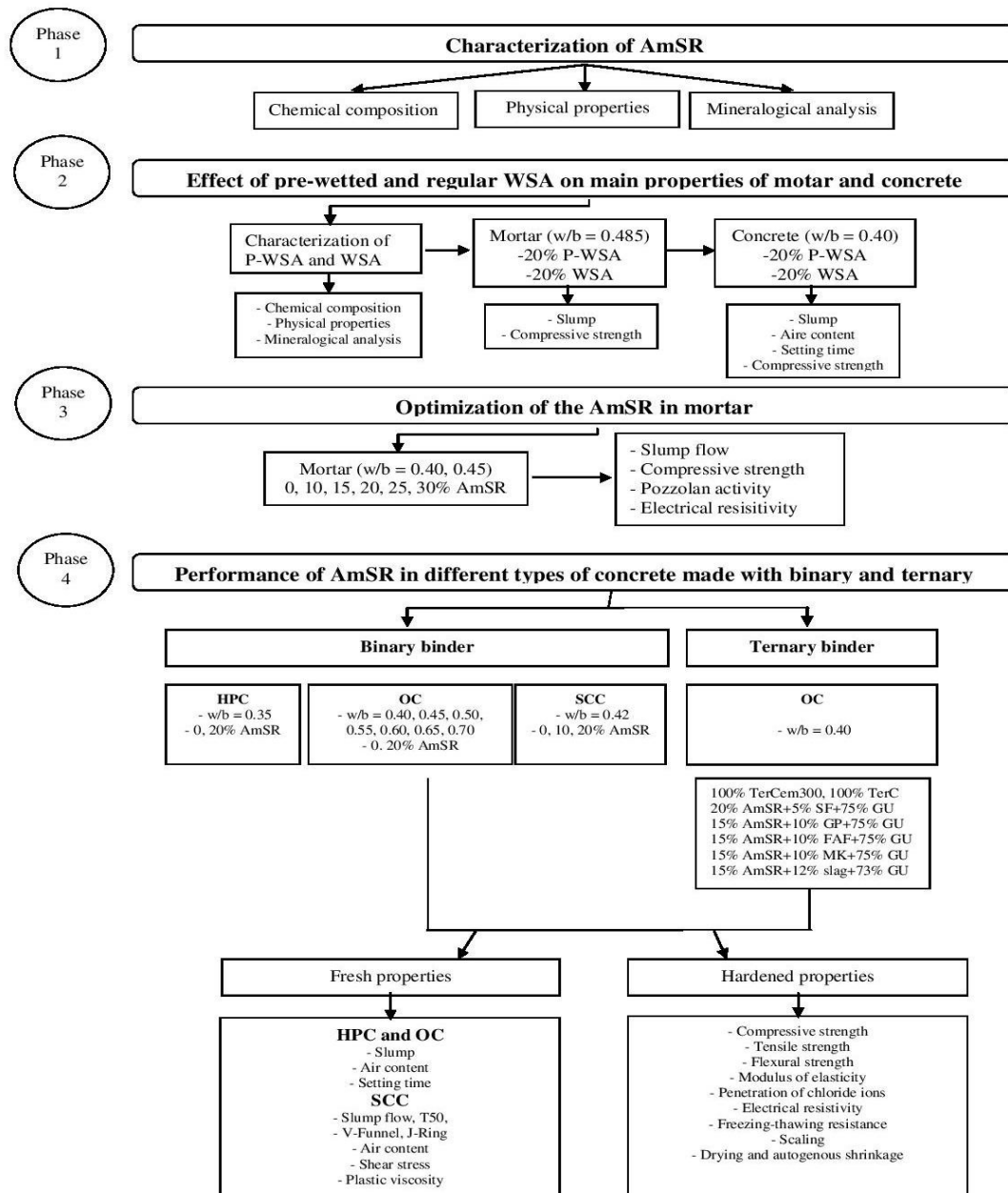


Figure 3-1: Organigram of the experimental phases

3.1.1 Phase 1 - Characterization of AmSR

This phase focuses on characterization of AmSR. The characterization includes chemical composition, mineralogical, and physical properties analysis. The test methods and evaluated characteristic are summarized in Table 3-1.

Table 3-1: Test methods and apparatuses for characterize of materials

Tests methods/ apparatuses	Evaluated characteristics
XRF (X-ray florescence)	Chemical composition
Unburned carbon	LOI (loss on ignition)
XRD (X-ray diffraction)	Mineralogical analysis
Pycnometer	Density
Laser particle size analyzer	Particle-size distribution
Blaine fineness or BET	Specific surface area

3.1.2 Phase 2 - Effect of pre-wetted and regular WSA on main properties of mortar and concrete

For consideration effect of pre-wetted WSA in mortar and concrete properties and comparison of pre-wetted and regular WSA, three steps are followed;

- a) characterization of pre-wetted and regular WSA
- b) performance of mortar incorporating pre-wetted and regular WSA
- c) performance of concrete incorporating pre-wetted and regular WSA

In this phase, first, physical properties, chemical composition and mineralogy of regular WSA are compared with pre-wetted WSA. The test methods and evaluated characteristic are summarized in Table 3-1.

✓ Pre-wetting procedure

- Weighing 5 kg of WSA and Put in a plastic bag,
- Spray water and mixing (Twenty times spraying and turn the bag that is filled by WSA, and spray water again in same quantity and turn the bag again, this process should

continue till all particles get wet and also it depends of water contents for pre-wetting WSA (water content was 50% of mass of WSA),

- Leave the mixed ash with water for 24 hours in plastic bag,
- Dry the pre-wetted WSA in oven at 50 °C,
- Grinding ,
- Sieving grinded of pre-wetted WSA on 1.25 mm sieve,

Thereafter, as presented in Table 3-2, mortar incorporating 20% WSA replacement of cement and 20% pre-wetted WSA is compared with reference mortar. The water-to-binder ratio (w/b) was 0.485. Then fresh properties and mechanical properties of concrete with 20% replacement of cement by pre-wetted and regular WSA are evaluated. The concrete mixtures were designed with 0.40 of w/b. The test on concrete incorporating regular and pre-wetted WSA showed in Table 3-2.

Table 3-2: Tests on mortar and concrete incorporating regular and Pre-wetted WSA

Mortar (w/b = 0.485)	Concrete (w/b = 0.40)
0, 20% WSA, 20% Pre-wetted WSA	
<ul style="list-style-type: none"> ✓ Slump flow ✓ Compressive strength at 1, 7, 28, and 56 days 	<ul style="list-style-type: none"> ✓ Slump ✓ Air content ✓ Setting time ✓ Compressive strength at 1, 7, 28, and 91 days

3.1.3 Phase 3 - Optimization of the AmSR in mortar

In this part, fresh, mechanical, and transport properties of mortar with partial replacement of cement by AmSR are investigated. As shows in Table 3-3, the rates of replacement of cement by AmSR are 0, 10, 15, 20, 25, and 30%. The w/b was 0.485 and 0.40. Finally, the optimum replacement rate of cement by AmSR is proposed to study of different type of concrete incorporating AmSR.

Table 3-3: Tests on mortar incorporating AmSR

Mortar	
w/b = 0.485	w/b = 0.40
0, 10,15, 20, 25, 30% AmSR	
✓ Slump ✓ Compressive strength at 1, 7, 28, 91, and 182 days ✓ Pozzolanic activity index ✓ Electrical resistivity	

3.1.4 Phase 4 - Performance of AmSR in different types of concrete made with binary and ternary system

3.1.4.1 Binary system

In this part, fresh and mechanical properties as well as durability of different types of concrete incorporating 20% AmSR are evaluated. As shown in Table 3-4, ordinary concrete (OC) with different w/b from 0.40 to 0.70, high performance concrete (HPC) with w/b of 0.35, and self-consolidating concrete (SCC) with w/b of 0.42 are done. The details of fresh and hardened tests are shown in Tables 3-5 and 3-6.

Table 3-4: w/b and rate of replacement of AmSR in ordinary and high performance concrete

Binary system						
HPC	Conventional concrete					
w/b = 0.35	w/b = 0.40	w/b = 0.45	w/b = 0.50	w/b = 0.55	w/b = 0.65	w/b = 0.70
0,20% AmSR						

Table3-5: Fresh properties tests for conventional and high performance concrete (HPC)

Tests	Standards
Slump	ASTM C 143
Air content	ASTM C 231
Unit weight	ASTM C 138
Temperature	ASTM C 1064
Setting time	ASTM C 403

Table 3-6: Hardened properties tests for conventional and high performance concrete (HPC)

Tests	Standard	Age
Compressive strength	ASTM C 39	1,7, 28 and 91days
Tensile strength	ASTM C 496	28 and 91days
Splitting Strength	ASTM C 78	28 and 91days
Modulus of elasticity	ASTM C 467	28 and 91days
Penetration of chloride ions	ASTM C 1202	28 and 91days
Electrical resistivity	-	28, 56 and 91days
Resistance of freeze-thaw cycle	ASTM C 666	28 and 91days
Scaling	BNQ 2621-900	28 and 91days
Drying shrinkage	ASTM C 157	-
Autogenous shrinkage	-	-

As shown in Table 3-7, the w/b for self-consolidating concrete (SCC) was 0.42. The rates of replacement of cement by AmSR were 0, 10 and 20%. Rheological properties of SCC are evaluated by ConTec rheometre. The details of fresh and hardened tests in this part are shown in Tables 3-8 and 3-9.

Table 3-7: Self consolidating concrete

Binary system
Self Consolidating Concrete (SCC)
w/b = 0.42
0, 10, 20%

Table 3-8: Fresh properties tests for self consolidating concrete (SCC)

Properties	Test methods	Standards
Deformability	Slump, T_{50}	ASTM C 1611
Passing ability	J-ring	ASTM C 1621
Dynamic stability and viscosity	Time flow, V-funnel	ACI 237
Air content	Air meter	ASTM C 231
Unit weight	Air meter	ASTM C 138
Rheology	Shear stress (τ_0), Plastic viscosity	[Wallevik, 2006]

Table 3-9: Hardened concrete tests for self consolidating concrete (SCC)

Tests	Standard	Age
Compressive strength	ASTM C 39	1,7, 28 and 56 days
Tensile strength	ASTM C 496	28 and 56 days
Flexural Strength	ASTM C 78	28 and 56 days
Modulus of elasticity	ASTM C 467	28 days
Penetration of chloride ions	ASTM C 1202	28 and 56 days
Electrical resistivity	-	28 and 56 days
Resistance of freeze-thaw cycle	ASTM C 666	28 days
Scaling	BNQ 2621-900	28 days
Drying shrinkage	ASTM C 157	-

3.1.4.2 Ternary system

Ternary system is combination of three different binders. Water to binder ratio for ternary concrete was 0.40. In this study ternary combinations are composed of Portland cement, AmSR and third binder is other SCMs as silica fume (SF), ground granulated blast furnace (GGBS), metakaoline (MK), fly ash f (FAF) and glass powder (GP). The results compared with two references concrete, which made with TerCem 3000 and TerC3 cements. The rates of replacement of cement by AmSR and other SCMs are shown in Table 3-10. The details of fresh and hardened tests of ternary concrete are shown in Table 3-11 and Table 3-12.

Table 3-10: Ternary concrete combinations

Ternary system						
w/b = 0.40						
100% TerCem 3000	100% TerC3	20% AmSR+5%SF+75% Portland cement	15% AmSR+10%GP+75% Portland cement	15% AmSR+10%FAF+75% Portland cement	15% AmSR+10%MK+75% Portland cement	15% AmSR+12%Slag+73% Portland cement

Table 3-11: Fresh properties tests for ternary concrete

Tests	Standards
Slump	ASTM C 143
Air content	ASTM C 231
Unit weight	ASTM C 138
Temperature	ASTM C 1064
Setting time	ASTM C 403

Table 3-12: Hardened properties test for ternary concrete

Tests	Standard	Age
Compressive strength	ASTM C 39	1,7, 28 and 91 days
Tensile strength	ASTM C 496	28 and 91days
Splitting Strength	ASTM C 78	28 and 91days
Modulus of elasticity	ASTM C 467	28 and 91days
Penetration of chloride ions	ASTM C 1202	28 and 91days
Electrical resistivity	-	28, 56 and 91days
Resistance of freeze-thaw cycle	ASTM C 666	28 and 91days
Scaling	BNQ 2621-900	28 and 91days
Drying shrinkage	ASTM C 157	-

3.2. Materials

3.2.1 Cement

In this project, three types of cement are used. Portland cement GU. Cement GUb-F / SF (TerC3) composed of 20% fly ash, 5% of silica fume and 75% of GU. Cement GUb-S / SF (Tercem3000) composed of 22% slag, 5% silica fume and 73% of GU. The physical and chemical analysis of three type of cement used are showed in Table 3-13.

Table 3-13: The physical-chemical analysis of three type of cement where used

Cement types were used	GU	Tercem 3000	TerC ³
Chemical composition (%)			
CaO	62.3	53.3	44.3
SiO ₂	20.4	27.2	33.4
Al ₂ O ₃	4.7	5.5	9.0
Fe ₂ O ₃	2.9	2.2	4.5
MgO	1.8	4.6	1.2
SO ₃	3.5	4.0	3.0
Na ₂ O eq.	0.80	0.80	0.85
Physical characteristics			
Density	3.15	3.05	2.98
Finesse Blaine (m ² /kg)	424	459	473
Retained 45 microns (≤24%)	6.0	6.2	10
Loss on Ignition (%)	2.51	-	2.4

3.2.2 Supplementary cementitious materials

The supplementary cementitious materials used in this project are silica fume (SF), fly ash F (FAF), Metakaolin (MK), ground granulate blast furnace slag (GGBS) and glass powder (GP).

3.2.2.1 Physical characteristics

Silica fume (SF) used in this project comes from the factory in Bécancour (Quebec). The Physical and chemical properties of this SF comply with Canadian standard CSA-A3001- 01. The specific surface area is between 18000 and 20 000 m²/kg. A type F Fly ash (FA-F) is used. It comes from the Belledune factory (New Brunswick). The specific surface area of used FA-F is 450 m²/kg. Its properties comply with CSA-3001-03 and ASTM C618 – 03 standards. The specific surface area of used MK is 2140 m²/kg. Ground granulate Blast furnace slag (GGBS) used in this study has 526 m²/kg of specific surface area. Specific surface area of used glass powder is 440 m²/kg. The relative density of SF, FAF, MK, GGBS and glass powder are 2.22, 2.36, 2.51, 2.89 and 2.54 respectively. The physical properties of used SCMs are shown in Table 3-14.

Table 3-14: physical properties of used SCMs

Materials	Density	SSA _(m²/kg)	D ₅₀ (µm)
SF	2.22	18000 - 20000	0.1-0.2
FA (F)	2.36	450	9.2
MK	2.51	2140	3.3
GGBS	2.89	526	8.4
GP	2.54	440	10.9

3.2.2.1 Chemical characteristics

The chemical composition of used Supplementary cementitious materials (SCMs) is shown in Table 3-15.

Table 3-15: Chemical analysis of used SCMs

Chemical composition (%)	SF	FA (F)	MK	GGBS	GP
SiO ₂	93	55.8	55.4	35.1	72.7
CaO	0.6	2.9	7.6	42.0	11.4
Al ₂ O ₃	0.4	20.9	30.1	10.7	1.6
Fe ₂ O ₃	0.8	10.1	1.6	0.4	0.4
MgO	0.6	0.9	0.7	7.9	1.2
SO ₃	0.4	1.4	0.4	1.0	0.1
Na ₂ O	0.2	0.3	0.1	0.2	12.9
K ₂ O	1.2	1.8	1.6	0.3	0.5
Na ₂ O eq.	1.0	1.5	1.2	0.4	13.2
Loss of ignition (LOI)	3.5	1.5	1.4	1.7	0.3

3.2.3 Aggregate

For the evaluating different mortar specimens, Ottawa sand is used which is standard sand according to ASTM C 778 standard. Natural sand used for doing concrete supplied by a local company. Coarse aggregates were crushed aggregate from the quarry St. Dominic. The physical properties of natural sand and coarse aggregates used are summarized in Table 3-16.

Table 3-16: The physical properties of natural sand and coarse aggregates used

Physical properties	Natural sand (0-5mm)	Aggregate (5-14 mm)	Aggregate (20 mm)
Density (SSD)	2.66	2.74	2.73
Absorption	0.99	0.64	0.49

3.2.4 Chemical admixture

a) Superplasticizer (SP)

Superplasticizers used in this project are plastol 5000, 6200, 6400, and Eucon 37. These types of SP are based high range water-reducing admixture, which enables concrete to produce with very low w/b. They have not contained chlorides, and will not promote corrosion in steel. In addition, they are compatible with air-entraining agents and many other admixtures. The relative density

for plastol 5000 is 1.07 and its solid content is 30.7%. The relative density of plastol 6400 is 1.08 and its solid content is 40%. The relative density of plastol 6200 is 1.085 and its solid content is 34%. The relative density of Ecoun 37 is 1.2. The properties of all superplasticizers complied with the requirements of ASTM C 494.

b) Water reducing agent (WRA)

Water reducer agent in this project was EuCon DX. EuCon DX provides a reduction of 5 to 10% of the total water in the mix depending on the quantity and characteristics of the cementitious material. It is an aqueous solution of hydroxy-carboxylic acids and a catalyst which provides a better hydration of the cementitious material. Relative density is 1.14 and solid content is 28.5%. EuCon DX complies with requirement of ASTM C 494.

c) Air-entrainer agent(AEA)

AireX-L is used as air entraining agent. It is a liquid solution of hydrocarbons used as an air entraining agent for concrete and complies with ASTM C260. When AireX-L is added to the concrete mix, it produces a system of microscopic air bubbles that remains very stable in the concrete. The entrainment of air with AireX-L improves ease of placement, workability and durability of the concrete while minimizing bleeding and segregation. Relative density of AireX-L is 1.007 and solid content is 5%.

3.3. Mixing procedures

3.3.1 Mortar mixing

According to ASTM C 305, the mortars are prepared in the Hobart mixer as following sequence: Place the dry paddle and the dry bowl in the mixing position in the mixer. Then introduce the materials for a batch into the bowl and mix in the following manner:

- Place all the mixing water in the bowl
- Add the cementitious materials and SPs to the water; then start the mixer and mix at the slow speed (140 ± 5 r/min) for 30 seconds
- Add the entire quantity of sand slowly over a 30 seconds period, while mixing at slow speed
- Stop the mixer, change to medium speed (285 ± 10 r/min), and mix for 30 seconds

- Stop the mixer and let the mortar stand for 90 seconds. During the first 15 seconds of this interval, quickly scrape down into the batch any mortar that may have collected on the side of the bowl; then for the remainder of this interval, close the mixer enclosure or cover the bowl with the lid
- Finish by mixing for 60 seconds at medium speed (285 ± 10 r/min).

3.3.2 Concrete mixing

All mixtures of concrete were made in a concrete mixer with vertical axis of rotation Monarch with a capacity of 110 L. All concrete are mixed in the same manner according to the following sequences:

- Introduction of all the sand into the mixer and mixing for 30 seconds
- Correcting sand according to its moisture content
- Introduction of coarse aggregates, mixing for 45 seconds to ensure good homogeneity between the aggregates
- Introduction half of water with air-entrainer agents and mixing another 45 seconds
- Reset the chronometer and stop mixer
- Introduction cementitious materials and mixing for 30 seconds,
- At $T = 30$, introduction the rest of water with superplasticizer and water reducing agent and mixing until 3 minutes
- At $T = 3$ minutes, break for 3 minutes
- At $T = 6$ minutes, mixing for 2 minutes
- At $T = 8$ minutes, starts fresh properties tests

3.4. Description of test methods

3.4.1 Characteristic tests of materials

3.4.1.1 Chemical analysis

a) X-ray fluorescence spectrometer (XRF)

The chemical analysis for WSA and AmSR is done by X-ray fluorescence spectrometer (XRF). X-ray Fluorescence spectrometry (XRF) determines chemical composition of given sample with characteristic analysis of X-ray emission lines. The analysis of major and trace elements in materials by x-ray fluorescence is made possible by the behavior of atoms when they interact with radiation. When materials are excited with high-energy, short wavelength radiation (X-rays), they can become ionized. The atom becomes unstable and an outer electron replaces the missing inner electron. When this happens, energy is released due to the decreased binding energy of the inner electron orbital compared with an outer one. The emitted radiation is of lower energy than the primary incident X-rays and is termed fluorescent radiation. Because the energy of the emitted photon is characteristic of a transition between specific electron orbital in a particular element, the resulting fluorescent X-rays can be used to detect the abundances of elements that are present in the sample. The results are present in the form of major oxides.

b) Free lime content

The free lime content of the WSA was determined by the lime extraction with ethylene glycol and subsequent titration of the slurry with hydrochloric acid (Javellana and JAWED, 1982). This test consists in heating the ethylene glycol at a temperature of 80-100 ° C and mix for 5 minutes with 1g of the analyzed sample then filtered and titrated with HCl 0,1005N.

3.4.1.2 Physical analysis

a) Density (specific gravity)

Relative density measured by helium pycnometer complies with ASTM C118. Helium pycnometre determine the volume of a powder (V_s) which it's mass (M) is known. This measurement is based on some method of gas displacement and the volume (pressure relationship known as Boyle's Law. The density is defined as the mass of a unit volume of given powder ($\rho = M/V_s$).

b) specific surface area

- Blaine

The specific surface area is a property of solids defined as the total surface area of a material per unit of mass (m^2/kg). Blaine test is a method for measuring the specific surface of the powder by the air permeability. This method is based on the fact that the time taken by a given volume of air to pass through a given volume of the compacted powder under the given pressure is a function of the specific surface of the powder. The Blaine specific surface area was determined according to ASTM C 204.

- Brunauer-Emmett-Teller (BET)

BET method determines the specific surface area of the sample as well as distribution of its pores according to their size by physical adsorption of gas molecules on surface sample. This technique involves measuring amount of condensed nitrogen in liquid state on given sample particles by forming a thin layer which covers entire particle surface. The value of BET method is significantly higher than Blaine method.

c) Particle size distribution

The particle size distribution is determined with laser granulometer. Laser granulometry is a technique for analyzing the distribution of the particles based on light diffraction. The particle size distribution is derived from the interaction between a set of particles and the incident laser beam by analyzing the diffraction of beam spot.

3.4.1.3 Mineral analysis (The X-ray diffraction (XRD))

The qualitative and semi-quantitative analysis of crystalline phases of cementitious materials characterize by X-ray diffraction (XRD) analysis. Quantitative determination can be carried out using some methods based on the comparison of the intensities of individual peaks (using an internal standard) or adjusting the entire spectrum (Rietveld). During this project, the XRD was used for identification of crystalline phases in WSA and AmSR. XRD works based on Bragg's law:

$$n\lambda = 2d \sin\theta$$

n is an integer called the order of reflection, λ is x-ray wavelength, d is the characteristic space between the crystal planes and θ is the angle between the incident beam and normal reflected lattice plane. By measuring the angles (θ) and consequently distanced between the lattice planes of each crystallographic phase can be determined. These data are compared with those reference files containing inter-planar spacing and the normalized intensity of the experimental peaks for each mineral which are available in a database. The interpretation of diagrams was performed using the JADE software and a database.

3.4.1.4 Morphology (Scanning electron microscope)

Scanning electron microscope analysis (SEM) is a technique used for the production of images of the surface of a sample based on the principle of electron-matter interactions. The images are produced from a scan of the sample surface by primary electrons (PE). At any point of scanned surface, each electron scattered from sample under the impact of the probe can be received by the respective detector. Scattered electrons are secondary electrons (SE), backscattered electrons (BSE) or X-ray photons. The images by secondary electrons (SE) have been used to describe the morphology of the samples. Elemental analysis is performed by using X-rays which called energy dispersive spectroscopy (EDS). EDS analyzes excited primary X-rays when atoms undergoing the interaction with the electrons of SEM electronic probe. Figure 3-2 shows the principal of SEM

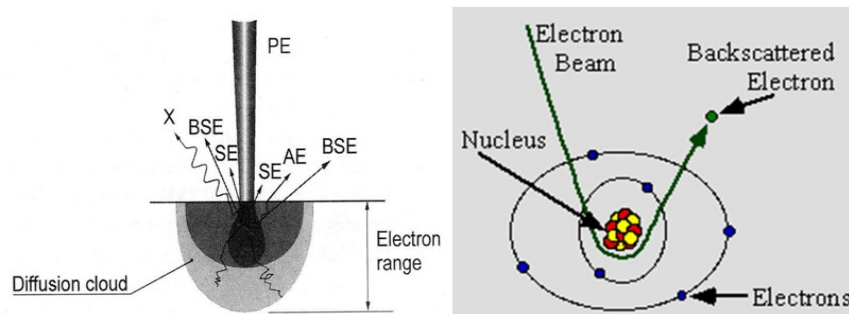


Figure 3-2: Principal of SEM

3.4.2 Test method for Mortar

Mortar mixtures are carried on according to ASTM C 109 and C 305 specifications. As long as the mortar is made, the slump flow will be measured according to the specification ASTM C 1437. The mortar is placed in cubes shape moulds with 50x50x50 (mm) dimension size. The cubes are de-molded after 24 hours for determination of compressive strength based ASTM C 109 specification. In addition, the strength activity index (SAI) is determined according to ASTM C 311 specification. SAI is relative strength between the WSA, AmSR mortars and control cube at the same period.

$$\text{SAI} = (\text{Strength of mortar containing tested material}) / (\text{Strength of the control mortar}) \times 100$$

3.4.3 Test method for concrete

3.4.3.1 Fresh properties

a) Slump

The measurement of slump gives us an indication of the workability of concrete. This measurement is done according to ASTM C 143 specification. The test is carried out by using a mould known as a slump cone or Abrams cone. The cone is placed on a hard non-absorbent surface. This cone is filled with fresh concrete in three stages. Each time, each layer is tamped 25 times with a rod of standard dimensions. At the end of the third stage, the mould is carefully lifted vertically upwards with twisting motion. Then the slump is defined by the vertical difference between the top of cone and the displaced original centre of the top surface of the specimen. Different types of slump shape are shown in Figure 3-3.

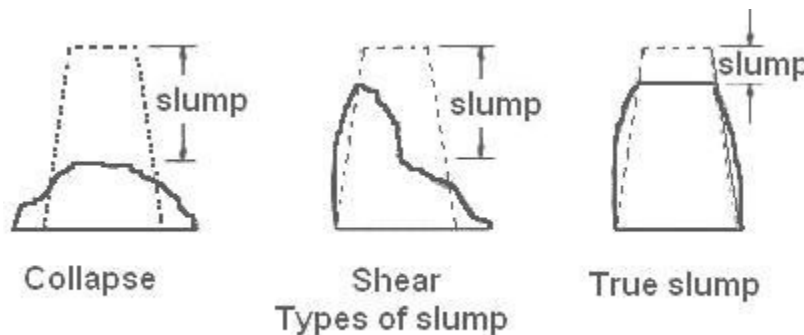


Figure 3-3: Types of slump shape (Concrete Society 2010)

b) Air content and density

Air content and density of the fresh concrete are determined according to ASTM C 231 and ASTM C 138 respectively. For measuring density of fresh concrete a container of 7.04 L for filling of samples is needed. The density is expressed in kilograms per cubic meter. Determination of air content of fresh concrete is based on Boyle's law, which relates pressure to volume.

c) Setting time

The setting time of concrete by the penetration resistance made at regular time intervals on mortar sieved from the fresh concrete by passing a 5 mm sieve. According to ASTM C 403 the initial and final setting time are defined as the time when the penetration resistance equals 500 and 4000 psi, respectively.

d) Slump flow

The measurement of slump flow gives us an indication of the deformability of self consolidating concrete (SCC). Slump flow is done in accordance with ASTM C 1611 by Abrams cone. This cone is placed on a clean and humidified base plate with sufficient dimensions. Then cone is filled with SCC. Thereafter cone is carefully raised. Therefore concrete spreads under its own power (without moving the base plate). Average diameter of circular shape concrete is value of slump flow ($\frac{d_1 + d_2}{2}$). The high slump flow value shows great ability to fill formwork or molds. In this project the range of slump flow is 660 ± 30 mm.

e) T_{50}

Measurement of T_{50} provides an indication of the relative viscosity of concrete and its free flow. T_{50} is flow time of concrete to receive 500 mm in diameter.

f) Visual stability index (VSI)

The Visual Stability Index (VSI) is a visual observation for determining the segregation stability of SCC. The VSI is determined through visually rating apparent stability of the slump flow patty based on specific visual properties of the spread. The SCC mixture is considered stable for the intended use when the VSI rating is 0 or 1, and a VSI rating of 2 or 3 gives an indication of segregation potential. According ASTM C 1611 Visual Stability Index Values criteria are as follow:

0 = highly stable, no evidence of segregation or bleeding, 1 = stable, no evidence of segregation and slight bleeding observed as a sheen on the concrete mass, 2 = unstable, a slight mortar halo, 10 mm and/or aggregate pile in the center of the concrete mass, 3 = highly unstable, clearly segregating by evidence of a large mortar halo > 10 mm, and/or a large aggregate pile in the center of the concrete mass.

g) J-ring

J-ring characterizes passing ability of SCC according to ASTM C 1621. This test evaluates the passage of concrete through the ring with reinforcing bars. J-ring is measuring the slump flow diameter of SCC through a central ring of 300 mm in diameter. The distance of each reinforcing bar with adjacent bar is 35 mm. According to ASTM C 1621, SCC has good passing ability if the difference between the slumps flow and the J-ring values is between 0 and 50 mm.

h) V-funnel

The V-funnel flow time is the period that defined volume of SCC needs to pass a narrow opening and gives an indication of the filling ability of SCC provided that blocking and/or segregation do not take place; the flow time of the V-funnel test is to some degree related to the plastic viscosity. The V-funnel is filled with 10 L of concrete and then closing flap is opened and measuring the time it takes for the concrete to flow fully from the funnel. A very fluid and homogeneous concrete will have a very short flow times. If concrete is fluid and unstable, the flow time will be slow with blocking aggregates at the bottom of the funnel. Figure 3-4 shows the dimension of V-Funnel.

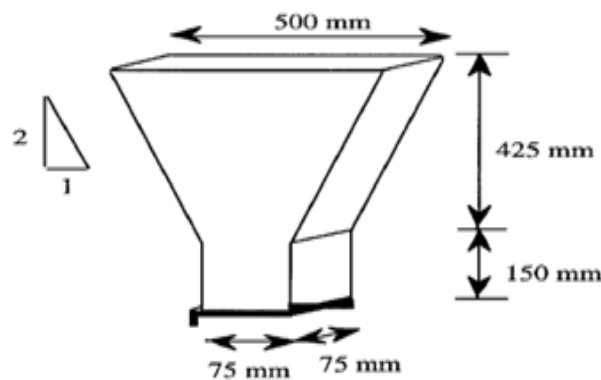


Figure 3-4: Schema of V-Funnel (Khayat, 1999)

i) ConTec 5 (rheometre)

Yield stress and plastic viscosity are two important rheological factors for SCC. To characterize rheological parameters of SCC, the rotational cylinder coaxial ConTec 5 is used. This rheometer consists of outer cylinder and inner blade cylindrical. Outer cylinder rotates and the inner cylindrical blade is fixed. The rotation speed increases from 0.025 to 0.5 rps in 10 points, in each point there are 50 resistance time measures. The data obtained are flow resistance (G) and viscosity factor (H). G represents the force required to initiate movement of the concrete and H represents the resistance of the concrete during the increase in speed of rotation. The yield stress and plastic viscosity are calculated from G and H respectively using the equation of Reiner-Riwlin (Feys et al, 2007).

3.4.3.2 Mechanical properties

a) Compressive strength

The compressive strength is measured by axial compression of cylinders 100x200 mm in accordance with ASTM C 39. After capping the samples, they are subjected to a load by rate of 120 KN/minutes until failure. Each time, two or three cylinders are measured and the compressive strength is obtained by the average value.

b) Splitting tensile strength

The tensile strength test includes crushing concrete cylinders in its axis horizontal between the plates of a press. The cylinder of 100x200 mm is prepared in accordance with ASTM C 496. The sample is putted with its axis horizontal between the plates of press apparatus, and the load is increased by rate of 1200 lb/ 10 seconds until failure takes place. The splitting tensile strength is calculated by the following equation:

$$F_{sp} = \frac{2P}{\pi DL}$$

P is maximum load during test (N), D is cylinder diameter (mm) and L is cylinder length (mm).

c) Flexural strength

Flexural strength is carried out in accordance with ASTM C 78 specification. A prismatic beam of 100 x100x400 mm is sampled. The prismatic beam is loaded at the third points along the span until the failure of sample in the middle. Flexural strength is determined by following equation:

$$F_s = \frac{PL}{bd^2}$$

P is maximum applied load indicated by the testing apparatus (N), L = 400 mm, b and d are width and depth of sample (mm) at the fracture

d) Modulus of elasticity

The modulus of elasticity of concrete cylinder 100x200 mm is determined in accordance with ASTM C 469 specification. The sample is subjected three loading cycles up to 40% of the compressive strength of concrete. Modulus of elasticity is the stress/deformation ratio of concrete in the elastic range of the stress-strain diagram. The modulus of elasticity (E) is calculated according to the following equation: $E = \frac{\sigma_2 - \sigma_1}{\varepsilon_2 - \varepsilon_1}$

E is modulus of elasticity (GPa), σ_2 is stress equivalent to 40% of the ultimate load (MPa), σ_1 is equivalent stress to the longitudinal strain ε_1 (MPa), ε_2 is longitudinal deformation caused by σ_2 and ε_1 is equal to 50 μ .

3.4.3.3 Durability

a) Chloride-ions penetrations

The penetration of chloride ions is carried out according to ASTM C 1202 specification. This test evaluates the pore inter-connectivity in concrete matrix. The tests specimens have diameter of 95 mm and 50 mm thick. These samples are extracted from a cylinder of 100x200 mm. The specimen is placed in a cell such that one of the circular faces immersed in a solution of 3% sodium chloride (NaCl) in where an electrode Cathode is located. The other circular face is immersed in a sodium hydroxide solution (0.3N of NaOH) where electrode anode. A potential

difference of 60 volts is maintained between the two ends of the specimen. The test consists of measuring the total electric charge in Coulombs that passes through the sample for 6 hours. The charge measured expresses the penetration of chloride ions across the sample. Different classes of penetration of chloride ions are shown in Table 3-17.

Table 3-17: Different classes of penetration of chloride ions (Whiting 1988)

Load (Coulombs)	penetration class	Type concrete corresponding estimated
load ≥ 4000	High	Concrete with W/C > 0.60
$2000 \leq \text{load} \leq 4000$	Moderate	Concrete with $0.40 < \text{W/C} < 0.60$
$1000 \leq \text{load} \leq 2000$	Low	concrete with W/C < 0.40
$100 \leq \text{load} \leq 1,000$	Very Low	Concrete Latex
load ≤ 100	Negligible	Polymer concrete

b) Electrical resistivity

The electrical resistivity can provide additional information about the quality of concrete matrix. The electrical resistivity of concrete is a physical quantity that is regularly considered as a durability indicator. It actually depends on the intrinsic characteristics of porous matrix (Archie, 1942). The principle of the measurement consists of injecting a current in the material and measuring the difference potential. Two electrodes are placed on the two parallel sides of the specimen and a voltage is applied followed by measuring the difference potential. The resistivity is calculated using Ohm's law:

$$\rho = \frac{VA}{IL}$$

Where ρ is the electrical resistivity, V is the potential difference across the test specimen, A and L are respectively the section and length of the sample and I is the intensity in the circuit. Durability classes with the indicative limit of the electrical resistivity are shown in Table 3-18.

Table 3-18: Durability classes with the indicative limit of the electrical resistivity (AFGC, 2004)

Electrical resistivity, $k\Omega \cdot \text{cm}$	potential Durability classes
< 5.0	Very low
5.0 – 10.0	Low
10.0 – 25.0	Moderate
25.0 – 100.0	High
> 100.0	Very High

c) Resistance of freeze-thaw cycle

Prisms of 75x75x350 mm are made for each concrete mix according to ASTM C 666 specifications. The freeze-thaw cycles begin at 14th day of maturing with 6 cycles per day under variable temperature of -18°C to + 4°C. The specimens are subjected by 300 freeze-thaw cycles. The measures are the relative elongation, the loss of mass and the speed of propagation of an ultrasonic wave.

d) De-icing scaling

De-icing scaling test is carried out on concrete slabs of 250x200x75 mm subjected to freezing and thawing in the presence of de-icing salt (3% NaCl, sodium chloride). De-icing scaling test is performed according to BNQ (2621-900) specification. Concrete slabs specimens are first matured in the moist chamber until 14 days. Then they are put in a room with 50% relative humidity and 23 ° C temperature. At 21 days, slabs concrete are framed and sealed to form an impermeable basin. At 28 days specimens are covered with 10 mm of saline solution containing 3% NaCl and maintained for 7 days. At 35th day, the freeze-thaw cycles begin for a total of 56 cycles. 16 ± 1 hours freezing at -18°C then 8 ± 1 h thaw at 23°C for each cycle. Measuring scaling consists of rinsing the plate surface with pure water. Scaling are collected on a sieve of 80 microns then washed and dried, thereafter weighed. This measurement is done in 7, 21, 35 and 56 cycles. The result is expressed as remain mass (g) by the area (m²). The surface of the slabs was visually evaluated at the end of each measurement. Table 3-19 provides the qualitative criterion to characterize the type of scaling.

Table 3-19: The visual observation criterion of scaling (BNQ 2621-900)

Rating	Condition of surface
0	No significant scaling observed
1-A	Very slight scaling of mortar on the surface (without the craters)
1-B	Substantial scaling of mortar on the surface (without the craters)
2-A	No significant scaling of mortar on the surface (with a few craters)
2-B	No significant scaling of mortar on the surface (with lots of craters)
3	Severely scaling of mortar over entire surface with coarse aggregate torn
4	Gravely coarse aggregate torn with scaling of mortar on the surface

e) Drying shrinkage

Drying shrinkage test consists of measuring the length change of the concrete prisms of 75x75x285 mm according to ASTM C 157. This test allows evaluating the potential for expansion or volumetric shrinkage of the concrete. The first measurement is made just after de-molding then concrete prism maintained in lime water saturated during 28 days. Thereafter, measuring the length change was continued in a room at $50 \pm 4\%$ relative humidity and 23 ± 2 °C temperatures until 64 weeks.

f) Autogenous shrinkage

Autogenous shrinkage test is carried out with an embedded vibrating wire strain gage in concrete specimens. This test is measured on prisms of 100x100x400 mm. measuring of autogenous shrinkage test starts after initial setting of concrete. Thermal variation and deformation of concrete measured with vibrating strain gage. The results recorded automatically by data acquisition system. The prisms are sealed immediately after de-molding at 24 hours and kept in a condition of 23 ± 2 °C until the end of testing.

4. Results and discussions

4.1. Phase 1 - Characterization of Physical and chemical composition of AmSR

The chemical composition of AmSR is shown in Table 4-1. As can be observed AmSR has 59.3% SiO₂, 15.8% MgO, and 1.48% Al₂O₃ contents. The calcium oxide CaO content of AmSR is 0.52%. The content of silicon which composed the reactive part of pozzolanic materials was same or more than the other classical mineral admixtures.

Table 4-1: The chemical composition of AmSR

Materials	Oxides (%)												
	CaO	SiO ₂	Al ₂ O ₃	MgO	Fe ₂ O ₃	K ₂ O	Ti ₂ O	P ₂ O ₅	NaO ₂	MnO	SO ₃	LOI	Na ₂ eq
AmSR	0.52	59.33	1.48	15.82	3.21	0.15	0.03	0.01	0.04	0.05	0.01	4.80	0.13
GU	62.39	20.43	4.70	1.81	2.97	0.95	-	-	0.18	-	3.53	2.51	0.80

Physical properties of AmSR are shown in Table 4-2. The fineness Blaine of AmSR was around 10 times more than Portland cement GU. The particle size and density of AmSR are smaller than Portland cement GU. The particle size distribution of AmSR is shown in Figure 4-1.

Table 4-2: The physical properties of AmSR

Materials	Physical properties			
	Density	Average diameter D ₅₀ (μm)	Fineness Blaine (m ² /kg)	Fineness BET (m ² /kg)
Portland cement GU	3.15	16.2	424	-
AmSR	2.45	8.4	4907	9775

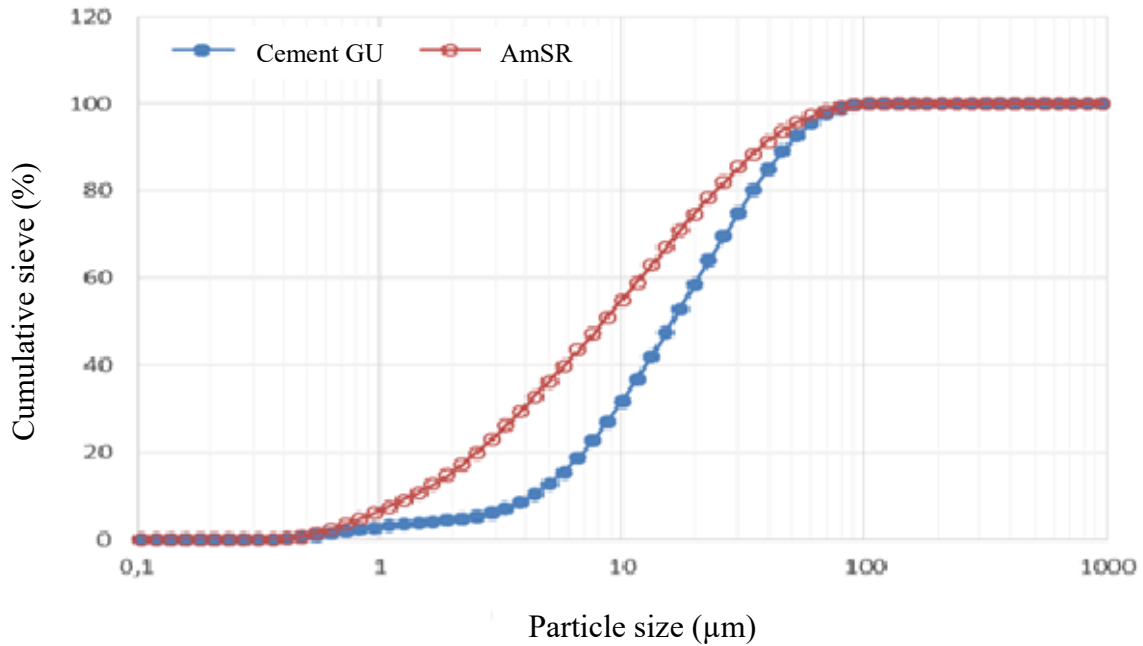


Figure 4-1: Particle size distribution of AmSR and Portland cement GU

Figure 4-2 shows result of XRD analysis of AmSR. Because the SiO_2 content in AmSR was amorphous, the peaks of SiO_2 were not detected.

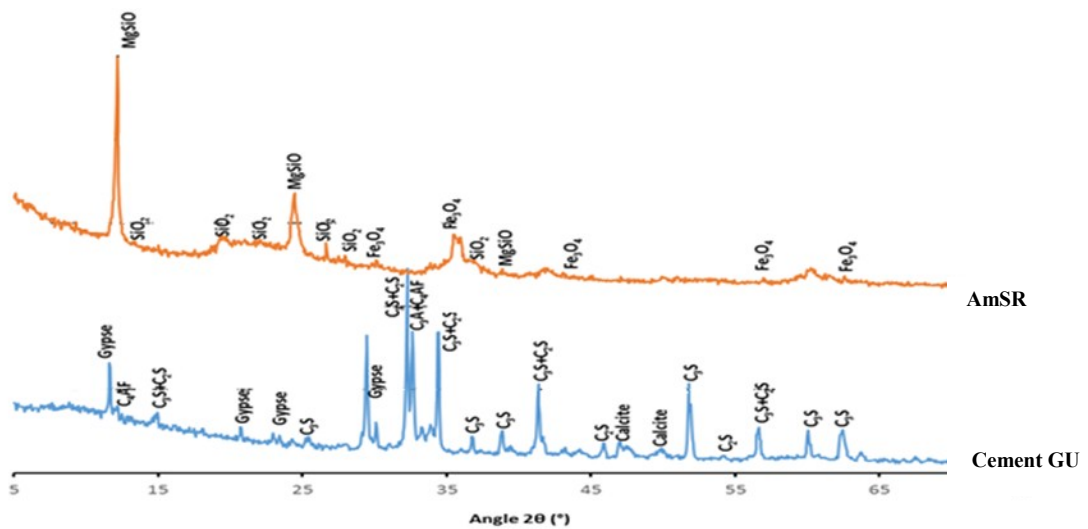


Figure 4-2: The XRD analysis of the AmSR

4.2. Phase 2 - Effect of pre-wetted and regular WSA on main properties of mortar and concrete

4.2.1 Characterization of pre-wetted and regular WSA

The chemical compositions of pre-wetted and regular WSA are shown in Table 4-3. The free lime of regular and pre-wetted WSA is 3.02 and 1.51 respectively.

Table 4-3: The chemical compositions of pre-wetted and regular WSA

Materials	Oxides (%)													
	CaO	SiO ₂	Al ₂ O ₃	MgO	Fe ₂ O ₃	K ₂ O	TiO ₂	P ₂ O ₅	Na ₂ O	MnO	SO ₃	Na ₂ eq	LOI	Free lime
WSA	42.0	22.21	12.26	2.40	3.62	0.77	1.85	1.74	0.587	0.1	7.8	1.09	8	3.02
Pre-wetted WSA	40.3	23.96	12.42	2.41	3.24	0.97	1.76	1.54	0.566	0.1	8.1	1.2	12	1.51

- Na₂O equivalent: 0.658K₂O+Na₂O

As seen in Figure 4-3, the particle size of pre-wetted WSA was larger than particle size of regular WSA and cement GU. The average diameter (D₅₀) for portland cement GU was 15.14 µm, for regular WSA was 47.6 µm, and for pre-wetted WSA was 89.41 µm.

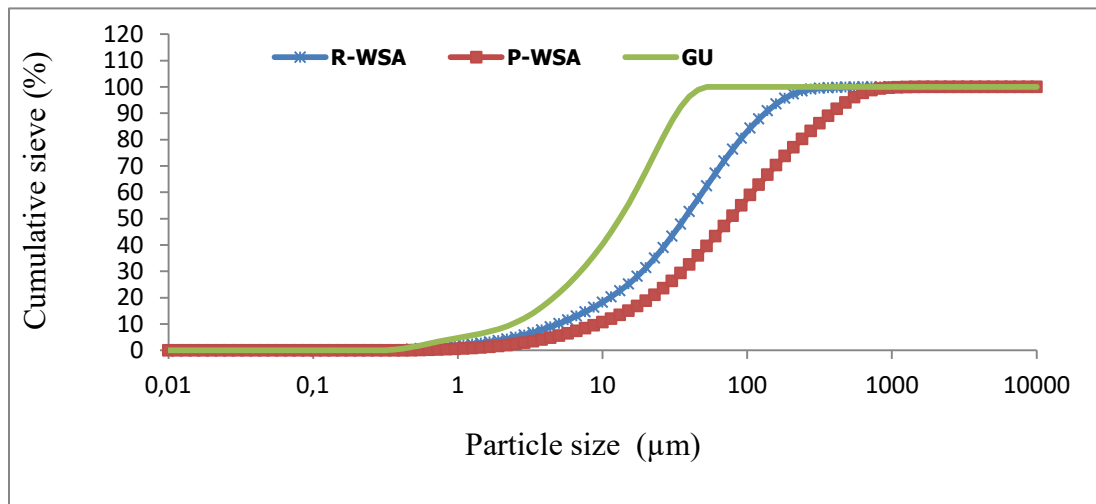


Figure 4-3: Particle size distribution of pre-wetted and regular WSA

The density, average diameter D_{50} and finenesses Blaine of pre-wetted WSA, regular WSA and Portland cement GU are shown in Table 4-4.

Table 4-4: Physical properties of pre-wetted and regular WSA

Materials	Physical properties		
	Density	Average diameter D_{50} (μm)	Fineness Blaine (m^2/kg)
Portland cement GU	3.15	16.2	424
WSA	2.72	47.6	-
Pre-wetted WSA	2.6	89.41	360

X-ray diffraction result of Pre-wetted and regular WSA is shown in Figure 4-4. As seen in XRD result by pre-wetting WSA, lime, meyenite and anorthite consumed in regular WSA, consequently ettringite is produced in pre-wetted WSA.

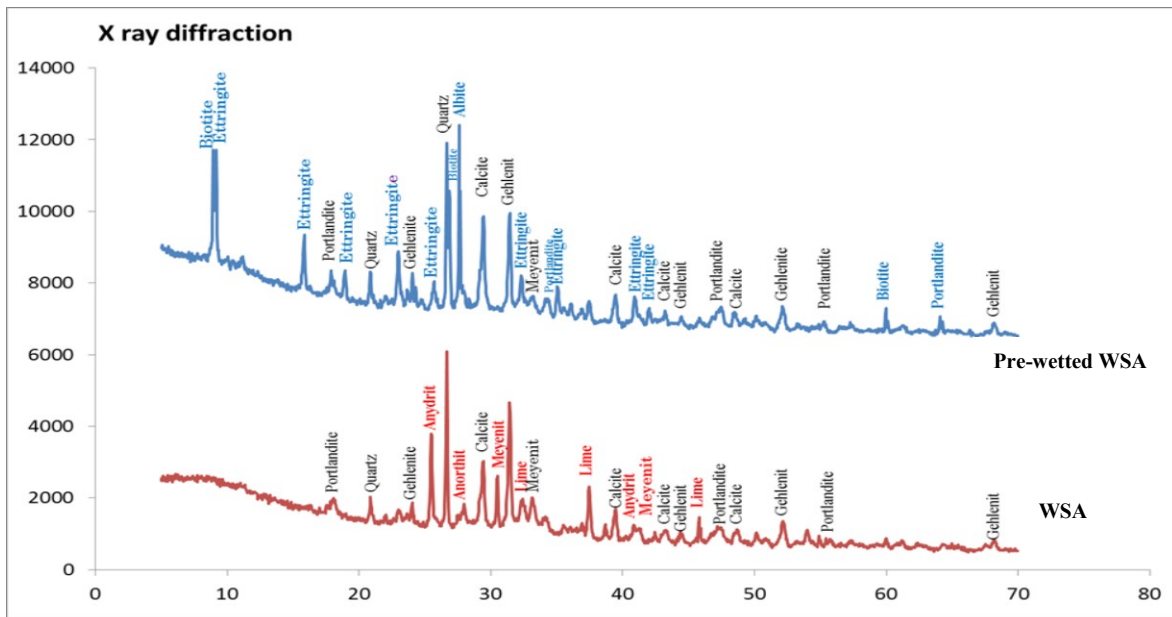


Figure 4-4: X-ray diffraction analysis of pre-wetted and regular WSA

Based on XRD results and literature survey, lime convert to portlandite, and partially react with meyenite to create carboaluminate and carboaluminates reacts with anydrite to create Ettringite (Segui et al, 2012).

4.2.2 Mortar incorporating regular and pre-wetted WSA

Mortars mixtures are made according to standard test method for compressive strength of hydraulic cement mortars (ASTM C 109). Three mortar mixtures are done. Control mix and two mortars incorporating pre-wetted and regular WSA. Rate of replacement of cement by regular and pre-wetted WSA was 20% and w/b was 0.485. The composition and fresh properties of mortar incorporating pre-wetted and regular WSA are shown in Table 4-5.

Table 4-5: Composition and fresh properties of mortars

w/b = 0.485				
Sand-to-binder ratio (s/b) = 2.75				
Ingredients	Unit	Control	WSA	pre-wetted WSA
Portland cement GU	g	1000	800	800
WSA		0	200	0
Pre-wetted WSA		0	0	200
Water		485	485	485
Sand		2750	2750	2750
Sp plastol 6200	% of binder	0	0.27	0.335
Temperature	°C	24.1	23.5	24.0
Slump flow	mm	200	205	200

- **Compressive strength**

The effect of regular and pre-wetted WSA on compressive strength of mortar is presented in Figure 4-6. The strength values were taken as the average of three cubes for each measurement. As seen in Figure 4-5, compressive strength of mortar incorporating 20% regular WSA is significantly less than control. Pre-wetted WSA improved about 13% of mortar compressive strength rather than regular WSA mortar in 56 days.

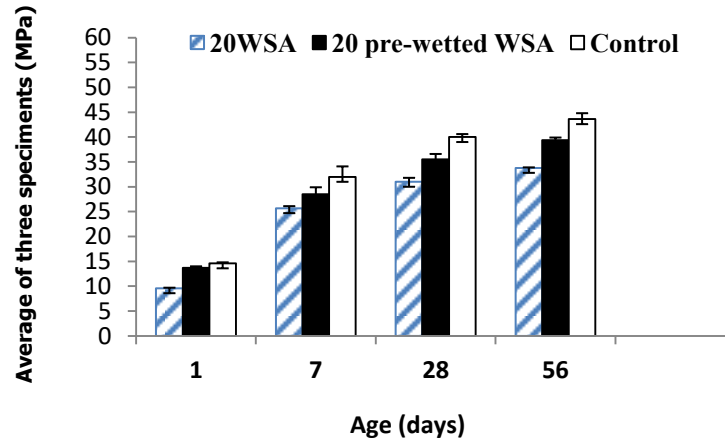


Figure 4-5: The compressive strength of mortar incorporating 20% pre-wetted and regular WSA

The strength activity index (SAI) was performed in accordance with ASTM C 311 standard. The SAI of cubes for 1, 7, 28 and 56 days are shown in Table 4-6, minimum limit of SAI recommended by ASTM C 618 when the mortar incorporates 20% of investigated ash is 75%. It can observe mortar incorporating regular WSA and pre-wetted WSA in 28 days surpassed minimum limit. The SAI of mortar incorporating 20% pre-wetted WSA was about 11% higher than mortar incorporating 20% regular WSA.

Table 4-6: Results of SAI of mortar cubes incorporating regular and pre-wetted WSA

Strength activity index (%)		
Time (days)	20% WSA	20% Pre-wetted WSA
1	65.7	93.8
7	80.3	89
28	77.5	88.7
56	77.5	90.3

4.2.3 Concrete incorporating regular and pre-wetted WSA

After the evaluation of regular and pre-wetted WSA in mortar, the concrete mixtures were designated for same workability. The control, 20% WSA and 20% pre-wetted WSA which referred to 100% Portland cement (PC), replacement of cement by 20% regular and pre-wetted WSA. The water to binder ratio (w/b) was 0.4. The compositions of control mix, concrete incorporating 20% regular WSA and 20% pre-wetted WSA are shown in Table 4-7.

Table 4-7: The composition of control mix, concrete incorporating 20% regular and pre-wetted WSA

Ingredients	Unit	density	w/b = 0.40		
			Control	20%WSA	20%Pre-wetted WSA
Portland Cement (GU)	kg	3.15	400	320	320
WSA		2.72	0	80	0
Pre-wetted WSA		2.6	0	0	80
Water		1.00	160	160	160
Sand (0-5 mm)		2.67	694	683	683
Aggregate (5-14 mm)		2.74	856	856	856
Aggregate (10-20 mm)		2.73	214	214	214
Air-entraining agent (Airx-l)	ml/100 kg	1.00	40	40	40
SP (plastol 6200)	l/m ³	1.08	0.8	1.0	1.8

Fresh properties of three concrete mixtures are shown in Table 4-8. As shown in Figure 4-6, for achieving same workability, concrete incorporating pre-wetted WSA needed significantly more quantity of SP compare to concrete incorporating 20% WSA and concrete incorporating 20%WSA required more quantity of SP compare to control mixture.

Table 4-8: Fresh properties of control mixture concrete incorporating 20% regular and pre-wetted WSA

Measured quantities	unit	w/b = 0.40					
		Control		20%WSA		20%Pre-wettedWSA	
Air-entraining agent (Airx-l)	ml/100 kg	40		40		40	
SP (plastol 6200)	l/m ³	0.8		1		1.8	
Time of measurement	minutes	10	30	10	30	10	30
Slump	mm	185	135	184	120	187	115
Air content	%	8.8	7.1	7.3	5.5	5.4	3.9
Unit weight	kg/m ³	2309	2337	2306	2354	2395	2416

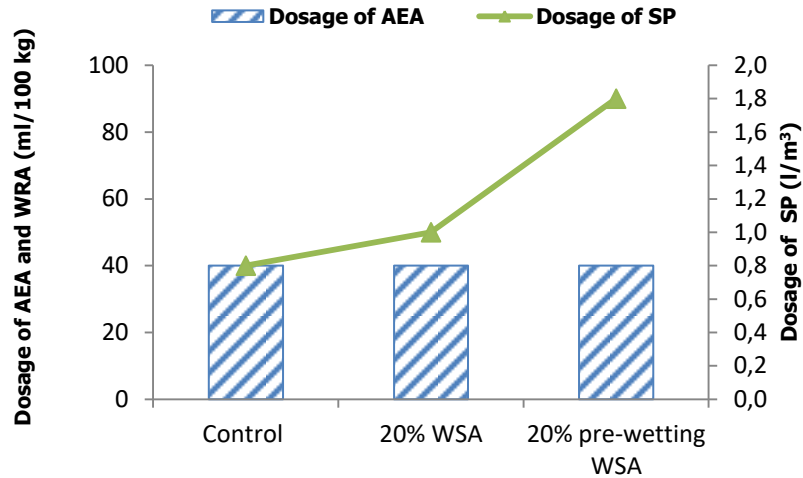


Figure 4-6: Required dosage of chemical admixtures for control, concrete incorporating 20 % pre-wetted and regular WSA

Figure 4-7 shows slump of concrete incorporating 20% pre-wetted WSA, 20% regular WSA, and control at 10 and 30 minutes. As can be observed slump loss of concrete incorporating 20% pre-wetted WSA was more than concrete incorporating 20% WSA and concrete incorporating 20% WSA was more than control. The reason can be high dosage of SP that used in concrete incorporating 20% pre-wetted WSA.

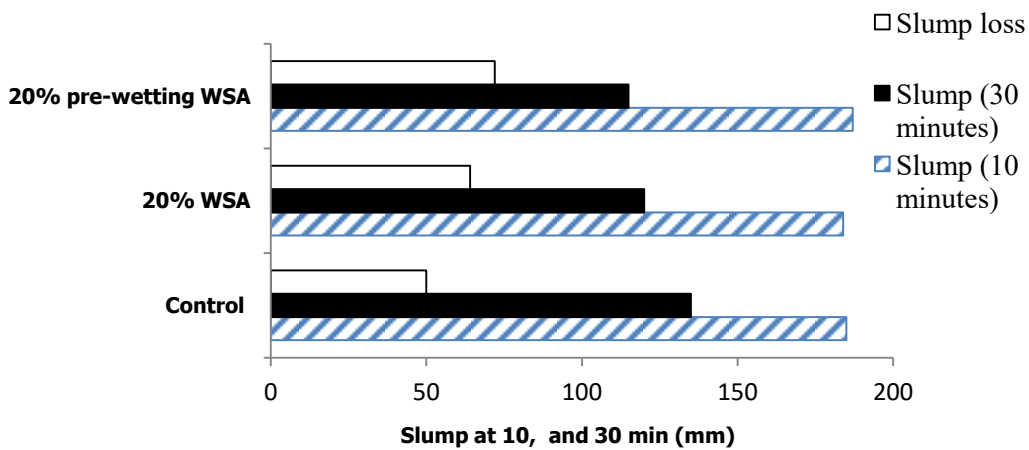


Figure 4-7: Slump of concrete incorporating 20% pre-wetted WSA, 20% regular WSA and control

- **Setting time**

Initial and final setting of three mentioned concrete mixes are shown in Figure 4-8. Concrete mixture incorporating 20% pre-wetted WSA showed rapid initial and final setting time compared to control mixture. Concrete incorporating 20% regular WSA showed slow initial and final setting time compare to control. Setting time of both concrete mixtures incorporating regular and pre-wetted WSA have satisfied limit of CSA 3004 specification. The requirement of CSA 3004 specification for setting time of concrete incorporating ASCMs, is not more than 1 hour earlier and 1.5 hours later than control mixture. Fineness and chemical composition are two principal parameters to explain hydration of cementitious materials and setting time. The reason of slow setting time of concrete incorporating WSA could be high content of sulfur SO_3 (7.8%) in WSA. The SO_3 directly cause generation of ettringite. The ettringite crystals create a thin coating around the anhydrated cement grains, hence preventing the quick reaction of calcium aluminates with water (Tzouvalas et al, 2004).

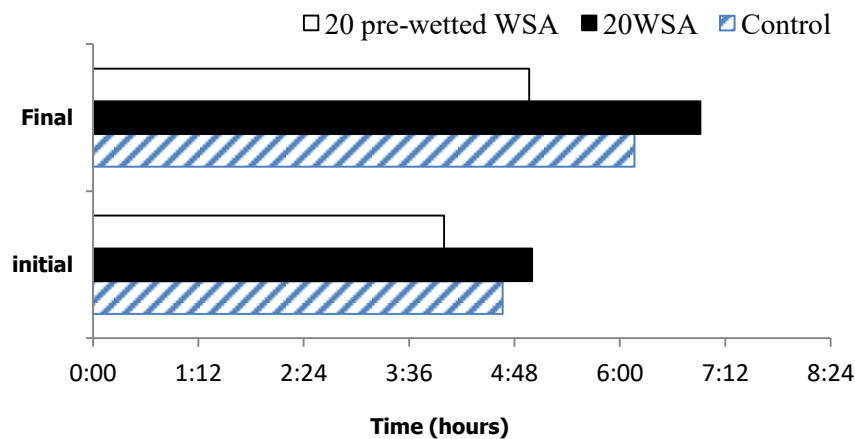


Figure 4-8: The initial and final setting time values of control, concrete incorporating 20% pre-wetted and regular WSA

- **Compressive strength**

As observed in Figure 4-9, pre-wetting of WSA significantly improved concrete compressive strength. Concrete incorporating pre-wetted WSA shows approximately same compressive strength with control mix at 91 days.

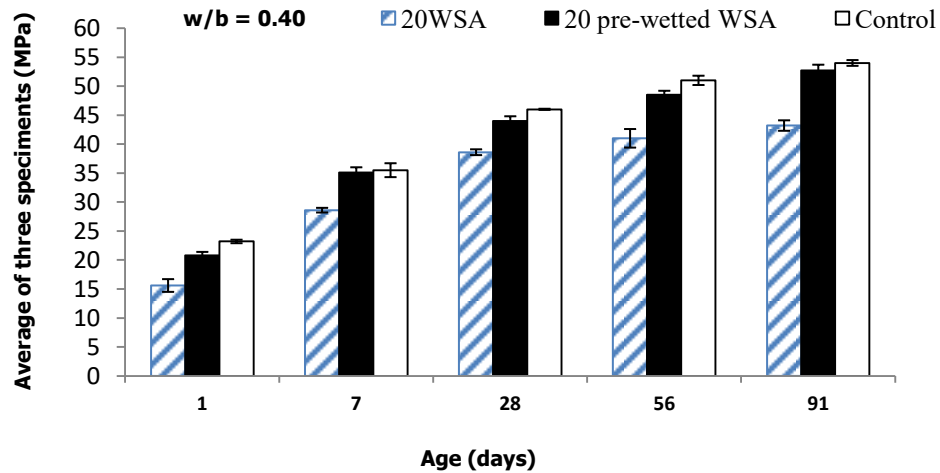


Figure 4-9: The compressive strength of control and concrete incorporating 20% pre-wetted and regular WSA

The compressive strength of concrete incorporating 20% of WSA was dramatically less than control. The reason can be due to expansion from hydration of WSA and generation unsoundness matrix. Two parameters are responsible of generation of expansion and unsoundness matrix, hydration of CaO in WSA and formation of Ca(OH)_2 (Bai et al, 2003; Mozaffari et al, 2006), oxidation of metallic aluminum in WSA and generation hydrogen bubbles (Aubert et al, 2004). By pre-wetting of WSA, disruptive hydration products are produced before setting of concrete and consequently, compressive strength is improved.

4.3. Phase 3 - Optimization of the AmSR content in mortar

For the optimization of AmSR content in mortar, the mortar mixtures were designated with different replacement rates of cement by AmSR and two different w/b ratios. The rates of replacement of cement by AmSR were 0, 10, 15, 20, 25 and 30% and the values of w/b were 0.485 and 0.40.

4.3.1 Composition and fresh properties

The composition and fresh properties of mortars with 0.485 and 0.40 of w/b are shown in Tables 4-9 and 4-10 respectively.

Table 4-9: Composition and fresh properties of mortars with 0.485 of w/b

w/b = 0.40							
s/b = 2.75							
Ingredients	Unit	control	10% AmSR	15% AmSR	20% AmSR	25% AmSR	30% AmSR
Portland cement (GU)	g	1000	900	850	800	750	700
AmSR		0	100	150	200	250	300
Ottawa sand		2750	2750	2750	2750	2750	2750
Water		400	400	400	400	400	400
SP Plastol 6400	% dry extract	0.165	0.190	0.247	0.272	0.312	0.327
Slump flow	mm	215	205	205	215	205	210
Temperature	°C	25.0	25.0	23.1	22.0	24.4	25.4

Table 4-10: Composition and fresh properties of mortars with 0.40 of w/b

w/b = 0.485							
s/b = 2.75							
Ingredient	Unit	Control	10% AmSR	15% AmSR	20% AmSR	25% AmSR	30% AmSR
Portland cement (GU)	g	1000	900	850	800	750	700
AmSR		0	100	150	200	250	300
Ottawa sand		2750	2750	2750	2750	2750	2750
Water		485	485	485	485	485	485
SP (ecoun 37)	% dry extract	0.27	0.31	0.42	0.52	0.78	0.88
Slump flow	mm	210	210	205	205	205	210
Temperature	°C	24.4	24.6	23.4	25.0	23.5	23.1

As can be observed in Tables 4-9 and 4-10, for achieving same slump flow by increasing rate of replacement of cement by AmSR, required dosage of SP were increased.

4.3.2 Compressive strength

The strength values were taken as the average of three cubes for each measurement. Figure 4-10 shows compressive strength of mortars with 0.485 of w/b at 1, 7, 28, 91 and 182 days. The compressive strength of mortars incorporating 10, 15, 20, and 25% was more than control mixtures. The compressive strength of 30% AmSR mortar was less than control mixture at 182 days. It was seen, by increasing replacement rate until 20%, rate of compressive strength development increased. Although, rate of compressive strength development of mortar

incorporating 25% AmSR was more than mortar with 15% AmSR and less than mortar with 20% AmSR.

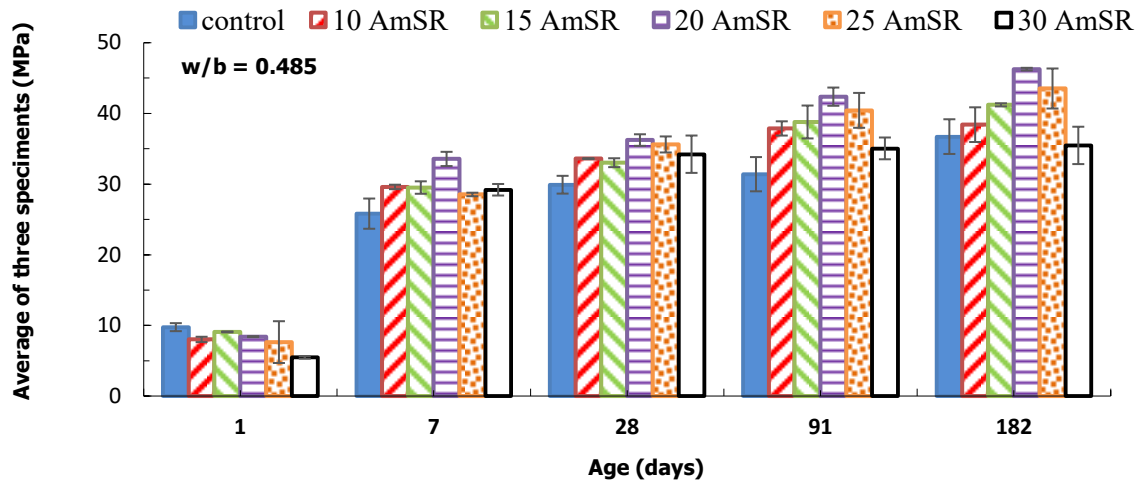


Figure 4-10: The compressive strength of mortar mixtures incorporating AmSR ($w/b = 0.485$)

Figure 4-11 shows compressive strength of mortars with 0.40 of w/b at 1, 7, 28, 91 and 182 days. Similar to mortars with 0.485 of w/b, the compressive strength of 0.40 w/b mortars incorporating 20% AmSR was significantly more than other mortar mixtures and control.

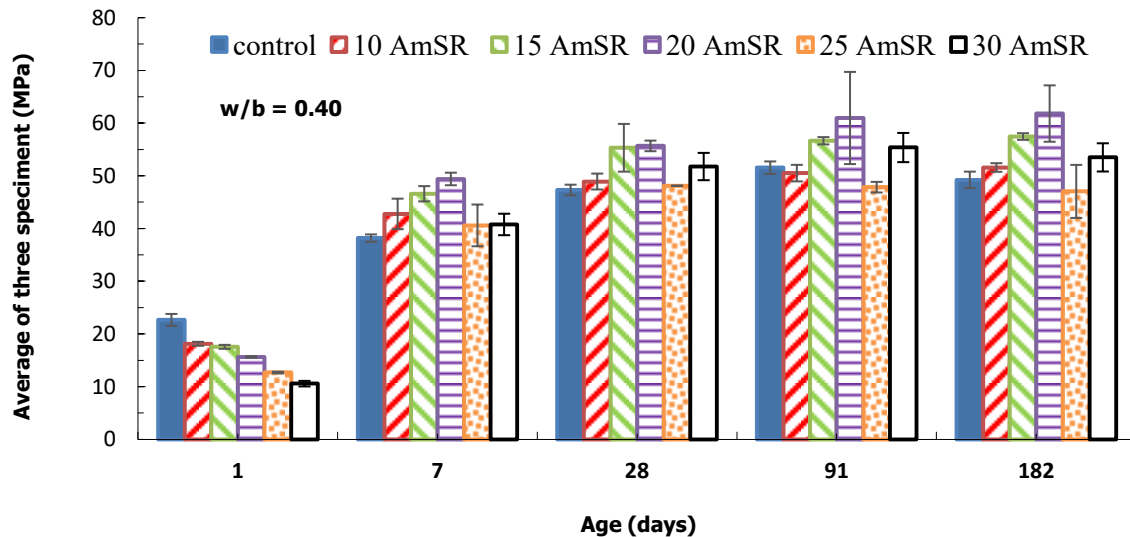


Figure 4-11: The compressive strength of mortar mixtures incorporating AmSR ($w/b = 0.40$)

As explained before, AmSR has high fineness and high amorphous silica content. Hence, AmSR generates dens matrix and develops compressive strength of mortar. Decreasing of w/b generates denser matrix by producing more C-S-H gel. It can be reason for development of compressive strength by decreasing of w/b from 0.485 to 0.40.

4.3.3 Strength activity index (SAI)

The strength activity index (SAI) was performed in accordance with ASTM C 311 standards. The SAI of mortar cubes for 1, 7, 28, 91 and 182 days are shown in Table 4-11. The SAI for all mortar mixtures except 30% AmSR were more than 100% since 7 days to 182 days. The SAI of mortar incorporating 20% AmSR was more than other mortar mixtures.

Table 4-11: Results of SAI of mortar cubes incorporating AmSR, w/b = 0.485

Strength activity index (%), w/b = 0.485					
Time (days)	10% AmSR	15% AmSR	20% AmSR	25% AmSR	30%AmSR
1	82.2	93.2	86.3	78.3	56.2
7	114.7	114.3	130.0	110.5	113.1
28	112.4	110.4	121.1	119.1	114.4
91	120.6	123.5	134.9	128.8	111.6
182	104.6	112.2	126.0	118.5	96.6

The SAI of mortar cubes with 0.40 of w/b at 1, 7, 28, 91 and 182 days are shown in Table 4-12. The SAI of mortar incorporating 20% AmSR was more than other mortar mixtures. The SAI for mortar incorporating 20% AmSR was 25% more than control at 182 days.

Table 4-12: Results of SAI of mortar cubes incorporating AmSR, w/b = 0.40

Strength activity index (%), w/b = 0.40					
Time (days)	10% AmSR	15% AmSR	20% AmSR	25% AmSR	30% AmSR
1	80.0	77.5	69.0	56.0	46.7
7	112.0	122.0	129.3	106.3	106.8
28	103.4	116.9	117.7	110.2	109.4
91	94.1	109.9	118.3	92.8	107.4
192	100.7	116.7	125.6	87.4	108.7

4.3.4 Electrical resistivity

The electrical resistivity depends on permeability and transfer properties of mortar matrix. Figure 4-12 shows results of electrical resistivity of mortar mixtures at 28 and 91 days. The electrical resistivity significantly increased by increasing rate of replacement of cement by AmSR.

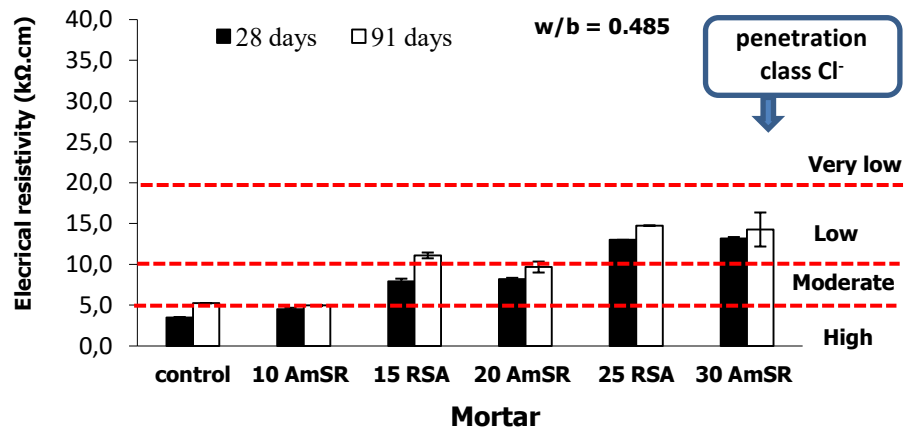


Figure 4-12: Electrical resistivity of mortar mixtures incorporating AmSR ($w/b = 0.485$)

Figures 4-13 shows results of electrical resistivity of mortar mixtures with 0.40 of w/b at 28 and 91 days. The electrical resistivity of mortars with 0.40 of w/b as well as mortar mixtures with 0.485 significantly increased by increasing rate of replacement of cement by AmSR.

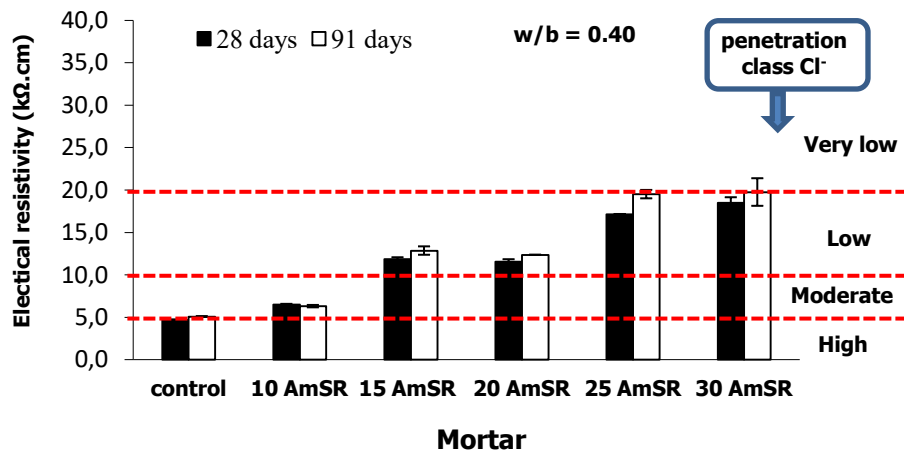


Figure 4-13: Electrical resistivity of mortar mixtures incorporating AmSR ($w/b = 0.40$)

Because of high fineness of AmSR, it fills micro pores in mortar matrix and generates impermeable matrix. Hence, electrical resistivity increased. The electrical resistivity of all

mortars with 0.40 of w/b was more than electrical resistivity of mortars with 0.485 of w/b. Decreasing of w/b generate denser matrix by producing more C-S-H gel. Hence, it can be reason for development of electrical resistivity by decreasing of w/b from 0.485 to 0.40.

4.4. Phase 4 - Performance of AmSR in different type of concrete with binary and ternary system

One of the principal objectives of this research project was to study the performance of AmSR in different types of concrete. Therefore, after definition of optimum rate of replacement of cement by AmSR in mortar, different types of concrete incorporating AmSR with different water to binder ratio were investigated, to evaluate fresh, hardened properties, and durability aspects.

4.4.1 Binary concrete

Binary system is combination of two different binders for concrete manufacturing. As explained before in methodology, three types of concrete were designed in this phase for binary system. The types of designed concrete are:

- ✓ Ordinary concrete (OC)
- ✓ Higher performance concrete (HPC)
- ✓ Self-consolidating concrete (SCC)

Ordinary concretes (OC) were designed with w/b of 0.40, 0.45, 0.50, 0.55, 0.65, and 0.70. The OC with w/b more than 0.45, are designed for residential purpose. High performance concrete (HPC) was designed with water to binder ratio (w/b) of 0.35. The rates of replacement of cement by AmSR were 0, 20%. Self-consolidating concrete was designed with w/b of 0.42 and the rates of replacement of cement by AmSR were 0, 10, and 20%.

4.4.1.1 Ordinary concrete (OC) and High performance concrete (HPC)

The composition of OC and HPC mixtures are shown in Tables 4-13 and 4-14. For each w/b, the control mixture with 100% PC (control) was used as a reference to compare with concrete incorporating with 20% AmSR (20AmSR).

Table 4-13: Composition of OC and HPC mixtures

Materials	Unit	Density	OC				HPC	
			w/b = 0.45		w/b = 0.40		w/b = 0.35	
			Control	20AmSR	Control	20AmSR	Control	20AmSR
Cement Portland (GU)	kg	3.15	375	300	400	320	430	344
AmSR		2.45	0	75	0	80	0	86
Water		1.00	168.8	168.8	160.0	160.0	150.5	150.5
Sand 0 - 5 mm		2.67	689	671	691	672	691	670
Aggregate 5 - 14 mm		2.71	856	856	856	856	856	856
Aggregate 10 - 20 mm		2.73	214	214	214	214	214	214
Air-entraining agent (Airx-l)	ml/100 kg	1.00	48	44	36	25	76	34
Water reducers (Eucon DX)	ml/100 kg	1.15	250	250	250	250	250	250
SP (Plastol 6400)	l/m ³	1.07	0.00	0.86	0.62	1.50	1.59	2.30

Table 4-14: Composition of OC residential mixtures

Materials	Unit	Density	OC residential							
			w/b = 0.50		w/b = 0.55		w/b = 0.65		w/b = 0.70	
			Control	20AmSR	Control	20AmSR	Control	20AmSR	Control	20AmSR
Cement Portland (GU)	kg	3.15	300	240	300	240	275	220	275	220
AmSR		2.45	0	60	0	60	0	55	0	55
Water		1.00	150	150	165	165	178.75	178.75	192.5	192.5
Sand 0 - 5 mm		2.67	802	788	762	748	747	733	710	697
Aggregate 5 - 14 mm		2.71	856	856	856	856	856	856	856	856
Aggregate 10 - 20 mm		2.73	214	214	214	214	214	214	214	214
Air-entraining agent (Airx-l)	ml/100 kg	1.00	30	30	25	30	0	0	21	21
Water reducers (Eucon DX)	ml/100 kg	1.15	250	250	200	200	61	241	0	125
SP (Plastol 6400)	l/m ³	1.07	0.35	0.70	0.00	0.90	0.00	0.60	0.00	0.20

4.4.1.1.1 Fresh properties

The measured fresh properties are slump at 10 and 50 minutes, fresh air contents, unit weight and temperatures. Results of fresh properties and required dosage of chemical admixtures for HPC and OC are shown in Tables 4-15 and 4-16.

Table 4-15: Fresh properties of OC and HPC mixtures

Characteristic	Unit	OC				HPC	
		w/b = 0.45		w/b = 0.40		w/b = 0.35	
		Control	20 AmSR	Control	20 AmSR	Control	20 AmSR
Air-entraining agent (Airx-l)	ml/100 kg	48	44	36	25	76	34
Water Reducer (Eucon DX)	ml/100 kg	250	250	250	250	250	250
SP (Plastol 6400)	l/m ³	0.00	0.86	0.62	1.50	1.59	2.30
Time of measurement	minutes	10 50	10 50	10 50	10 50	10 50	10 50
Slump	mm	140 105	160 140	210 180	185 110	210 155	215 140
Air content	%	8.6 7.6	7.0 6.4	8.1 8.0	6.9 4.1	7.8 5.8	6.1 4.9
Unit weight	kg/m ³	2200 2230	2250 2285	2281 2309	2260 2355	2295 2366	2318 2330
Temperature	°C	23.0 23.2	23.4 23.2	- -	22.4 22.2	20.8 20.1	23.0 23.0

Table 4-16: Fresh properties of residential OC mixtures

Characteristic	Unit	OC residential							
		w/b = 0.50		w/b = 0.55		w/b = 0.65		w/b = 0.70	
		Control	20AmSR	Control	20AmSR	Control	20AmSR	Control	20AmSR
Air-entraining agent (Airx-l)	ml/100 kg	30	30	25	30	0	0	21	21
Water Reducer (Eucon DX)	ml/100 kg	250	250	200	200	61	241	0	125
SP (Plastol 6400)	l/m ³	0.35	0.70	0.0	0.9	0.0	0.6	0.0	0.2
Time of measurement	minutes	10 50	10 50	10 50	10 50	10 50	10 50	10 50	10 50
Slump	mm	175 120	155 80	160 120	150 80	170 155	142 95	185 160	155 110
Air content	%	7 6.4	7.5 5.3	8 6.9	7.8 6.5	2.4 1.8	3.7 3	4.5 4	6.2 4.6
Unit weight	kg/m ³	2255 2263	2240 2306	2206 2225	2207 2247	2375 2381	2322 2334	2329 2336	2248 2291
Temperature	°C	19.0 19.1	22.0 21.7	21.0 20.8	19.1 19.0	20.7 20.6	19.0 18.9	21.2 20.8	21.0 21.0

- **Slump**

The comparison of required quantities of chemical admixtures is shown in Figure 4-14. The required dosage of SP (Plastol 6400), WRA (Eucon DX) and AEA (AireX-L) increased with decreasing the w/b. The required dosage of chemical admixture to having same slump of concrete incorporating 20% AmSR is significantly more than control mixtures with same w/b. Slump of all mixtures was in defined target. Measured slump at 10 and 50 minutes, and slump

loss of all mixtures are presented in Figure 4-15. As it observed in Figure 4-15, for same w/b except concrete with w/b of 0.45, the slump loss of concrete incorporating of 20% AmSR is more than control mixtures. The slump loss can be affected by dosage of chemical admixtures and initial slump of concretes.

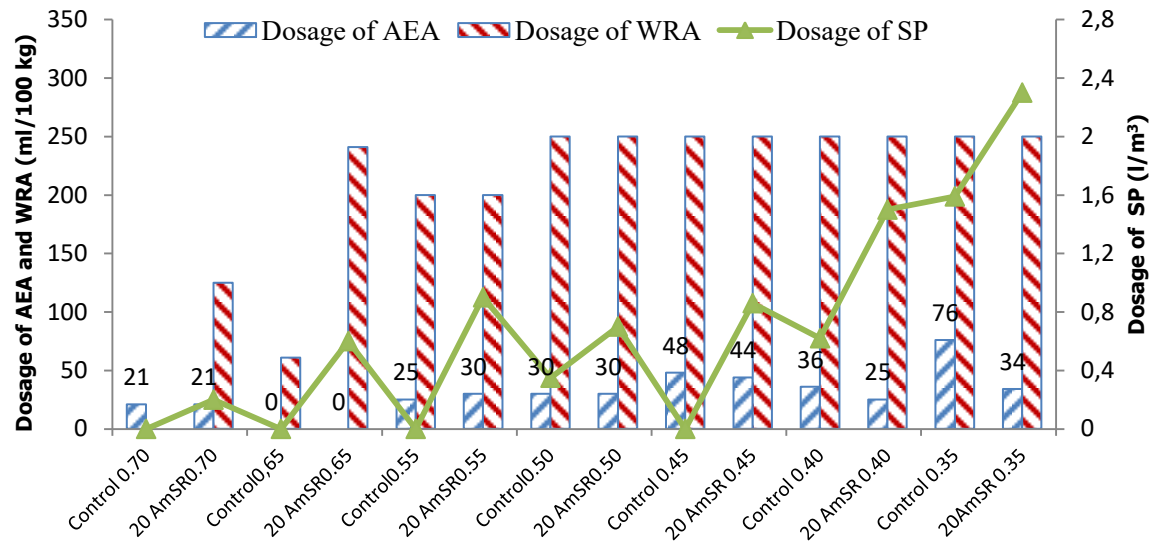


Figure 4-14: The comparison of required quantities of chemical admixtures of HPC and OC mixtures incorporating 20% AmSR and control mixtures

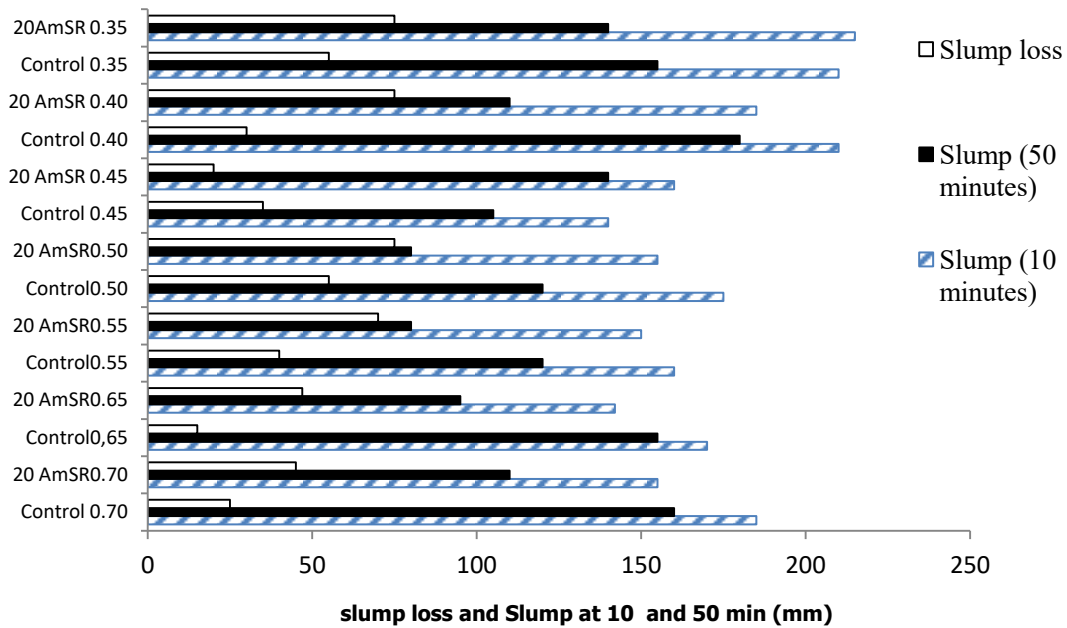


Figure 4-15: Measured slump and slump loss of HPC and OC mixtures incorporating 20% AmSR and control mixtures

- **Air content**

The fresh targeted air volume was in the range of 5 to 8% and was determined at 10 and 50 minutes. All mixtures met fresh air content target except of residential OC mixtures with 0.65 of w/b and control with 0.70 of w/b. These two types of concrete were designed for interior usage purpose and resistance of freeze-thaw cycle is not important. So, these concrete have not air entraining agent. The results were compared as presented in Figure 4-16.

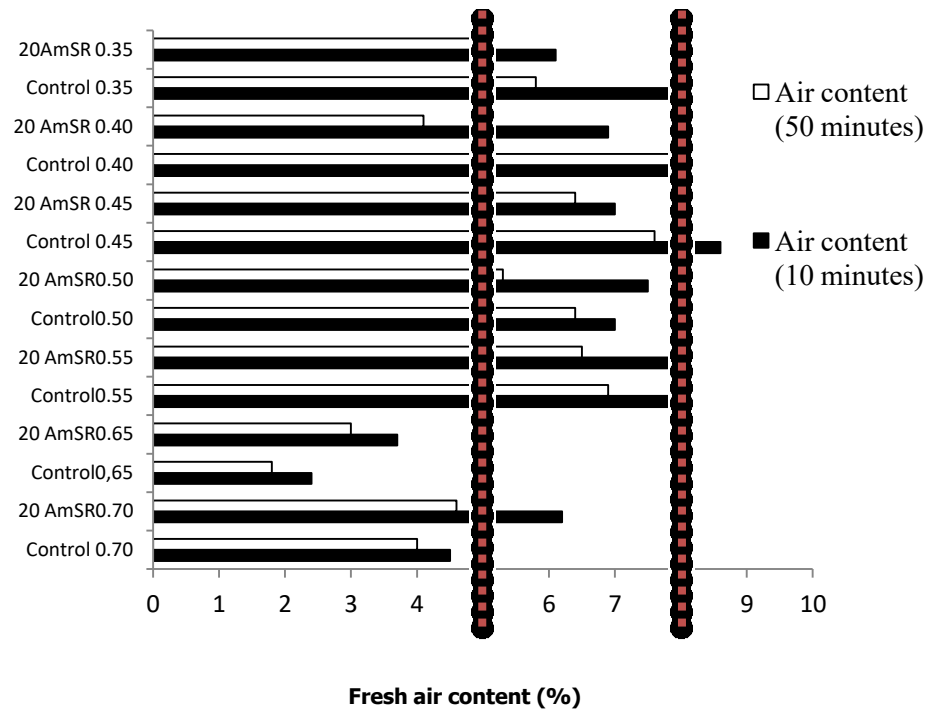


Figure 4-16: Fresh air content of HPC and OC mixtures incorporating 20% AmSR and control mixtures

- **Setting time**

The initial and final settings of OC and HPC mixtures are presented in Figure 4-17. As can be seen in Figure 4-17, except concretes with 0.65 and 0.70 of w/b, concrete incorporating 20% AmSR showed rapid initial and final setting time compared to control mixture with same w/b. The reason can be dosage of chemical admixture used in mixtures incorporating 20% AmSR compared to the control concrete. In control mixtures, concrete with 0.65 and 0.70 of w/b did not need WRA and SP to achieve required slump. The chemical admixtures can cover binder particles and reduce rate of hydration reaction. Setting time of all concrete mixtures incorporating AmSR met limit of CSA 3004 specification. Fineness and chemical composition are two principal parameters to explain hydration of cementitious materials and therefore setting time. The reason of rapid setting time of concrete incorporating AmSR could be high fineness of AmSR. Its fineness is about 10 times higher than of cement portland.

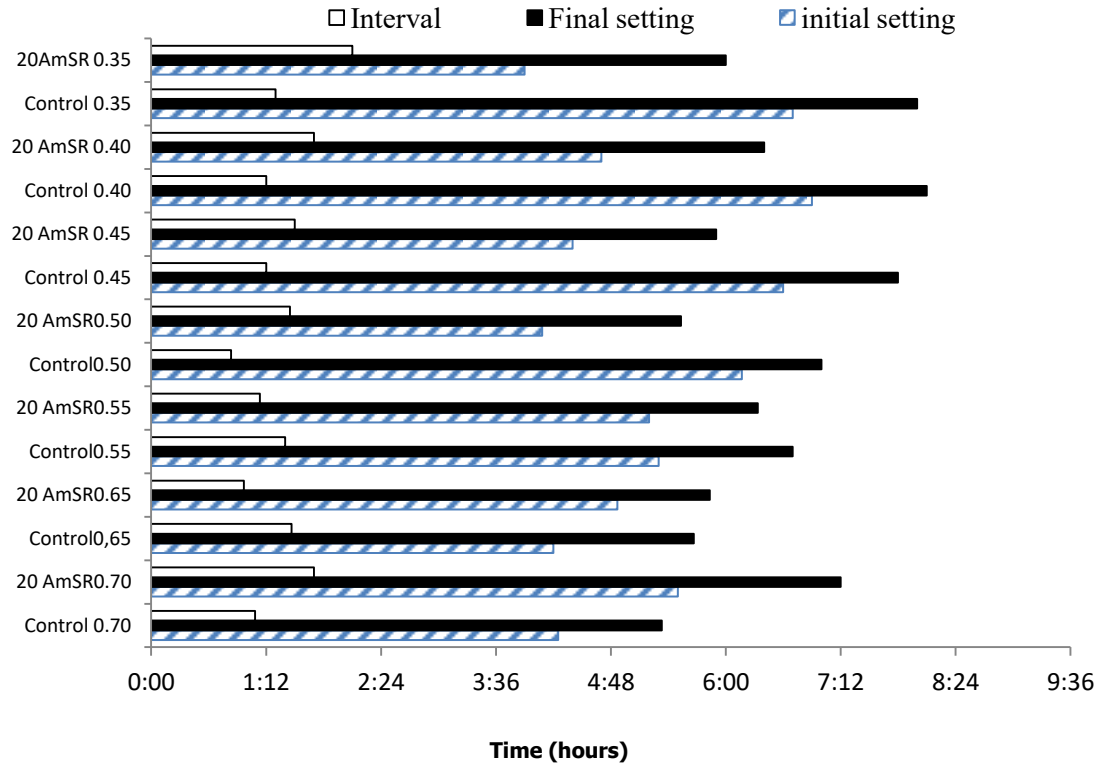


Figure 4-17: The initial and final settings of OC and HPC mixtures incorporating 20% AmSR and control mixtures

4.4.1.1.2 Mechanical properties

- Compressive strength

The results of compressive strength of the high performance concrete (HPC) with 0.35 of w/b at 1, 7, 28, and 91 days under the standard curing conditions is shown in Figure 4-18. The HPC incorporating 20% AmSR showed significantly lower resistance at 1 and 3 days compared to control mixture. With increasing curing time, compressive strength of 20AmSR HPC is significantly improved. The rate of compressive strength development was remarkably high between 3 to 7 days. It is observed that compressive strength of 20AmSR HPC had reached near to control mixture at 91 days. The compressive strength of concrete incorporating 20% AmSR and control concrete were respectively 69.5 MPa and 71.5 MPa. In addition 20AmSR HPC compressive strength met the specified compressive strength at 28 days.

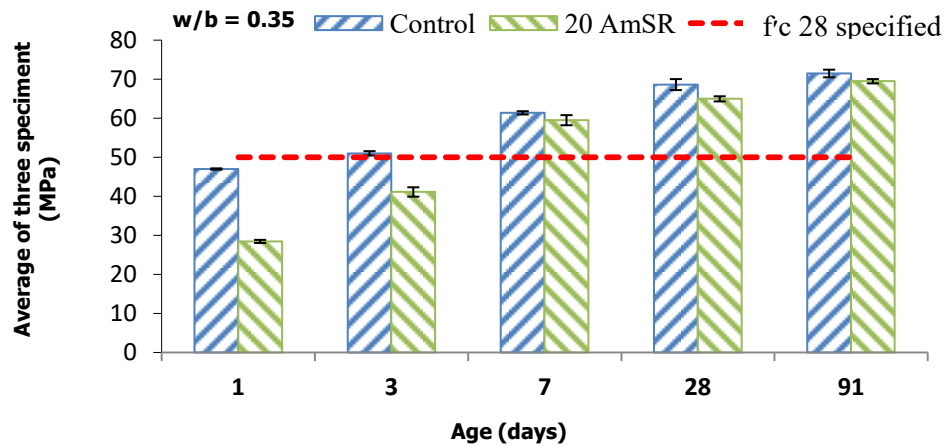


Figure 4-18: Compressive strength of HPC incorporating 20% AmSR and control mixture ($w/b = 0.35$)

The results of compressive strength of ordinary concrete (OC) with 0.40, 0.45, 0.50, 0.55, 0.65, and 0.70 of w/b , are shown in Figures 4-19 to 4-24. It was observed that OC mixtures incorporating 20% AmSR had lower compressive strength compared to control mixtures until 7 days. The compressive strength of all OC mixtures incorporating 20% AmSR surpassed the compressive strength of control mixtures with same w/b at long term curing times except concrete with 0.70 of w/b . The difference between compressive strength of concrete with 0.70 of w/b incorporating 20 % AmSR and control mixture was less than 1.5 MPa.

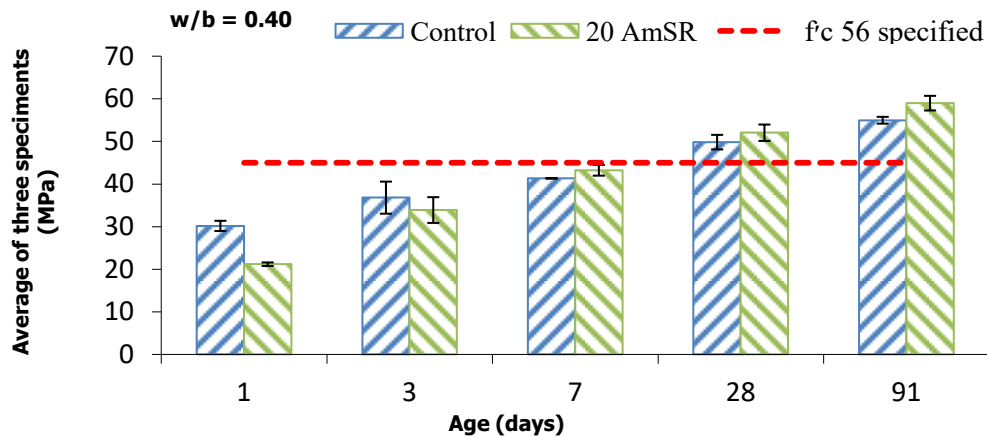


Figure 4-19: Compressive strength of OC incorporating 20% AmSR and control mixture ($w/b = 0.40$)

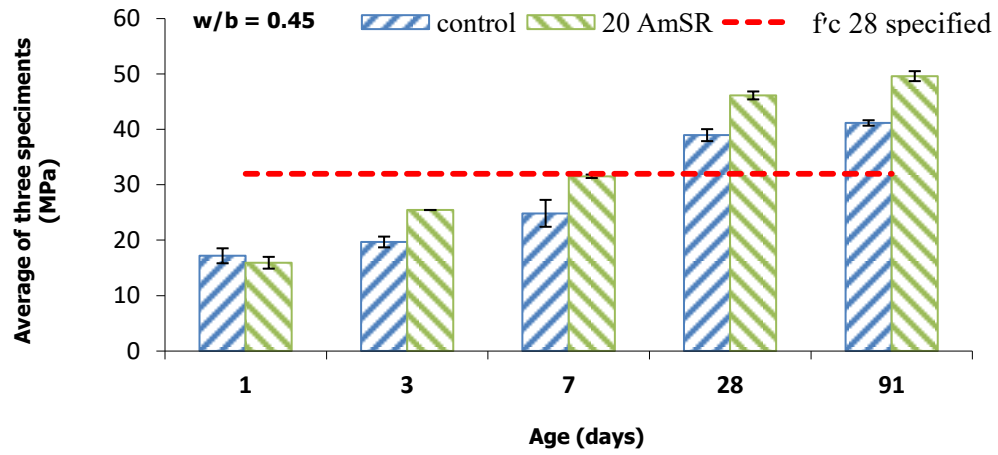


Figure 4-20: Compressive strength of OC incorporating 20% AmSR and control mixture ($w/b = 0.45$)

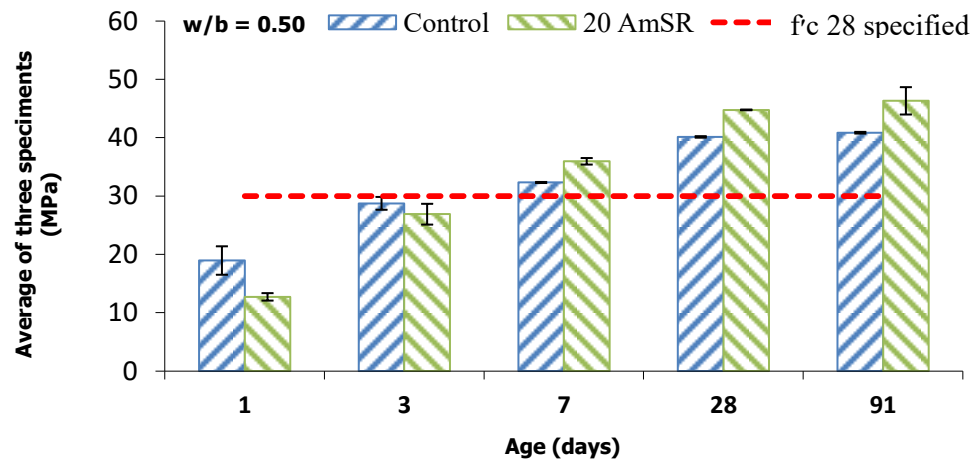


Figure 4-21: Compressive strength of OC incorporating 20% AmSR and control mixture ($w/b = 0.50$)

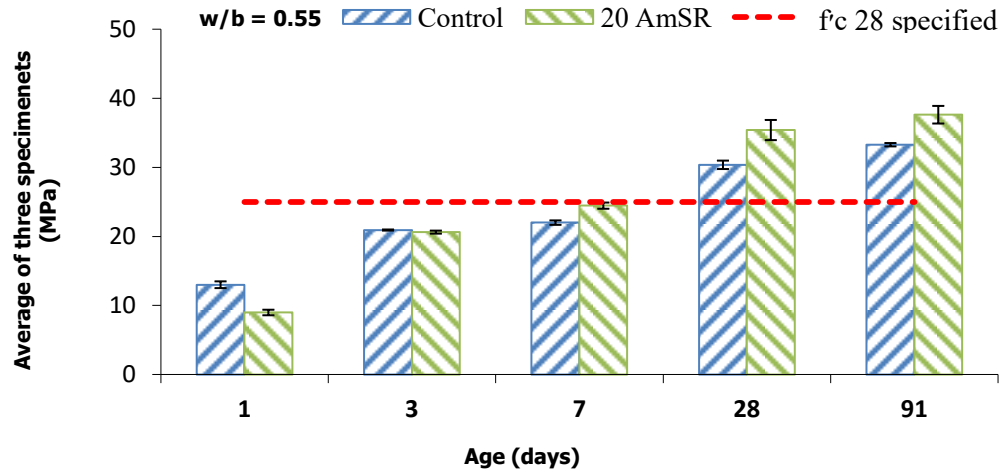


Figure 4-22: Compressive strength of OC incorporating 20% AmSR and control mixture ($w/b = 0.55$)

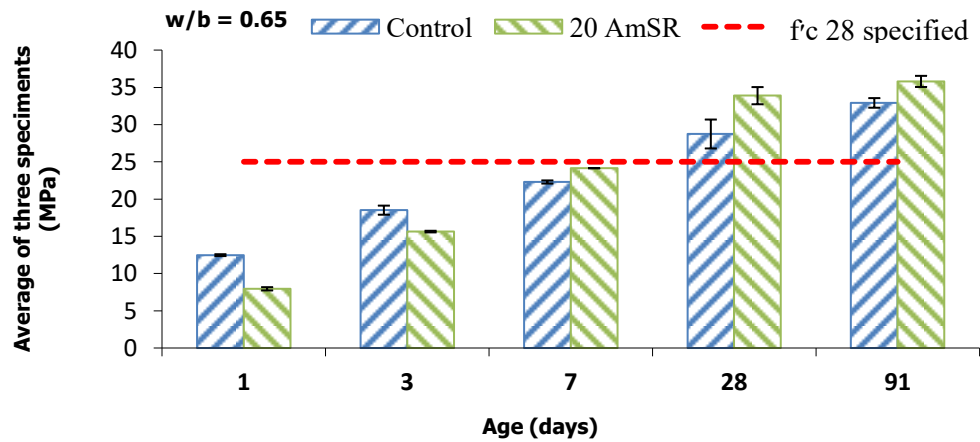


Figure 4-23: Compressive strength of OC incorporating 20% AmSR and control mixture ($w/b = 0.65$)

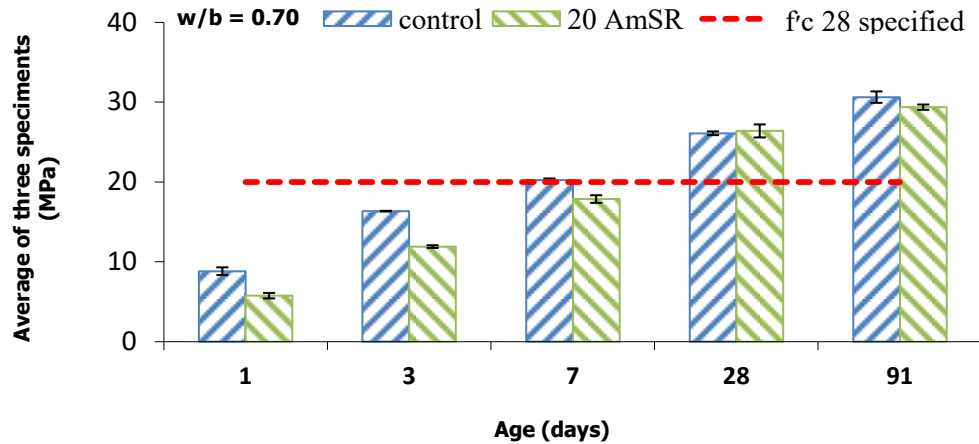


Figure 4-24: Compressive strength of OC incorporating 20% AmSR and control mixture ($w/b = 0.70$)

The compressive strength development at 91 days for concrete incorporating 20% AmSR with w/b of 0.45 compared to control concrete was higher than other mixtures with different w/b . As shown in Figure 4-25, the rate of improvement of compressive strength of HPC with 0.35 of w/b and OC mixtures with 0.40, 0.45, 0.50, 0.55, 0.65 and 0.70 of w/b incorporating 20% AmSR compared with their control mixtures were -2.7%, +7.3%, +20%, +13.2%, +12.9%, +8.8%, and -3.9%.

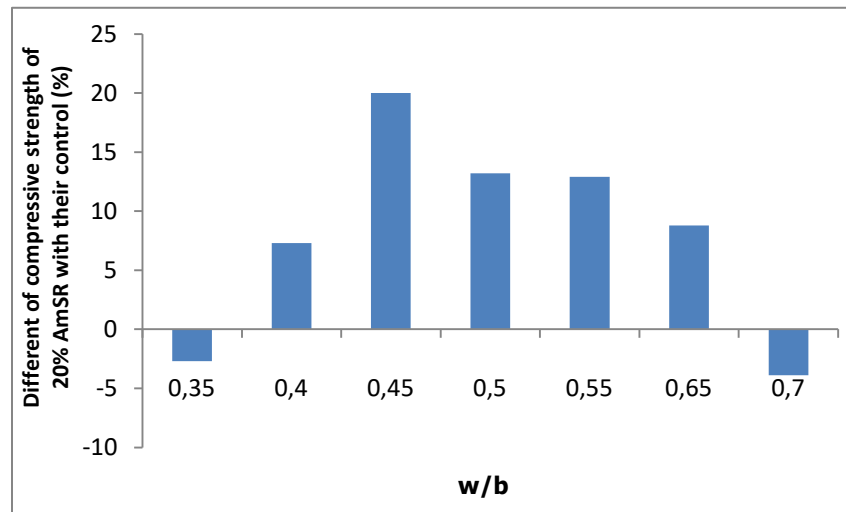


Figure 4-25: Different of compressive strength of 20%AmSR concrete with their control at 91 days

Hence, the w/b affected on rate of improvement of concrete incorporating AmSR compared with control mixtures. The OC 20AmSR with 0.45 of w/b showed more compressive strength development. The possible reason is generation of more C-S-H with 0.45 of w/b. The change of w/b, can affect on quantity of C-S-H gel production. The reason of development of compressive strength of OC concrete mixtures incorporating of 20% AmSR is high fineness of AmSR particles and high content of amorphous silica in AmSR. Adding fine AmSR brings millions of very small particles to a concrete mixture. They fill in the spaces between cement particles. This phenomenon is frequently referred to as particle packing or micro-filling. This phenomenon improves performance of concrete incorporating 20% AmSR. Moreover, because of its high amorphous silicon dioxide content, AmSR was a very reactive pozzolanic material in concrete.

- **Tensile splitting strength**

Comparison of tensile splitting strength of the HPC incorporating 20% AmSR and control concrete at 28 and 91 days is shown in Figure 4-26. The results obtained at 28 and 91 days are compared with estimated results by ACI 363 specification based on compressive strength. Generally, the trend of tensile strength is similar to compressive strength of each concrete mixture. The tensile strength of HPC incorporating 20% AmSR had reached near to control concrete tensile strength. The tensile strength of 20%AmSR and control at 91 days were respectively 6.3 and 6.8 MPa. Therefore, the HPC incorporating 20% AmSR exhibits very good tensile splitting strength.

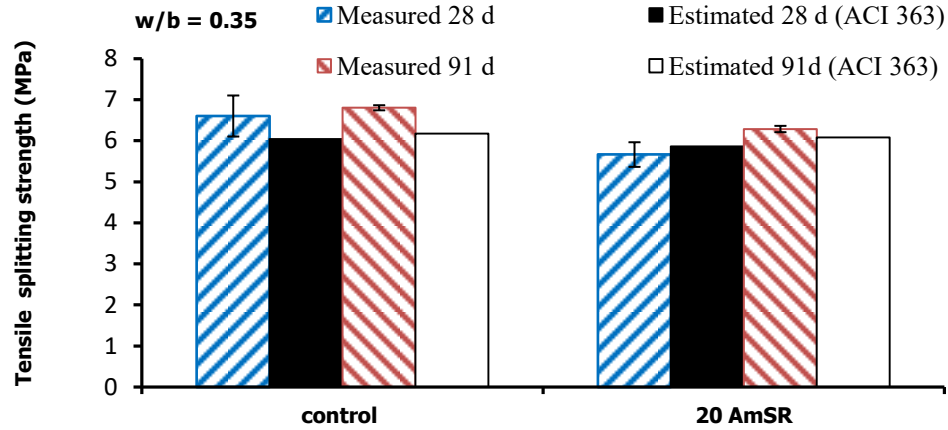


Figure 4-26: Tensile splitting strength of HPC incorporating 20% AmSR and control mixture ($w/b = 0.35$)

The results of tensile strength of ordinary concrete (OC) with 0.40, 0.45, 0.50, 0.55, 0.65, and 0.70 of w/b , are shown in Figures 4-27 to 4-32. It was observed that the tensile strength of all OC mixtures show same trend of their compressive strength. The tensile strength of OC mixtures incorporating 20%AmSR at 91 days surpassed tensile strength of control mixtures with same w/b except concrete with 0.70 of w/b .

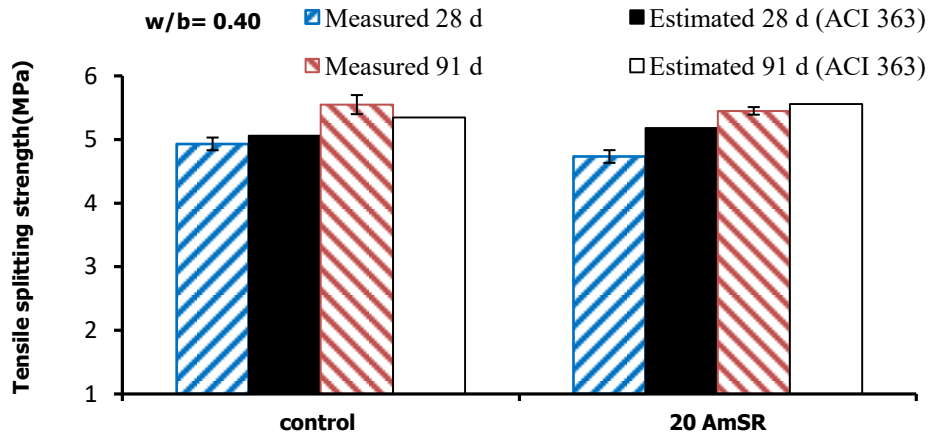


Figure 4-27: Tensile splitting strength of OC incorporating 20% AmSR and control mixture ($w/b = 0.40$)

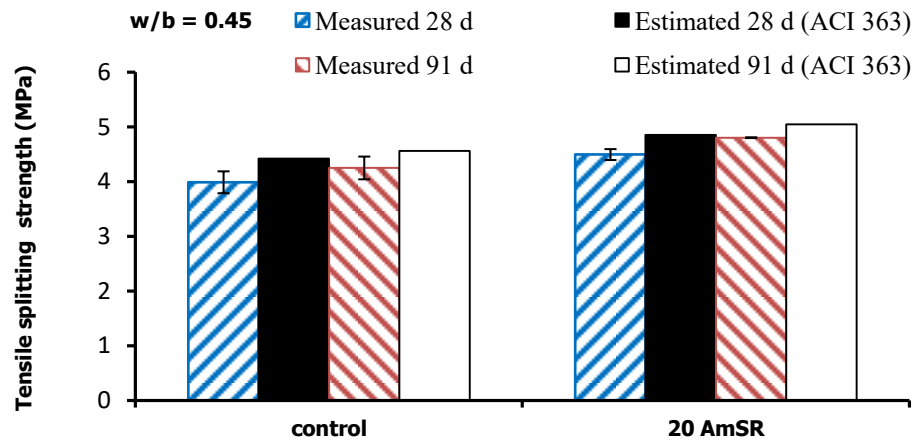


Figure 4-28: Tensile splitting strength of OC incorporating 20% AmSR and control mixture ($w/b = 0.45$)

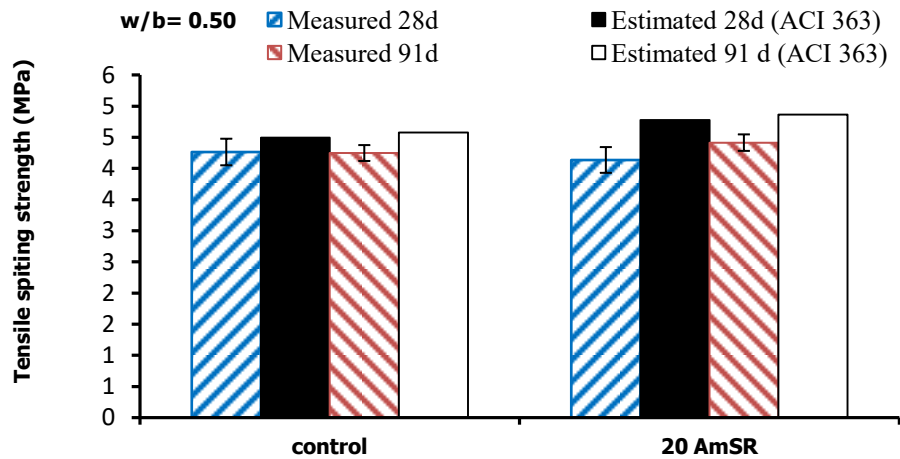


Figure 4-29: Tensile splitting strength of OC incorporating 20% AmSR and control mixture ($w/b = 0.50$)

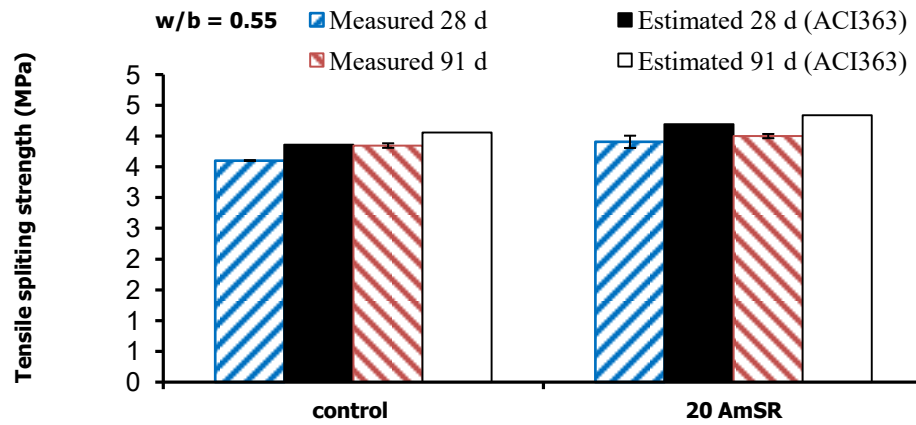


Figure 4-30: Tensile splitting strength of OC incorporating 20% AmSR and control mixture ($w/b = 0.55$)

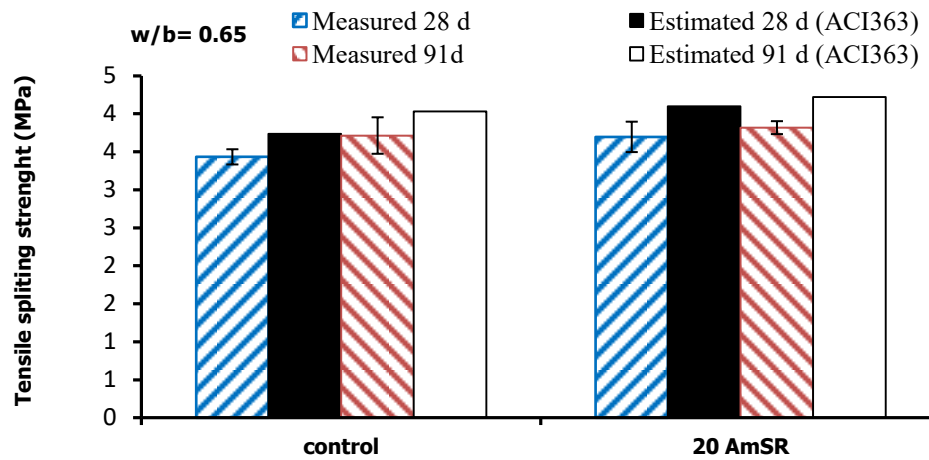


Figure 4-31: Tensile splitting strength of OC incorporating 20% AmSR and control mixture ($w/b = 0.65$)

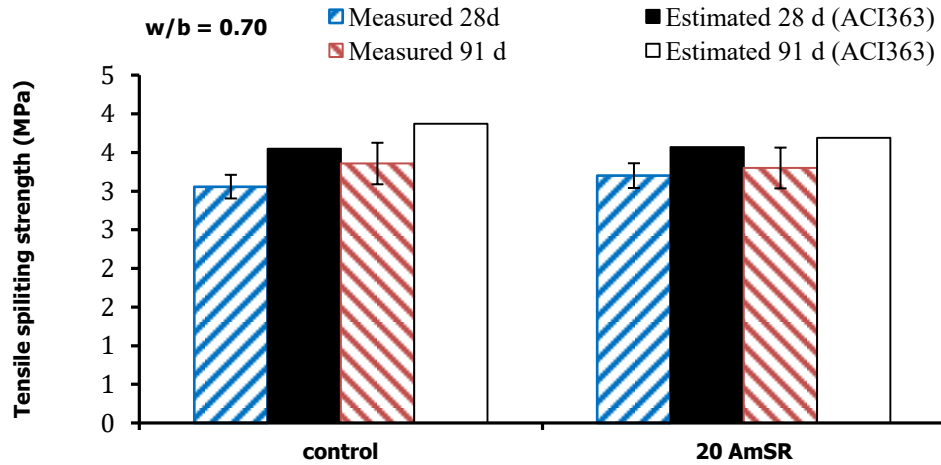


Figure 4-32: Tensile splitting strength of OC incorporating 20% AmSR and control mixture ($w/b = 0.70$)

- **Flexural strength**

The flexural strength results of HPC with 0.35 of w/b at 28 days are shown in Figure 4-33. It was observed, same as compressive and tensile strength of HPC, flexural strength of concrete incorporating 20% AmSR at 28 days was lower than control concrete. As shown in Figures 4-34 and 4-35, flexural strength of OC with 0.40 and 0.45 of w/b incorporating 20% surpassed flexural strength of control mixtures. As well as compressive and tensile strength results trend, concrete with 0.45 of w/b incorporating 20% AmSR showed high improvement of flexural strength compared to other concrete mixtures. As shown in all figures, the flexural strength of HPC and OC are compared with theoretical values estimated by the equation of ACI 363 specification.

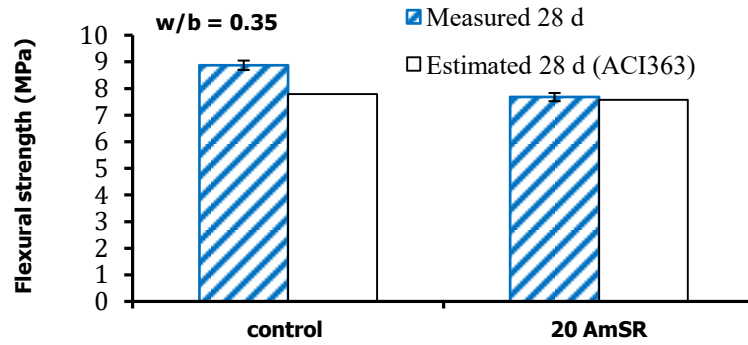


Figure 4-33: Flexural strength of HPC incorporating 20% AmSR and control mixture ($w/b = 0.35$)

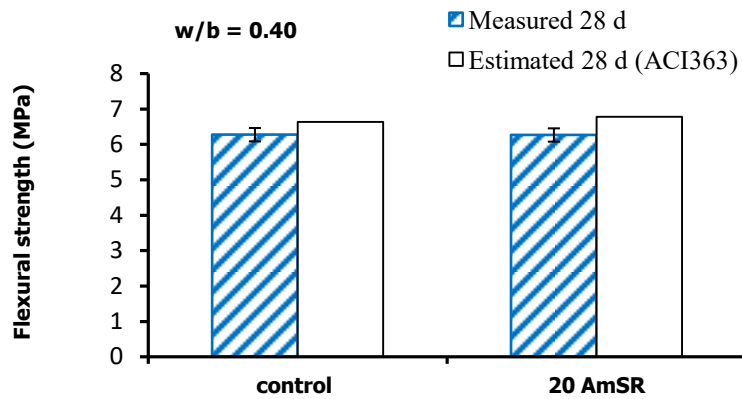


Figure 4-34: Flexural strength of OC incorporating 20% AmSR and control mixture ($w/b = 0.40$)

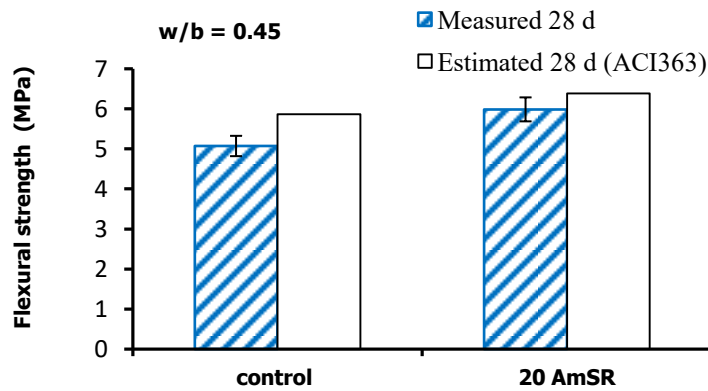


Figure 4-35: Flexural strength of OC incorporating 20% AmSR and control mixture ($w/b = 0.45$)

- **Modulus of elasticity**

The comparison of modulus of elasticity values, for HPC and OC mixtures with 0.40 and 0.45 of w/b at 28 and 91 days are shown in Figures 4-36 to 4-38 respectively. The modulus of elasticity of HPC and OC mixtures showed same trend of other mechanical properties as compressive, tensile and flexural strength. The modulus of elasticity of HPC incorporating 20% AmSR at 28 and 91 days were lower than control mixture but the difference was not significant. It observed that the modulus of elasticity of OC incorporating 20% AmSR at 28 and 91 days were more than control mixture. Same as other mechanical properties, modulus of elasticity improvement of OC incorporating 20% AmSR with 0.45 of w/b compared to its control was more than OC mixtures with 0.40 of w/b. In addition, modulus of elasticity values is compared with BEAL equation. It observed that the estimated values were close to the real obtained results.

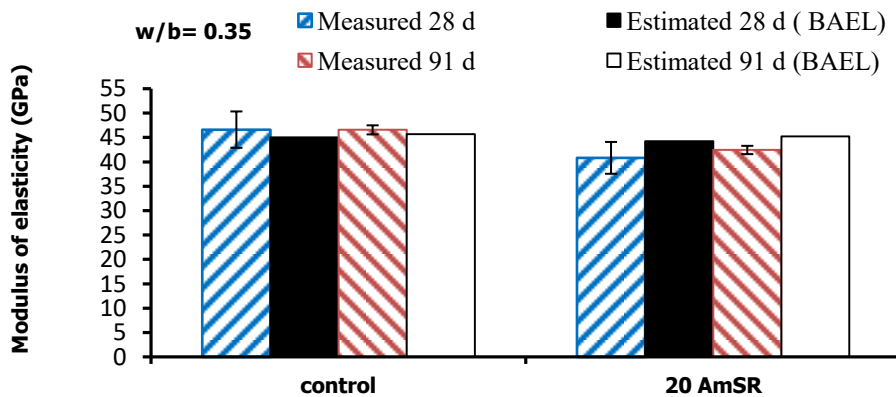


Figure 4-36: Modulus of elasticity of HPC incorporating 20% AmSR and control mixture (w/b = 0.35)

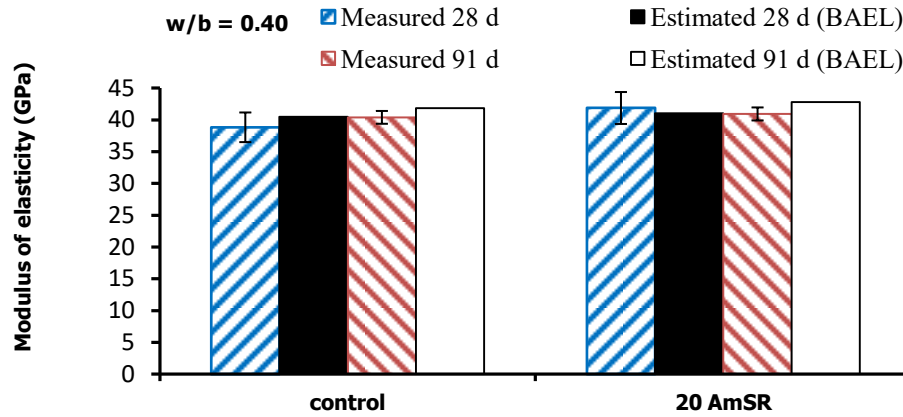


Figure 4-37: Modulus of elasticity of OC incorporating 20% AmSR and control mixture ($w/b = 0.40$)

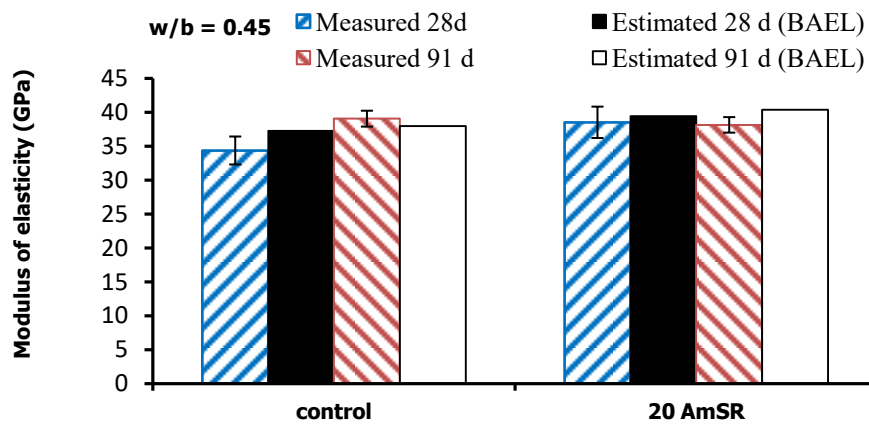


Figure 4-38: Modulus of elasticity of OC incorporating 20% AmSR and control mixture ($w/b = 0.45$)

4.4.1.1.3 Durability

- **Electrical resistivity**

There is a correlation between the electrical resistivity and durability of concrete. The electrical resistivity depends on permeability and transfer properties of concrete. The electrical resistivity is often used to determine the corrosivity of concrete. The concrete with high electrical resistivity shows low risk of corrosion. Figure 4-39, shows results of electrical resistivity of HPC mixtures at 28, 56 and 91 days. It was observed that electrical resistivity of HPC incorporating 20%

AmSR at 28, 56 and 91 days had higher electrical resistivity compared with control mixture. HPC incorporating 20% AmSR were in very low penetration class and control concrete was in low penetration class at all measurement ages.

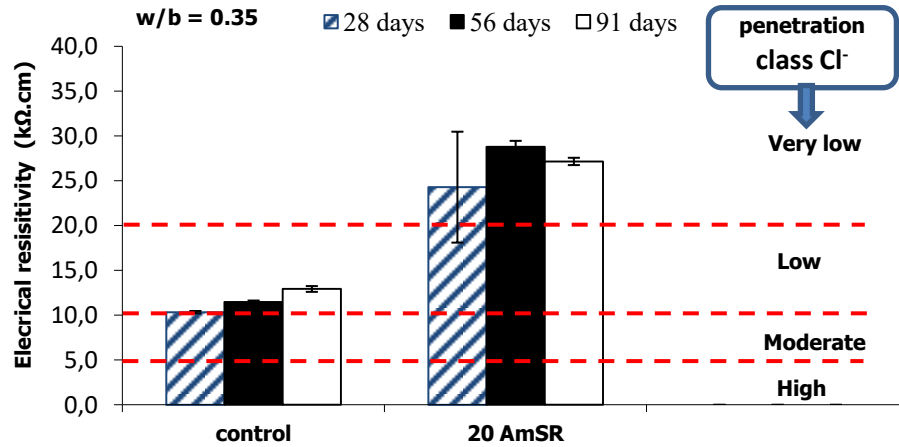


Figure 4-39: Electrical resistivity of HPC incorporating 20% AmSR and control mixture (w/b = 0.35)

The results of electrical resistivity of OC mixtures with 0.40, 0.45, 0.50, 0.55, 0.65 and 0.70 of w/b at 28, 56 and 28 days are shown respectively in Figures 4-40 to 4-45. It was observed that electrical resistivity of all OC mixtures incorporating 20% AmSR were significantly more than electrical resistivity of control mixture with same w/b. Generally the electrical resistivity decreased with increasing w/b of 0.35 to 0.70. The class of permeability of concrete with 0.40 of w/b, incorporating 20% AmSR was very low and its control concrete was in moderate level. Other OC mixtures incorporating 20% AmSR were in low class of permeability and their control mixtures were in moderate level. Therefore, AmSR as partial replacement of cement in concrete significantly increased electrical resistivity and consequently significantly improved durability of concrete. It can conclude fine particles and high content of amorphous silica in AmSR are the reasons of generation of less permeable matrix and hence, provides high electrical resistivity. It was observed that, by increasing w/b electrical resistivity decreased. The reduction of w/b generate denser matrix by producing more C-S-H gel. Hence, it can be reason for development of electrical resistivity by decreasing of w/b.

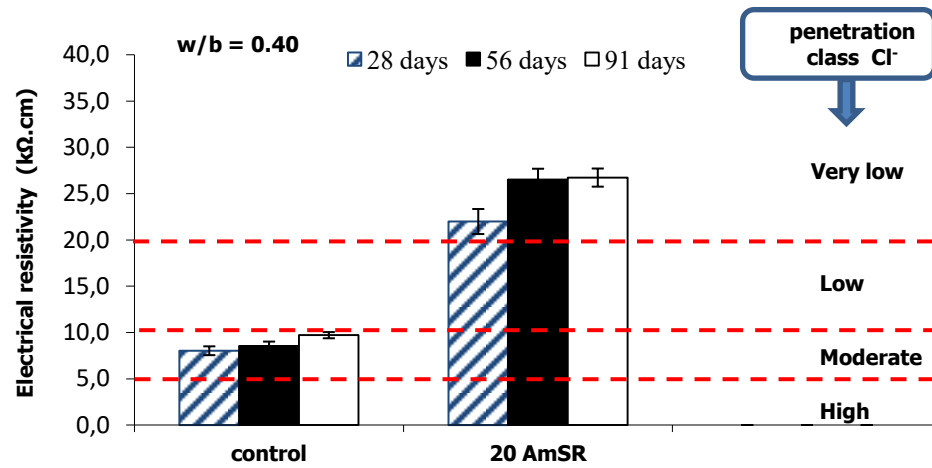


Figure 4-40: Electrical resistivity of OC incorporating 20% AmSR and control mixture ($w/b = 0.40$)

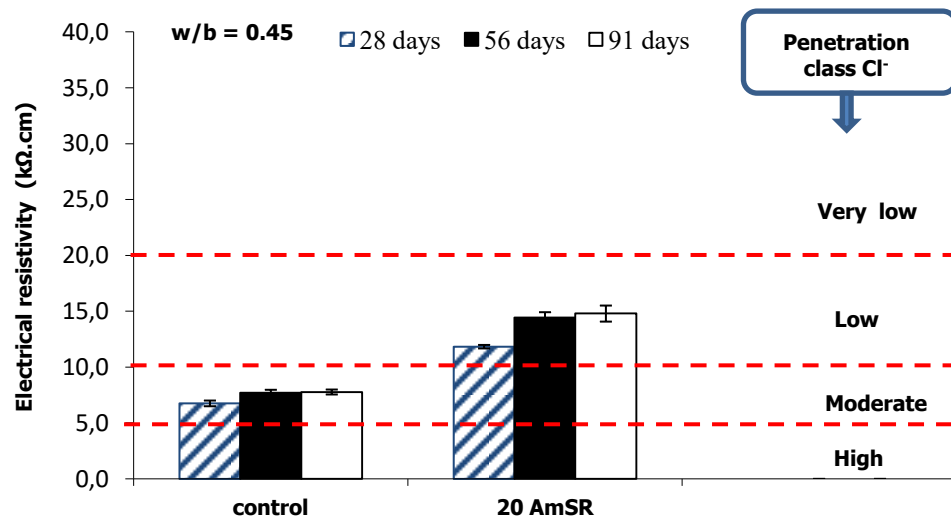


Figure 4-41: Electrical resistivity of OC incorporating 20% AmSR and control mixture ($w/b = 0.45$)

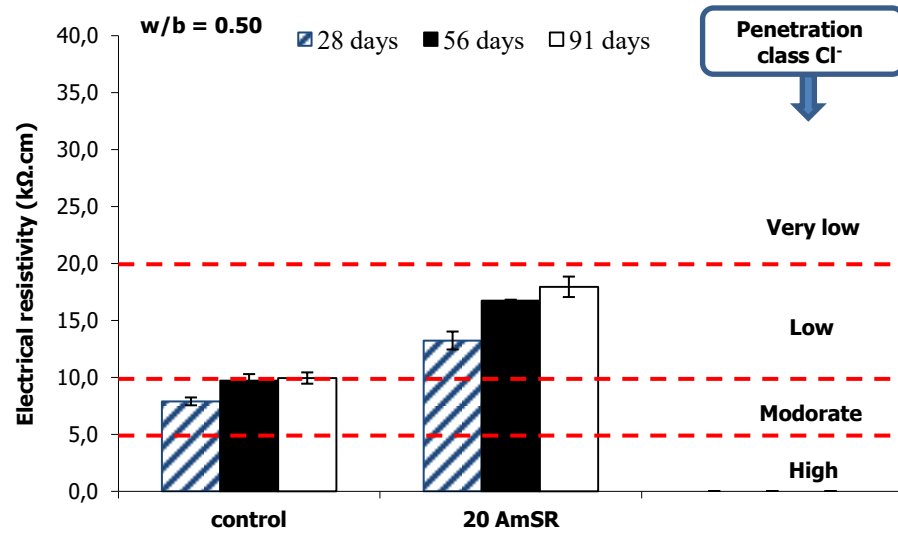


Figure 4-42: Electrical resistivity of OC incorporating 20% AmSR and control mixture ($w/b = 0.50$)

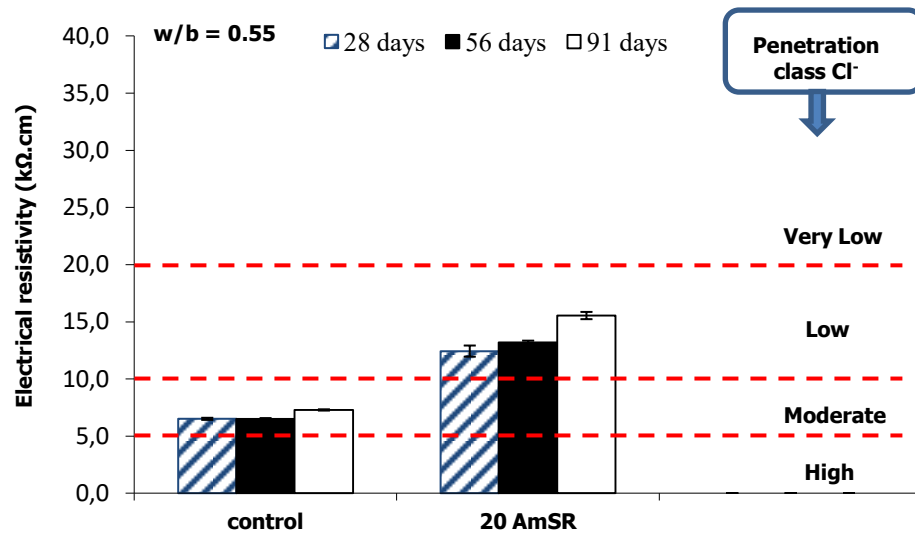


Figure 4-43: Electrical resistivity of OC incorporating 20% AmSR and control mixture ($w/b = 0.55$)

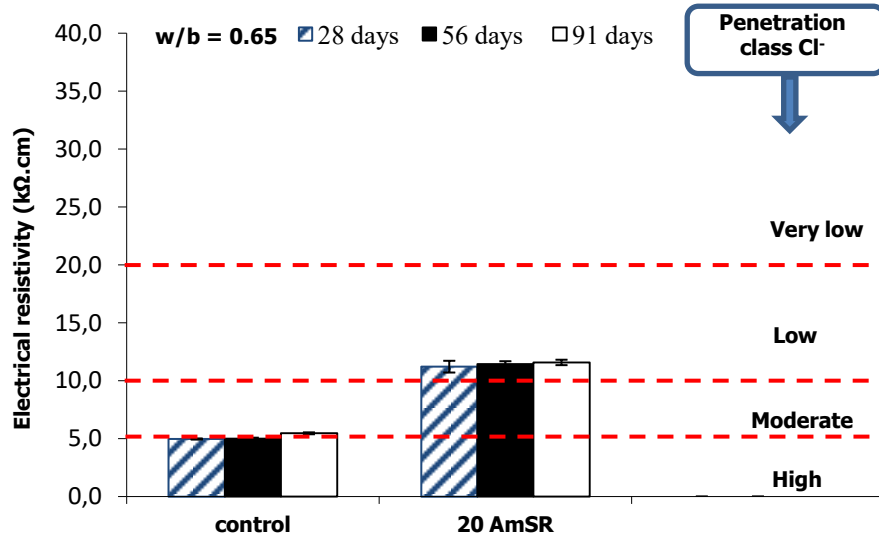


Figure 4-44: Electrical resistivity of OC incorporating 20% AmSR and control mixture ($w/b = 0.65$)

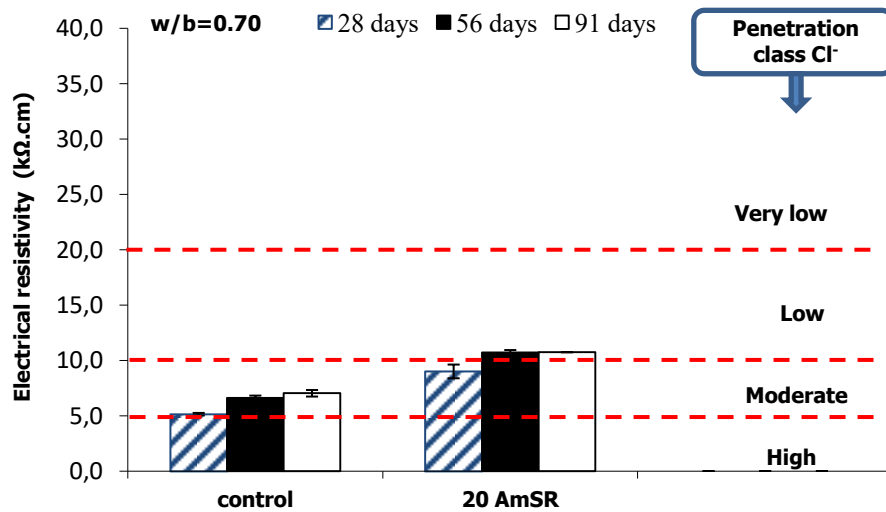


Figure 4-45: Electrical resistivity of OC incorporating 20% AmSR and control mixture ($w/b = 0.70$)

- **Chloride-ions penetration**

The results of penetration of chloride ions of HPC and OC mixtures with 0.40, 0.45, 0.50 and 0.70 of w/b at 28 and 91 days are shown in Figures 4-46 to 4-50. The results of chloride ions penetration of all mixtures were in agreement with their electrical resistivity results. It was observed that concrete with high electrical resistivity showed low chloride ions penetration. Opposite of the electrical resistivity results with increasing w/b, chloride ions penetration increased. The mixtures incorporating 20% AmSR showed significantly low penetrations chloride ions compared with their control mixtures. It can conclude that the replacement of cement by AmSR generates dens matrix, therefore, increased electrical resistivity and reduced permeability. According to ASTM C 1202 specification the class of penetration of chloride ions of concrete incorporating 20% AmSR with 0.35 and 0.40 of w/b, at 28 and 91 days were in very low level. The concrete incorporating 20% AmSR with 0.45 and 0.50 of w/b, at 28 and 91 days were in low level. The class of penetration of concrete incorporating 20% AmSR with 0.70 of w/b, at 28 and 91 days was in moderate level. It was seen that chloride ions penetration increased by increasing w/b. decreasing w/b leads to generation more gel in concrete. More quantity of gel generate denser matrix. Hence, decreasing w/b increases chloride ion penetration.

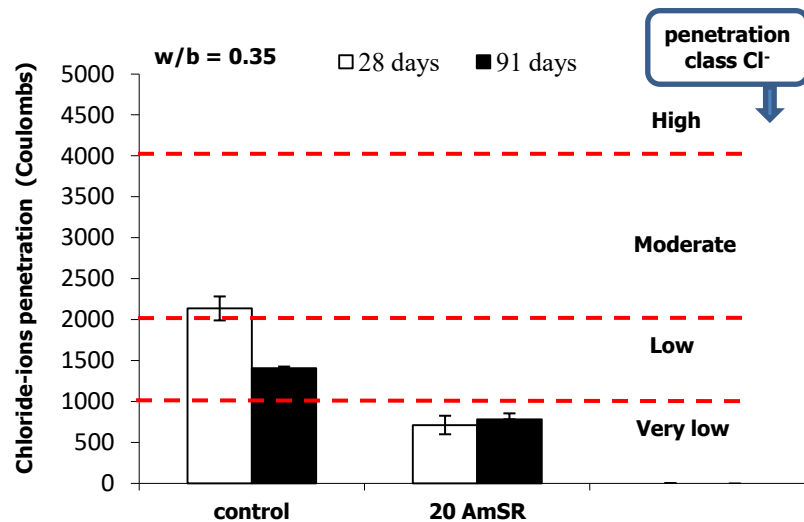


Figure 4-46: Chloride-ions penetration of HPC incorporating 20% AmSR and control mixture (w/b = 0.35)

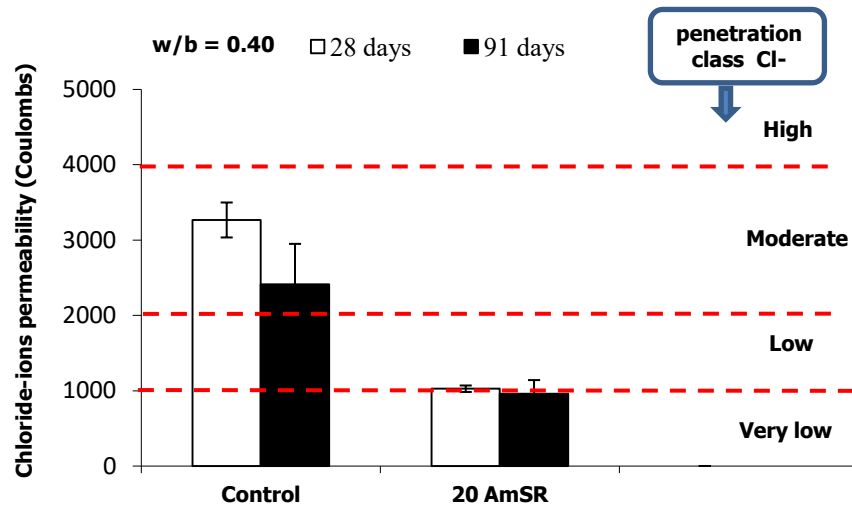


Figure 4-47: Chloride-ions penetration of OC incorporating 20% AmSR and control mixture ($w/b = 0.40$)

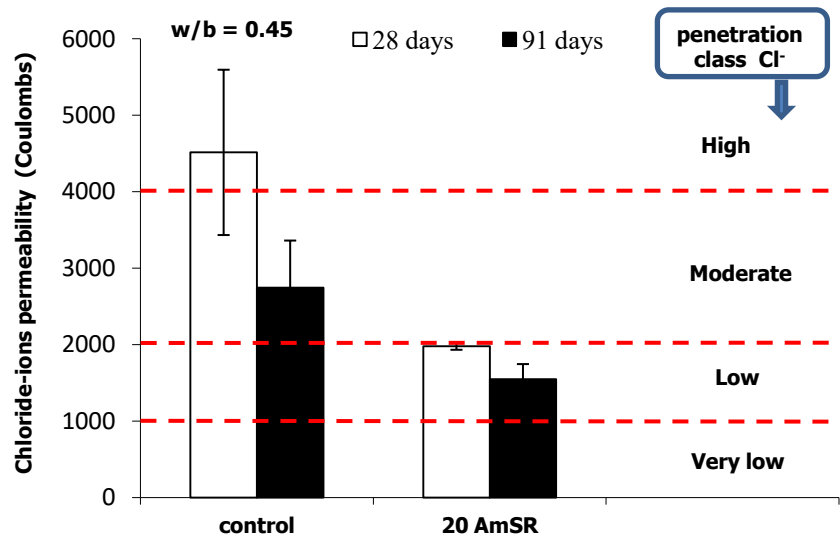


Figure 4-48: Chloride-ions penetration of OC incorporating 20% AmSR and control mixture ($w/b = 0.45$)

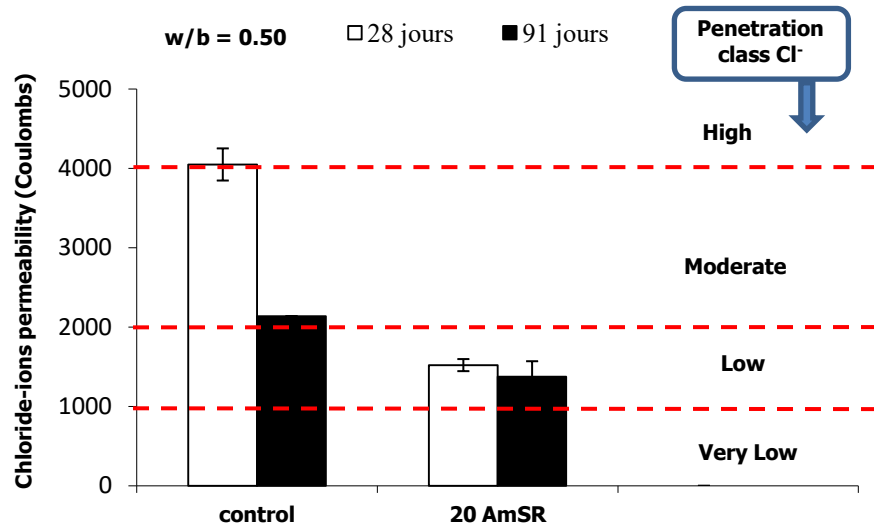


Figure 4-49: Chloride-ions penetration of OC incorporating 20% AmSR and control mixture ($w/b = 0.50$)

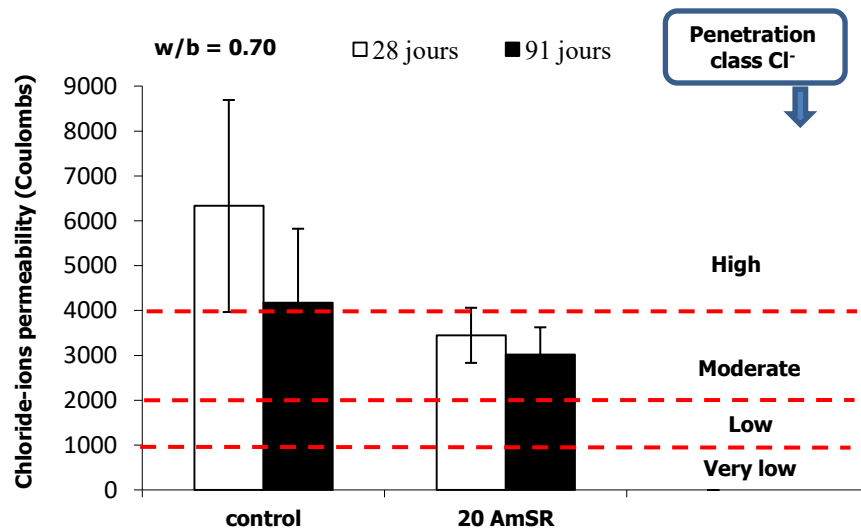


Figure 4-50: Chloride-ions penetration of OC incorporating 20% AmSR and control mixture ($w/b = 0.70$)

- **Autogenous shrinkage**

Autogenous shrinkage of cement paste and concrete is defined as the macroscopic volume change occurring with no moisture transferred to the exterior surrounding environment. It is a

result of chemical shrinkage affiliated with the hydration of cement particles (Holt, 2001). Autogenous shrinkage correspond water removed internally by a chemical reaction during hydration of binder. As the use of high-performance concrete has increased, problems with early age cracking have become prominent. The reduction in w/b contributes to this problem (Aitcin, 1998). The fundamental parameters contributing to the autogenous shrinkage and consequently early age cracking of high performance concrete could include the surface tension of the pore solution, geometry of the pore network, visco-elastic response of the developing solid framework, and kinetics of the cementitious reactions (Bentz et al, 2001; Bentz et al, 2004; Bentz et al, 2008). Because the capillary stresses are a function of the size of the pores being emptied, autogenous deformation is an extremely strong function of w/c ratio, increasing dramatically as the w/b is lowered below 0.35 in Portland cement systems. Figure 4-51 shows the results of autogenous shrinkage of concrete incorporating 20% AmR and control mixture with 0.35 of w/b. it was observed autogenous shrinkage of concrete in presence of AmSR was significantly less than control mixture. Consequently AmSR reduced risk of early age cracking in HPC.

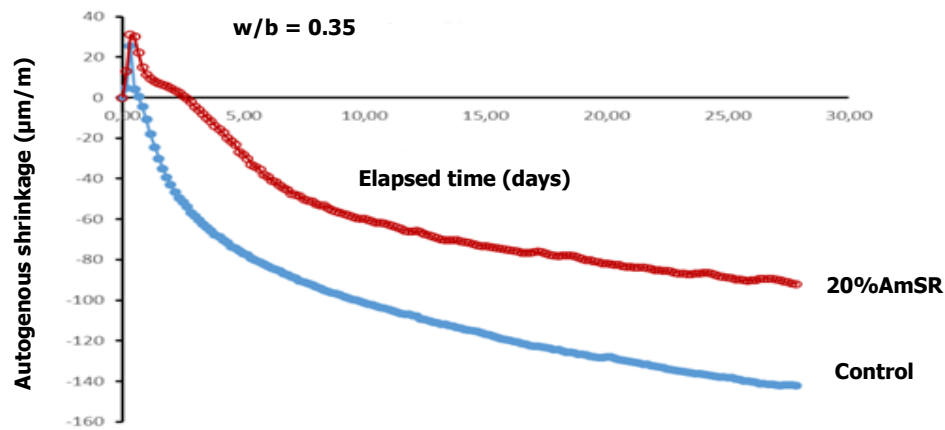


Figure 4-51: The autogenous shrinkage of HPC incorporating 20% AmR and control mixture (w/b = 0.35)

As shown in Figure 4-52, the variation of temperature of concrete incorporating 20% AmSR and control with 0.35 of w/b was substantially same during 30 days.

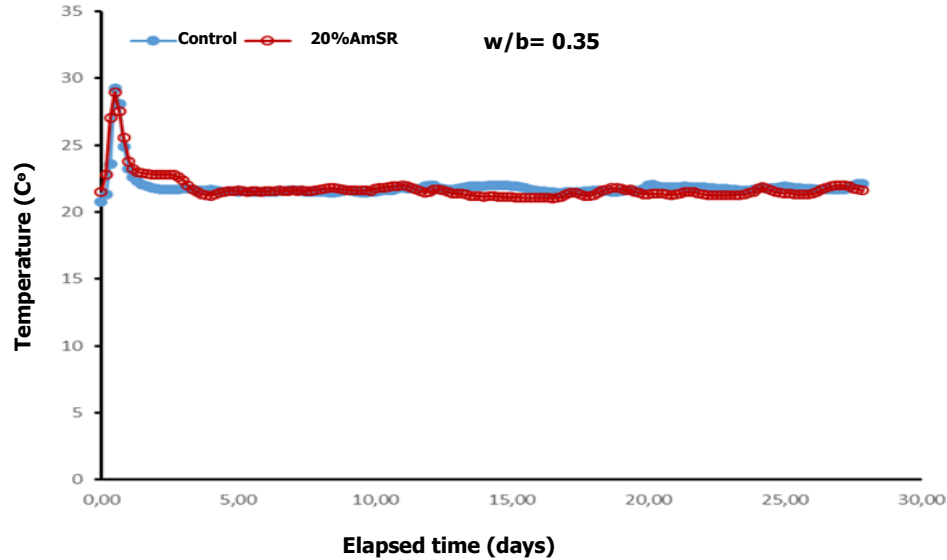


Figure 4-52: The variation of temperature of HPC incorporating 20% AmSR and control mixture ($w/b = 0.35$)

- Drying shrinkage**

The results of the drying shrinkage of HPC with 0.35 of w/b during 140 days are shown in Figure 4-53. It was observed that the expansion of HPC incorporating 20% AmSR and control mixture was same during 28 days curing period in lime water. After 28 days the test specimens are stored in air at room with temperature of 23 °C and about 50% humidity. The drying shrinkage of HPC 20AmSR was slightly more than control.

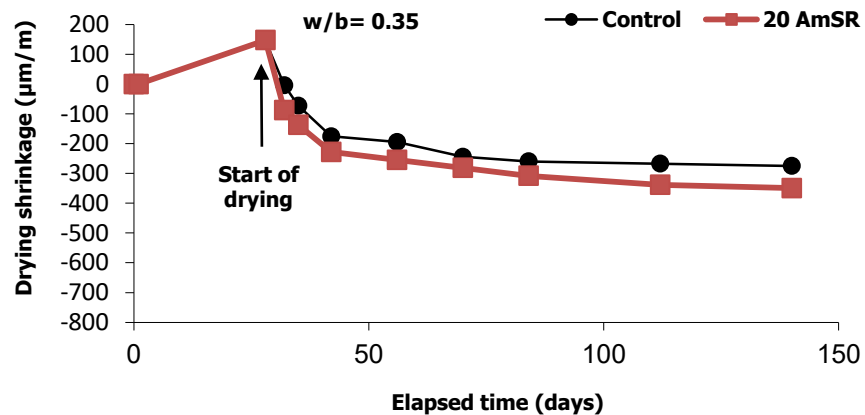


Figure 4-53: The drying shrinkage of HPC incorporating 20% AmSR and control mixture ($w/b = 0.35$)

The drying shrinkage of the OC series was measured up to 140 days after casting. All mixtures showed initial expansion during first 28 days, because of procedure of immersing the samples in lime-saturated water. This expansion may be helpful in limiting the contraction over drying period when air curing is started. As seen in Figure 4-54, OC incorporating 20 % AmSR with w/b of 0.40 showed slightly more expansion during first 28 days and less shrinkage until 140 days compare with control mixture.

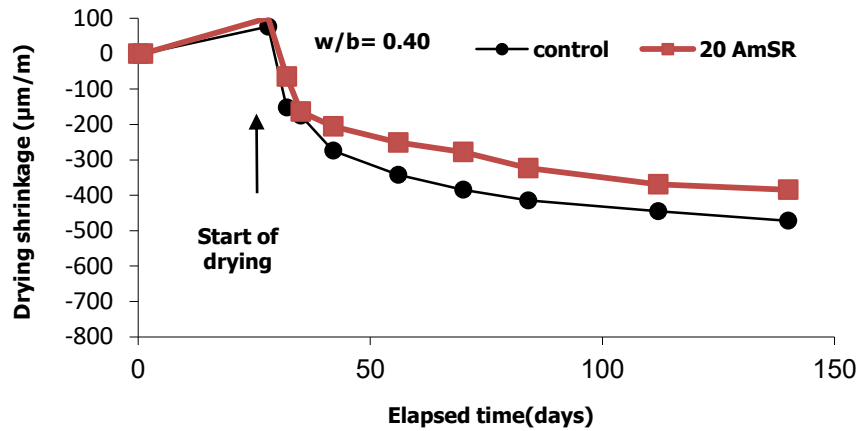


Figure 4-54: The drying shrinkage of OC incorporating 20% AmSR and control mixture (w/b = 0.40)

Generally, the required w/b to hydrate portland cement is 0.42 (Aitcin, 2007). The OC concrete with 0.45, 0.50, 0.55, 0.65 and 0.70 of w/b have more free water. The high free water in concrete can increase drying shrinkage. The results of drying shrinkage of OC with 0.45, 0.50, 0.55, 0.65 and 0.70 of w/b are presented in Figures 4-55 to 4-59. It was observed all OC mixtures incorporating 20% AmSR showed more expansion during first 28 days and more shrinkage after first 28 days. It can conclude that presence of AmSR in OC increased drying shrinkage.

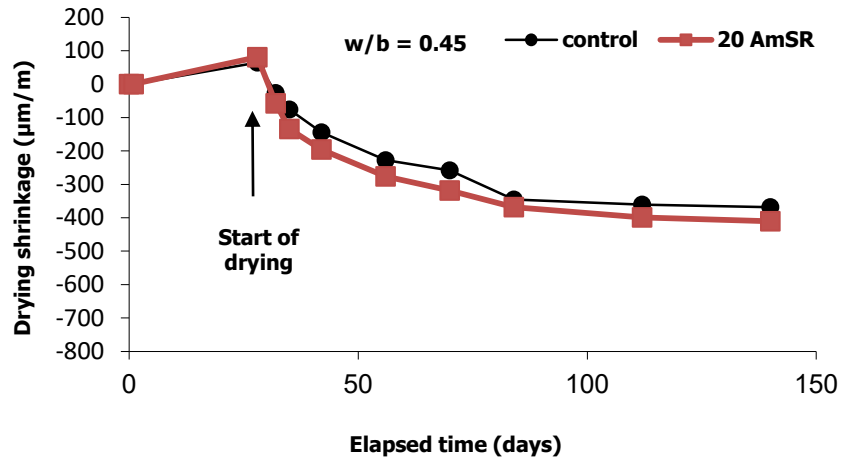


Figure 4-55: The drying shrinkage of OC incorporating 20% AmSR and control mixture ($w/b = 0.45$)

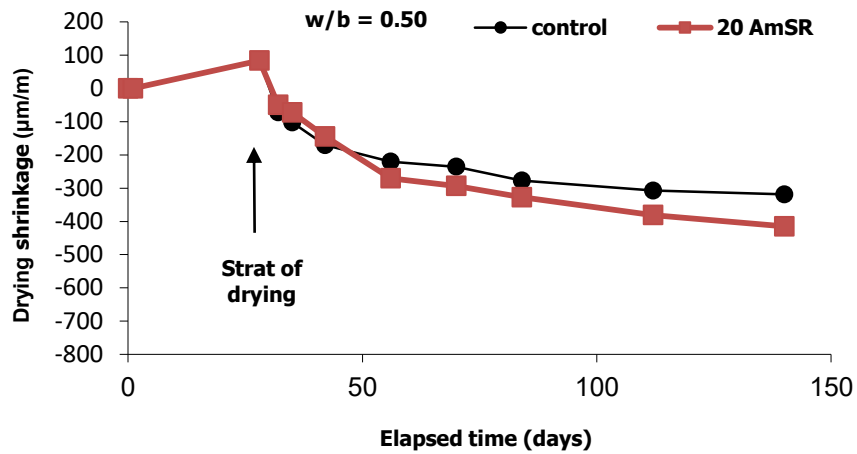


Figure 4-56: The drying shrinkage of OC incorporating 20% AmSR and control mixture ($w/b = 0.50$)

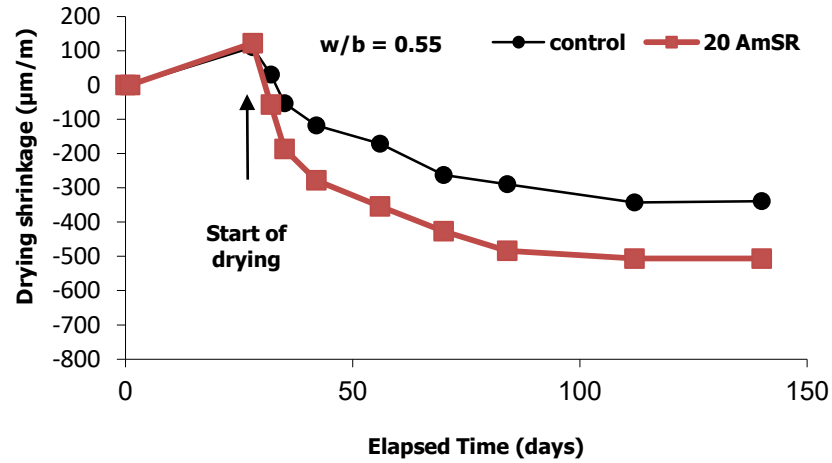


Figure 4-57: The drying shrinkage of OC incorporating 20% AmSR and control mixture ($w/b = 0.55$)

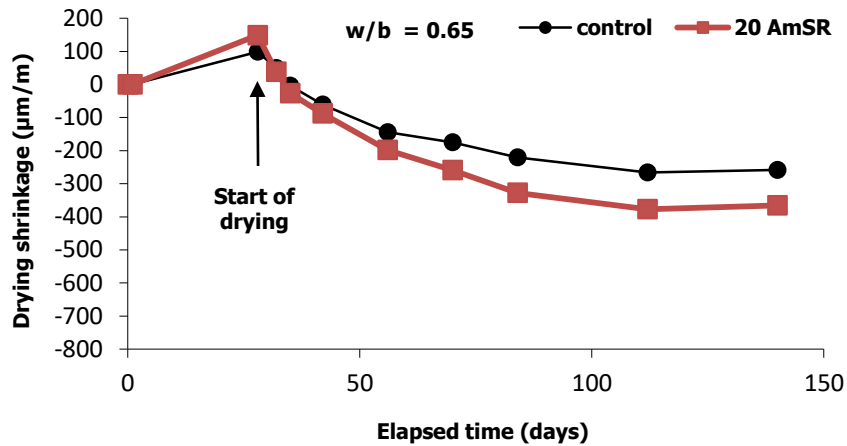


Figure 4-58: The drying shrinkage of OC incorporating 20% AmSR and control mixture ($w/b = 0.65$)

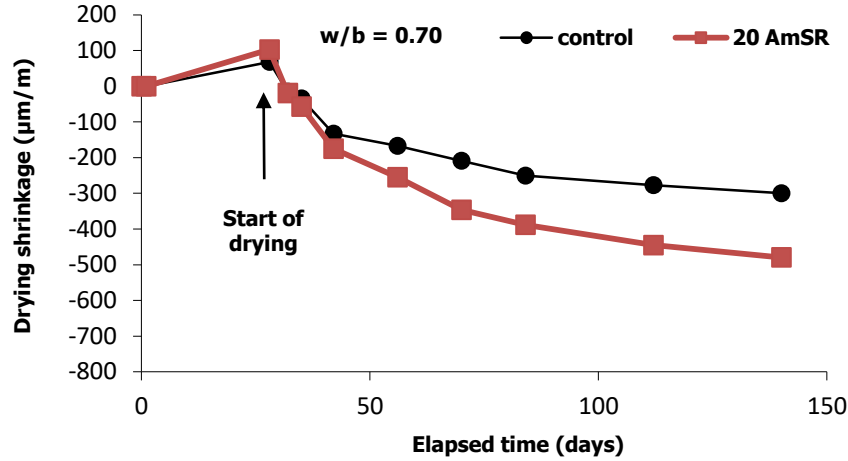


Figure 4-59: The drying shrinkage of OC incorporating 20% AmSR and control mixture ($w/b = 0.70$)

- **De-icing scaling**

According to BNQ 2621-900, a concrete is considered resistant to scaling when the average scaled residue on two slabs does not surpass 500 g/m^2 during 56 cycles of freezing and thawing. Figure 4-60 shows de-icing scaling results of HPC with 0.35 of w/b . It is observed that HPC 20AmSR had very low scaling residue. Its scaling residue was less than 170 g/m^2 at 28 days. The results of de-icing scaling of OC mixtures with 0.40, 0.45, 0.50 and 0.55 at 28 days are showed in Figures 4-61 to 4-64. It can be seen OC mixtures with 0.40 and 0.45 incorporating 20% AmSR and control satisfied the BNQ standard specification limit. Their scaling residues at 28 days measurement were less than 500 g/m^2 . The OC mixtures with 0.50 and 0.55 of w/b incorporating 20% AmSR had high scaling residue at 28 days. Their scaling residue surpassed BNQ 261-900 specification limit. This trend is mainly due to the increasing of w/b . The finishing process of the slabs surface can considerably change the air-void system, and thus it affects on resistance freezing and thawing action in the presence of de-icing salt (Bilodeau et al, 1994).

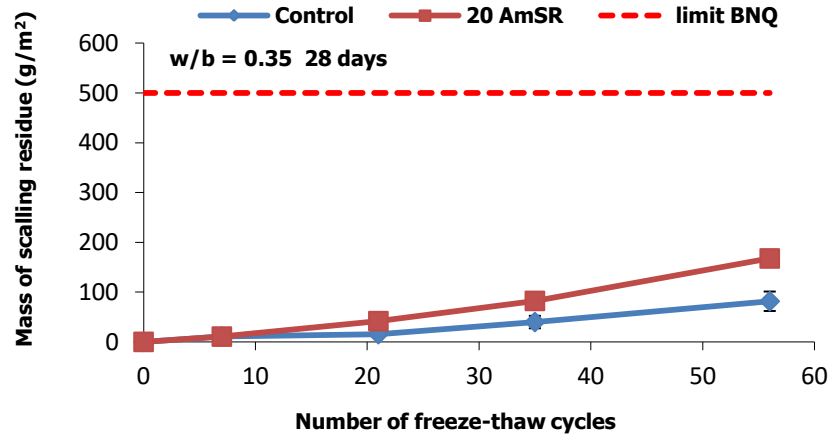


Figure 4-60: The de-icing scaling of HPC incorporating 20% AmSR and control mixture ($w/b = 0.35$)

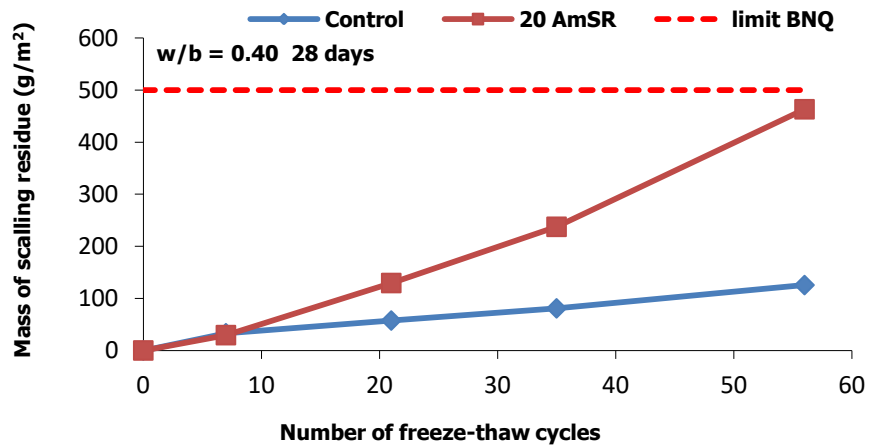


Figure 4-61: The de-icing scaling of OC incorporating 20% AmSR and control mixture ($w/b = 0.40$)

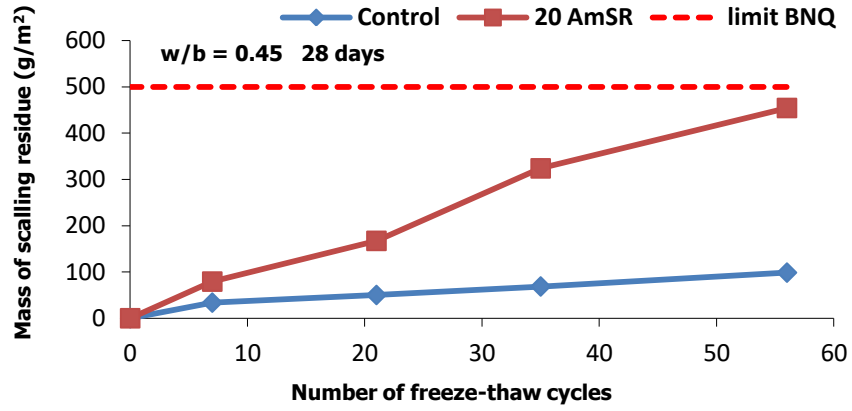


Figure 4-62: The de-icing scaling of OC incorporating 20% AmSR and control mixture ($w/b = 0.45$)

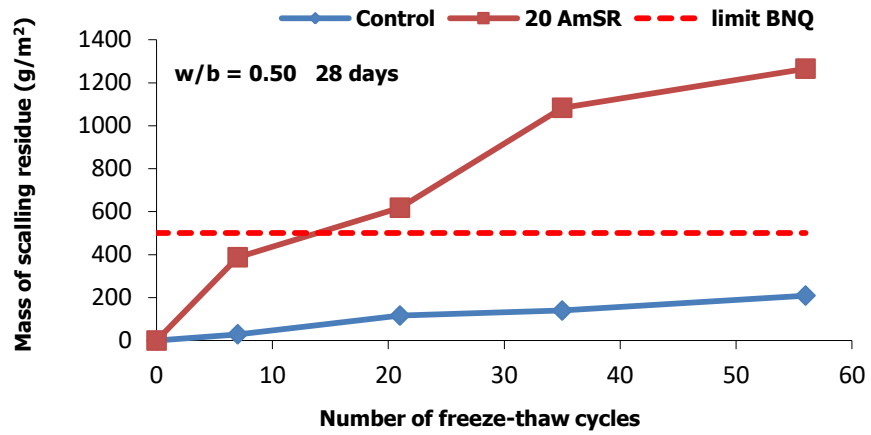


Figure 4-63: The de-icing scaling of OC incorporating 20% AmSR and control mixture ($w/b = 0.50$)

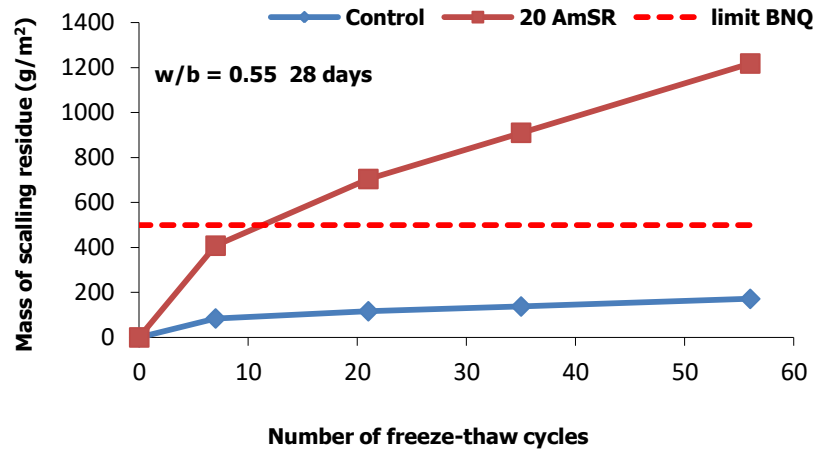


Figure 4-64: The de-icing scaling of OC incorporating 20% AmSR and control mixture ($w/b = 0.55$)

- Freezing thawing resistance

Freezing and thawing tests were started after 14 days of curing. The air content in concrete is important parameter that affects resistance to freezing and thawing. Table 4-17 shows durability coefficient of HPC with 0.35 of w/b and OC with 0.40, 0.45 and 0.50 of w/b . All of mixtures showed excellent durability after 300 freezing and thawing cycles. The durability coefficient of all mixtures is surpassed 60% which is minimum requirement of ASTM C 666 specification.

Table 4-17: The results of freezing thawing resistance

Durability coefficient (%)		
Mixtures	control	20% AmSR
HPC $w/b = 0.35$	104	102
OC $w/b = 0.40$	101	92
OC $w/b = 0.45$	102	101
OC $w/b = 0.50$	102	94

4.4.1.2 Self-consolidating concrete (SCC)

To evaluate fresh properties, mechanical, and durability of self consolidating concrete (SCC) incorporating AmSR, three concrete mixtures are done. The control mixture, and concrete incorporating 10 and 20% AmSR. For all SCC mixtures, type of SP was plastol 5000 and air entraining agent was Airex-L. The dosage of SP is adjusted to achieve 660 ± 30 of slump flow. The w/b was 0.42 and maximum size of aggregate was 14 mm. Table 4-18 shows composition of SCC mixtures. The fresh properties of SCC mixture are shown in Table 4-19.

Table 4-18: The composition of SCC mixtures

Materials	Unit	Density	SCC w/b = 0.42		
			Control	10 AmSR	20 AmSR
Cement GU	kg	3.15	425	382.5	340
AmSR		2.45	0	42.5	85
Water		1.00	178.5	178.5	178.5
Sand 0 - 5 mm		2.67	872	862	852
Aggregate 5 - 14 mm		2.71	905	905	905
Air-entraining agent (Airex-l)	ml/100 kg	1.00	7	7	7
SP (Plastol 5000)	l/m ³	1.07	2.4	3.4	4.5

Table 4-19: Fresh properties of SCC mixtures

Slump target = 660 ± 30				
characteristic	Unit	SCC w/b = 0.42		
		Control	10 AmSR	20 AmSR
Slump flow	mm	680	640	665
T ₅₀	s	2.3	2.6	2.5
Slump-J Ring	mm	20	50	55
VSI	-	1	0	0
J-Ring	mm	660	590	610
V-Funnel	S	5.75	6.46	5.84
Air content	%	8.2	8.1	8.6
Unit weight	kg/m ³	2234.6	2251.9	2180
Temperature	°C	20.8	21.3	21.6
τ^0	Pa	54.7	132.3	145.3
μ	Pa.s	14.5	17	18.5

4.4.1.2.1 Fresh properties

It was seen to achieve slump flow target, by increasing rate of replacement of cement by AmSR, dosage of SP significantly increased. Figure 4-65 shows the slump flow and dosage of SP for concrete incorporating 0, 10, and 20% AmSR.

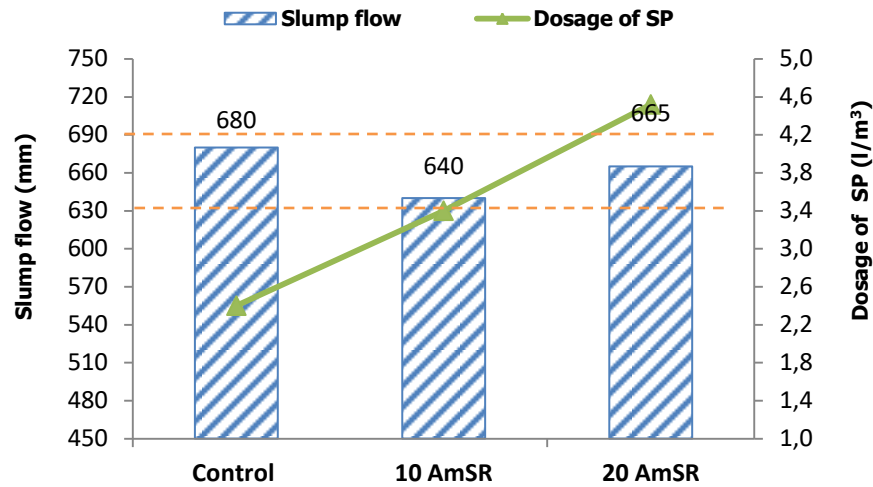


Figure 4-65: Comparison of dosage of SP and slump flow of SCC mixtures ($w/b = 0.42$)

Figure 4-66 shows the variation of the slump flow, V-Funnel and T_{50} of SCC mixtures. The passage facility without blockage through a thin section is measured by the flow time through the V-Funnel. The T_{50} is the flow time of SCC through the Abrams cone to 500 mm in diameter. These measurements give an indication of the viscosity of the concrete and its free flow. The SCC for structural applications with a slump flow between 620 and 720 mm should have a V-Funnel time and $T_{50} \leq 8$ seconds (Hwang et al, 2006). It was observed that all SCC mixtures in this project are in this range. The results of V-Funnel and T_{50} showed the same trend. The V-Funnel and T_{50} of SCC mixtures incorporating 10 and 20% were more than control. Because of high fineness of AmSR, viscosity of SCC increased by increasing of rate of replacement of cement by AmSR. Hence, T_{50} and V-Funnel increased by increasing rate of replacement.

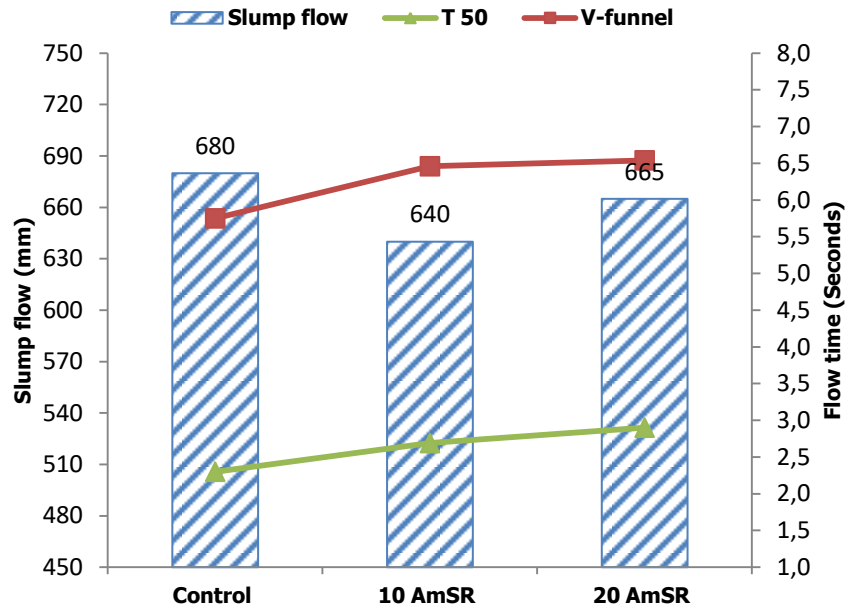


Figure 4-66: The comparison of V-funnel, T_{50} and slump flow of SCC mixtures ($w/b = 0.42$)

- **J-ring**

According to ASTM C 1621, if the difference between the slump flow and J-ring be less than 50 mm, hence, the SCC has good passage ability. As seen in Table 4-19, the difference between of slump flow and J-ring of control, SCC incorporating 10 and 20% AmSR were respectively 20, 50, 55 mm. The difference between of slump flow and J-ring for concrete incorporating 20% AmSR was 5 mm over limit of ASTM C 1621 specification. By increasing SP or viscosity agent can overcome this slight instability.

- **Plastic viscosity and shear yield stress**

The rheological parameters of studied SCC are shown in Figure 4-67. The shear yield stress of control mixture, SCC incorporating 10 and 20% AmSR were 54.7, 132.27 and 145.24 Pa.s respectively. The plastic viscosities were 14.5, 17 and 18.5 Pa respectively. Cruz in 2012 reported the concrete is considered self-compacting when their yield stress is between 50 to 200 Pa and the plastic viscosity between 20 to 100 Pa·s (Sotomayor Cruz, 2012).

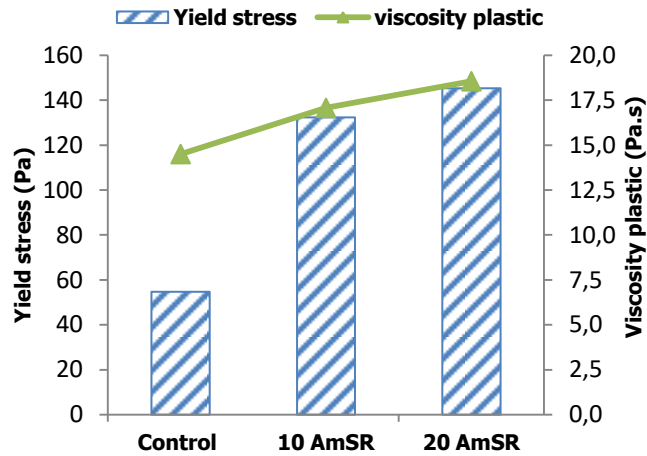


Figure 4-67: The yield stress and plastic viscosity of SCC mixture ($w/b = 0.42$)

It was observed that the replacement of cement by AmSR increased yield stress and plastic viscosity. It can conclude increasing rate of replacement of cement by AmSR decreased fluidity of SCC. The results of yield stress and plastic viscosity were in accordance with other fresh properties as T_{50} V-Funnel, slump flow and J-ring.

4.4.1.2.2 Mechanical properties

The evaluated mechanical properties of SCC were compressive strength at 1, 3, 7, 28 and 56 days, tensile splitting strength at 28 and 56 days, the flexural strength and modulus of elasticity at 28 days.

- **Compressive strength**

The results of compressive strength at 1, 7, 28 and 56 days are shown in Figure 4-68. It was seen, at early age the compressive strength of 10AmSR and 20AmSR SCC were less than control mixture. At 28 and 56 days the compressive strength of both SCC incorporating 10 and 20% were surpassed control compressive strength. Compressive strength of SCC incorporating 10% AmSR was more than 20%% AmSR at 28 and 56 days. The reason could be slightly high air content of SCC with 20% AmSR rather than SCC with 10% AmSR.

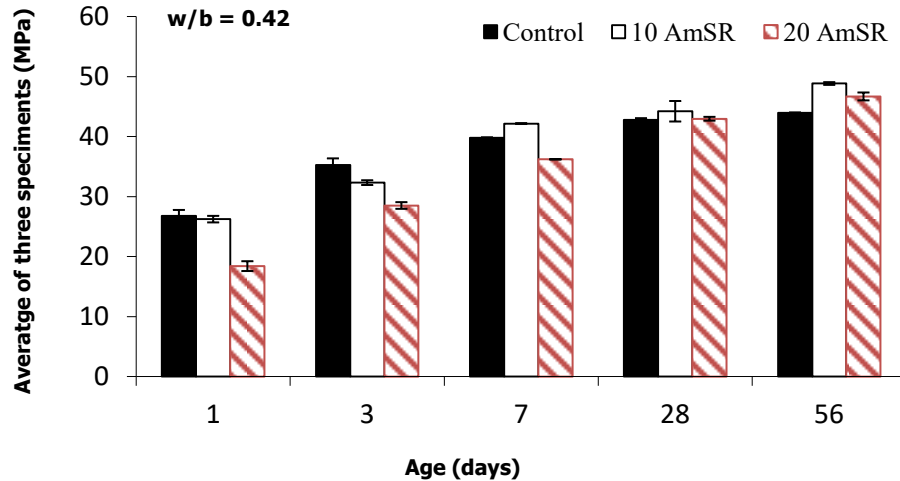


Figure 4-68: The compressive strength of SCC incorporating AmSR and control mixture ($w/b = 0.42$)

- Tensile splitting strength**

Figure 4-69 shows tensile splitting strength at 28 and 56 days. The trend of SCC tensile splitting strength was similar to compressive strength. The tensile strength of SCC incorporating 10% AmSR was more than that of SCC incorporating 20% AmSR and both of them were more than control mixture as well as trend of compressive strength results. The results obtained at 28 and 56 days compared with estimated results by ACI 363 specification based on compressive strength.

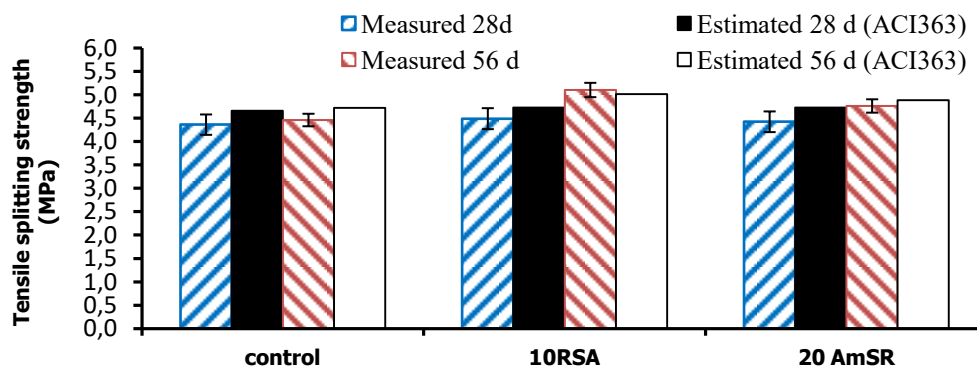


Figure 4-69: The tensile strength of SCC incorporating AmSR and control mixture ($w/b = 0.42$)

- **Flexural strength**

The flexural strength results of SCC at 28 days shows in Figure 4-70. It was observed that the flexural strength of SCC incorporating 10 and 20% AmSR at 28 days were near to control concrete. The flexural strength of control, 10AmSR and 20AmSR were 6.3, 6.28 and 6.2 MPa respectively. The flexural strength of SCC is compared with theoretical values estimated by the equation of ACI 363 specification.

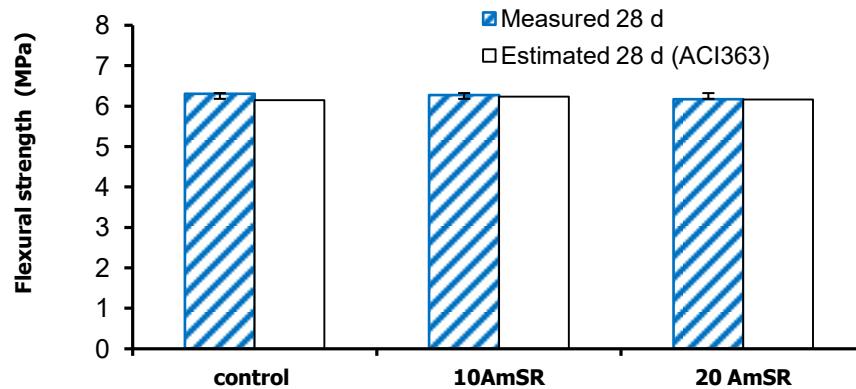


Figure 4-70: The flexural strength of SCC incorporating AmSR and control mixture ($w/b = 0.42$)

- **Modulus of elasticity**

The results of modulus of elasticity of SCC at 28 days are shown in Figure 4-71. The result of modulus of elasticity of all SCC was approximately same at 28 days. The modulus of elasticity of SCC incorporating 10, 20% and control were 33, 33.9 and 33 GPa respectively. Moreover, modulus of elasticity values is compared with BEAL equation.

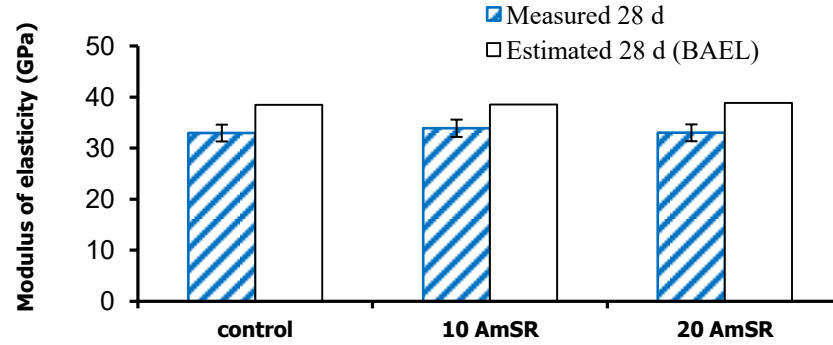


Figure 4-71: The modulus of elasticity of SCC incorporating AmSR and control mixture ($w/b = 0.42$)

4.4.1.2.3 Durability

- **Electrical resistivity**

Figure 4-72 shows results of electrical resistivity of SCC mixtures at 28 and 56 days. As seen before, for OC and HPC, adding AmSR as alternative supplementary cementitious material in concrete increased electrical resistivity. It was observed that the electrical resistivity of SCC incorporating 10 and 20% AmSR at 28 and 56 were in low penetration class. The penetration class of control SCC was in moderate level at 28 and 56 days. The electrical resistivity increased with increasing rate of replacement of cement by AmSR from 0 to 20%.

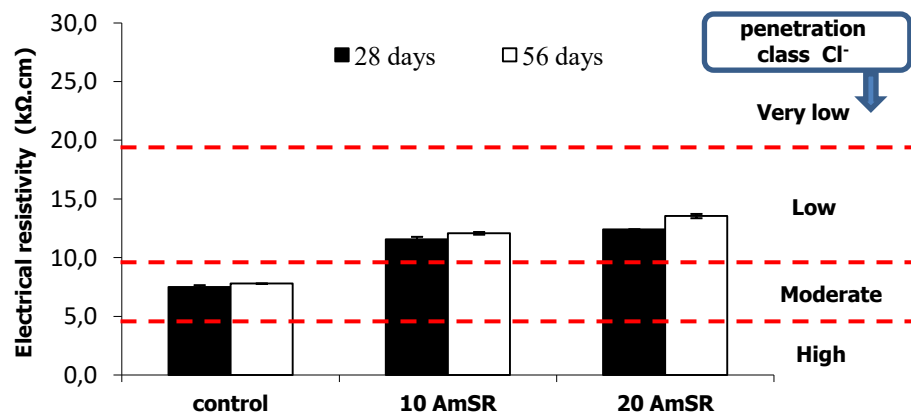


Figure 4-72: Electrical resistivity of SCC mixtures incorporating AmSR and control ($w/b=0.42$)

- **Chloride-ions permeability**

Figure 4-73 shows chloride ions permeability of SCC mixtures at 28 and 56 days. According to ASTM C 1202 specification, the class of penetration of chloride ions of SCC incorporating 10 and 20% AmSR at 56 days were in very low level. The control mixture at 56 days was in moderate penetration class. The chloride ions penetration significantly decreased with increasing rate of replacement of cement by AmSR from 0 to 20%.

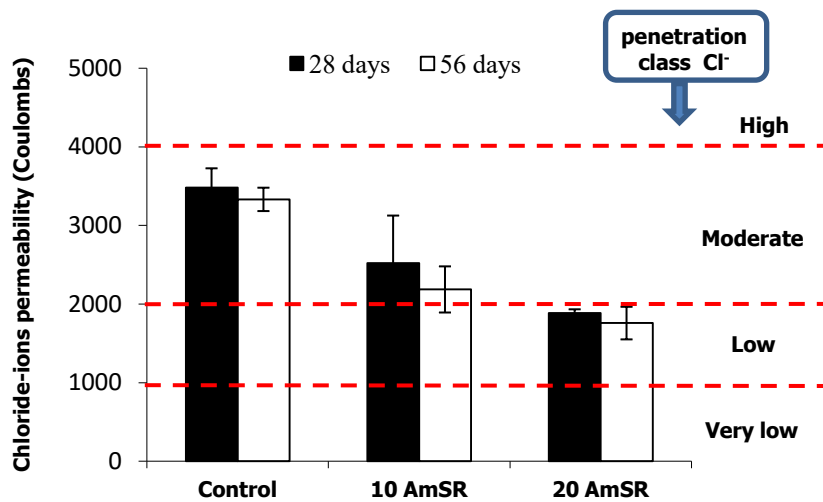


Figure 4-73: Chloride-ions penetration of SCC incorporating AmSR and control ($w/b = 0.42$)

- **Drying shrinkage**

The results of the drying shrinkage of SCC with 0.42 of w/b during 140 days are shown in Figure 4-74. The SCC incorporating 10% AmSR showed less drying shrinkage compare with control and the SCC incorporating 20 % AmSR showed more drying shrinkage compare with control during 140 days.

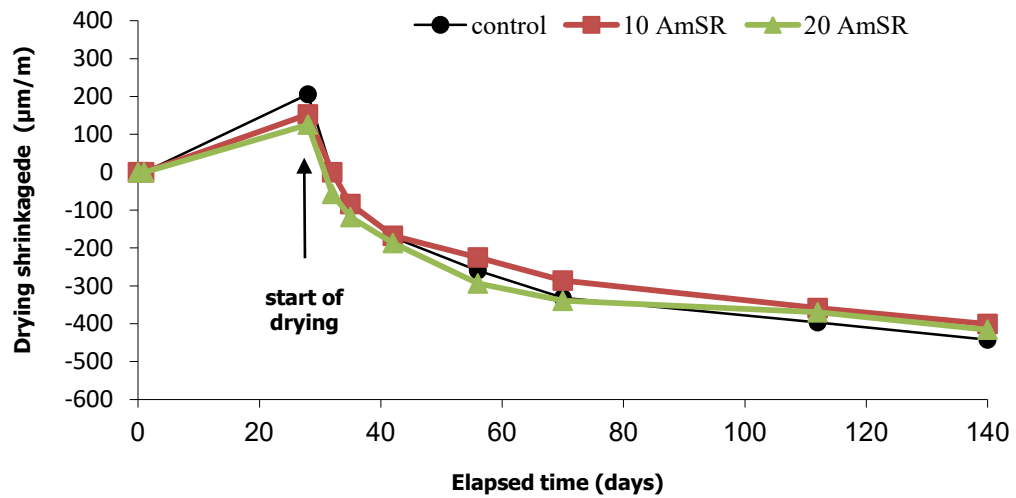


Figure 4-74: Drying shrinkage of SCC incorporating AmSR and control ($w/b = 0.42$)

- Freezing-thawing resistance

The results of freezing-thawing resistance of SCC mixtures are shown in Table 4-20. All of SCC mixtures showed excellent durability after 300 freezing and thawing cycles. The durability coefficient of SCC control, 10AmSR and 20AmSR were 100, 98 and 102% respectively, which surpassed 60% set by ASTM C 666 specification.

Table 4-20: The durability coefficient of SCC

Durability coefficient (%)			
Mixtures	control	10AmSR	20AmSR
SCC $w/b = 0.42$	100	98	102

4.4.2 Ternary concrete

Ternary concrete is manufactured with three different binders. The w/b for ternary concrete was 0.40. As explained in methodology, ternary combinations are composed of portland cement, AmSR and third binder was other SCMs as silica fume (SF), ground granulated blast furnace (GGBS), metakaolin (MK), fly ash F (FAF) and glass powder (GP). The results are compared with two controls concrete, which made with 100% TerCem 3000 and 100% TerC3 cements. The compositions of studied ternary concrete are presented in Table 4-21.

Table 4-21: The compositions of ternary concretes

Materials	Unit	Density	Ternary w/b = 0.40						
			Control#1	Control# 2	Ter-SF	Ter-GP	Ter-FAF	Ter-Slag	Ter-MK
Cement Portland (GU)	kg	3.15	0	0	300	300	300	292	300
Cement Ternary (Tercem 3000)		3.05	400	0	0	0	0	0	0
Cement Ternary (Ter C3)		2.98	0	400	0	0	0	0	0
AmSR		2.45	0	0	80	60	60	60	60
SF		2.22	0	0	20	0	0	0	0
GP		2.6	0	0	0	40	0	0	0
FA		2.53	0	0	0	0	40	0	0
GGBS		2.89	0	0	0	0	0	48	0
MK		2.51	0	0	0	0	0	0	40
Water		1.00	160	160	160	160	160	160	160
Sand 0 - 5 mm		2.67	660	660	664	668	670	673	668
Aggregate 5 - 14 mm		2.71	856	856	856	856	856	856	856
Aggregate 10 - 20 mm		2.73	214	214	214	214	214	214	214
Air-entraining agent (Airx-I)	ml/100 kg	1.00	40	46	38	0	22	32	44
Water reducers (Eucon DX)	ml/100 kg	1.15	250	250	250	250	250	250	250
SP (Plastol 6400)	l/m ³	1.07	0.72	0.83	2.17	1.40	1.40	1.60	2.00

The fresh properties and required dosage of chemical admixtures of ternary concrete are shown in Table 4-22. The slump, air content, unit weight, and temperature are measured at 10 and 50 minutes.

Table 4-22: The fresh properties and required dosage of chemical admixtures of ternary concrete

Characteristic	Unit	Ternary w/b = 0.40							
		Control#1	Control#2	Ter-SF	Ter-GP	Ter-FAF	Ter-Slag	Ter-MK	
Air-entraining agent (Airx-l)	ml/100 kg	40	46	38	0	22	32	44	
Water Reducer (Eucon DX)	ml/100 kg	250	250	250	250	250	250	250	
SP (Plastol 6400)	l/m ³	0.72	0.83	2.17	1.40	1.40	1.60	2.00	
Time of measurement	minutes	10 50	10 50	10 50	10 50	10 50	10 50	10 50	
Slump	mm	185 130	190 135	160 85	150 105	165 90	170 105	175 105	
Air content	%	7.2 6	5.9 4.6	7.1 5.2	7.3 6	6.6 4.7	6.9 5.8	7.8 5.9	
Unit weight	kg/m ³	2245 2288	2291 2338	2244 2311	2229 2259	2260 2305	2268 2292	2228 2286	
Temperature	°C	21.2 21.1	21.3 21.5	21 21	23.1 23	21.9 22	21.6 20.7	23 22.7	

4.4.2.1 Fresh properties

Figure 4-75 shows required chemical admixtures for studied ternary concrete. The required dosage of SP for Ter-SF and Ter-MK were more than other mixtures. The one of the reasons can be high fineness of SF and MK rather than other third binders. The Ter-SF has 20% AmSR, but other ternary mixtures have 15% AmSR.

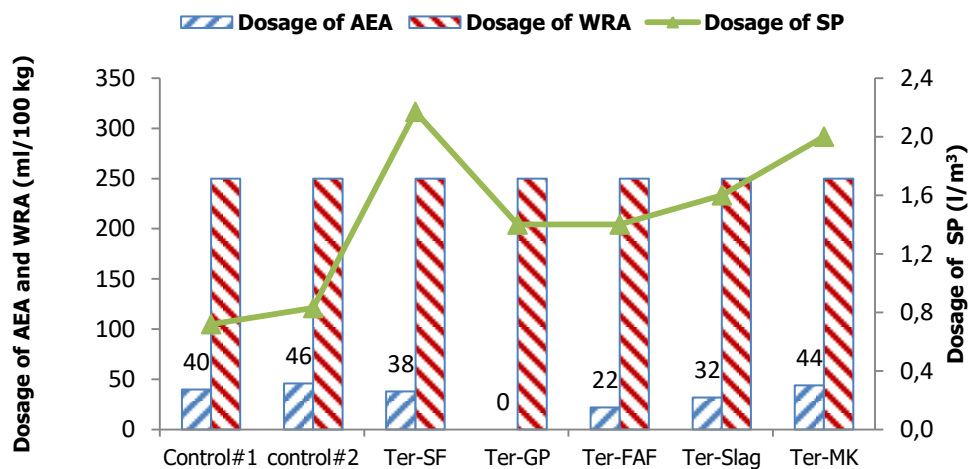


Figure 4-75: The required chemical admixtures for studied ternary concrete (w/b = 0.40)

The slump of ternary mixtures at 10 and 50 minutes are shown in Figure 4-76. The Ter-SF, Ter-FAF and Ter-Mk showed high slump loss compared to other mixtures. The Ter-GP showed less slump loss compared to other ternary mixtures. The air content at both 10 and 50 minutes is shown in Figure 4-77. The air content for all the mixtures was between 5 to 8% at 10 minutes.

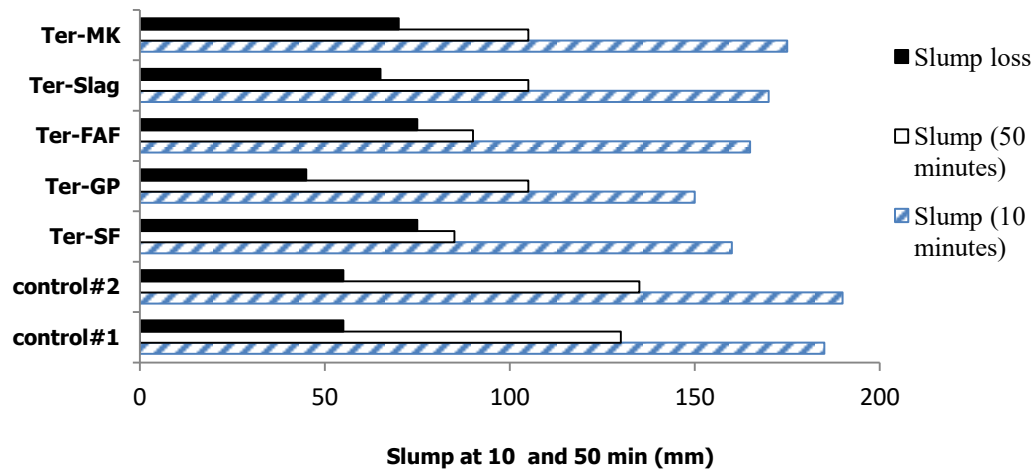


Figure 4-76: The slump and slump loss of ternary concretes ($w/b = 0.40$)

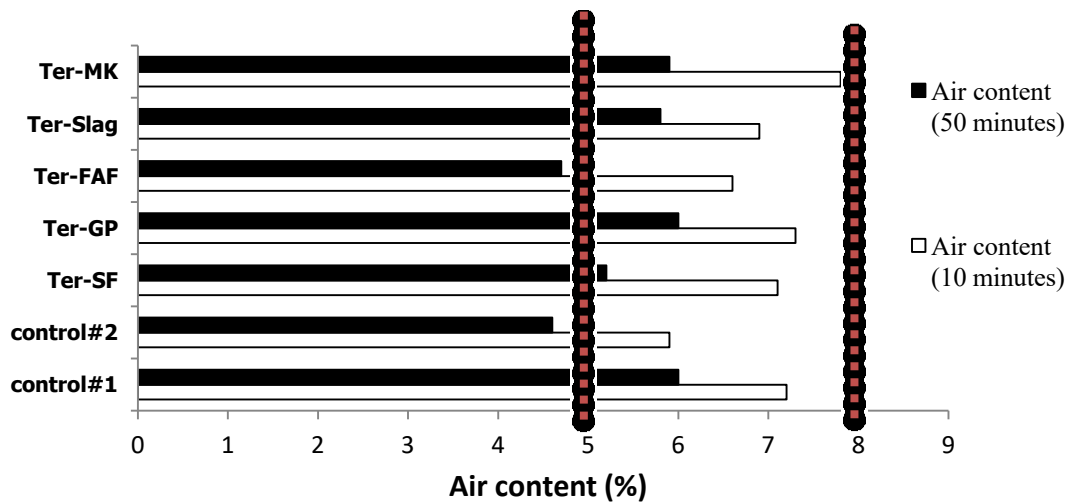


Figure 4-77: The fresh air content of ternary concretes ($w/b = 0.40$)

- **Setting time**

Figure 4-78 shows the initial, final setting times and the duration between the initial and final setting times. It should be noted that the dosage of chemical admixtures, quantity of AmSR and other used SCMs in ternary mixtures can affect on rate of hydration system. As shown in Figure 4-78, the ternary mixtures had rapid initial and final setting time compared to two controls mixtures.

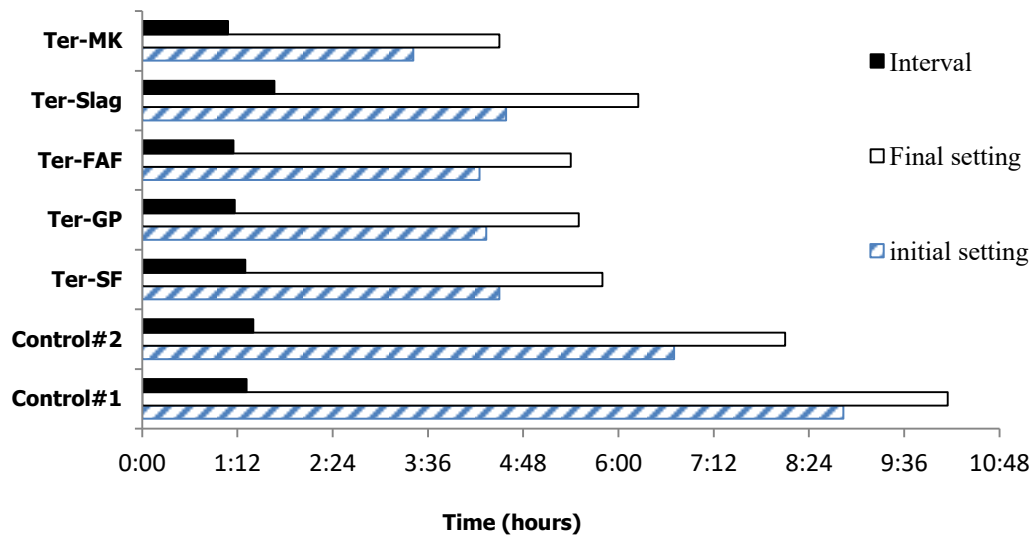


Figure 4-78: The initial and final setting time of ternary concretes ($w/b = 0.40$)

4.4.2.2 Mechanical properties

- **Compressive strength**

The results of compressive strength of ternary mixtures at 1, 3, 7, 28, 56 and 91 days under the standard curing conditions are shown in Figure 4-79. It was seen at 56 days all the mixtures surpassed specified compressive strength (50 MPa) except Ter-GP. The compressive strength of Ter-SF was more than control#1 and approximately same as control#2 at 56 days. The compressive strength of Ter-Mk was more than other mixtures at 28, 56 and 91 days. It was observed AmSR had very good synergy with other binders.

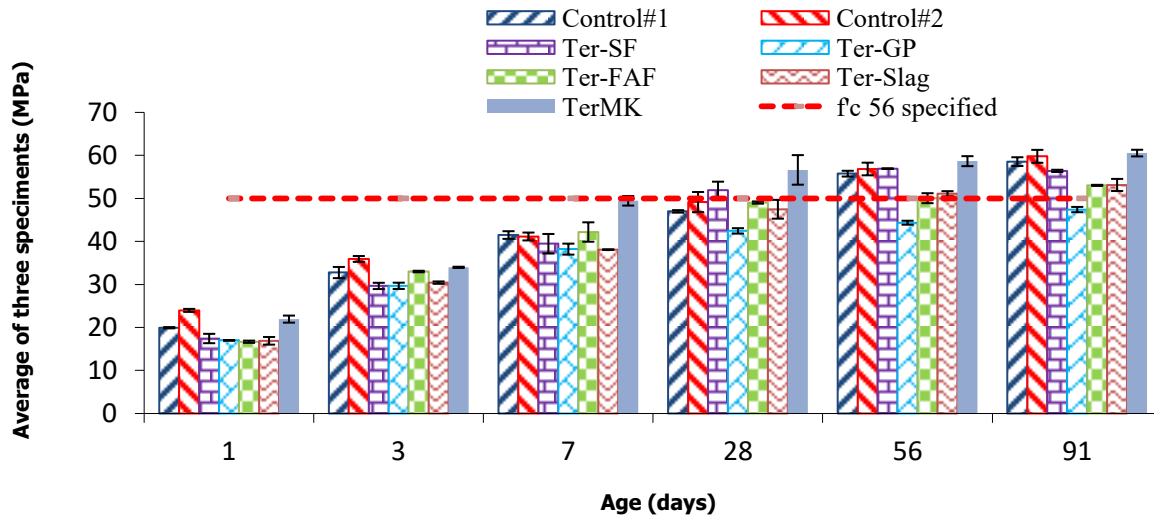


Figure 4-79: The compressive strength of ternary concretes ($w/b = 0.40$)

- Tensile strength**

The comparison of tensile splitting strength of ternary mixtures and two control mixtures at 28 and 91 days is shown in Figure 4-80. The results obtained at 28 and 91 days are compared with estimated results by ACI 363 specification based on compressive strength. The estimated values by ACI 363 show relatively same trend of measured values. This observation shows that ACI 363 provides very good estimation of tensile strength of concrete. It can see the trend of tensile strength is similar to compressive strength of each concrete mixture.

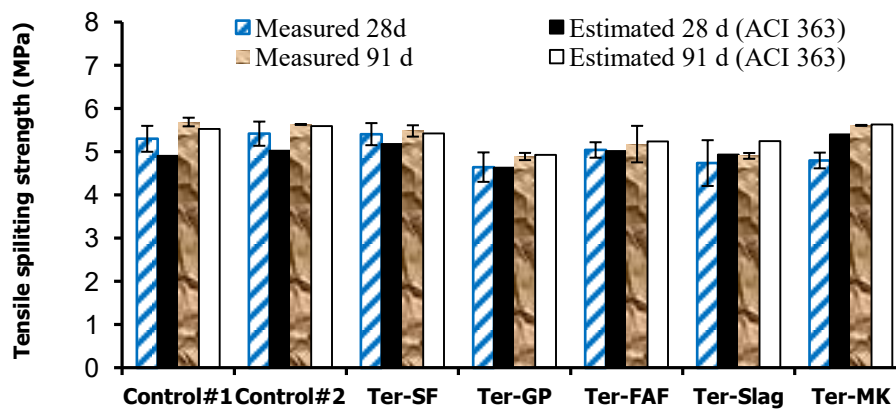


Figure 4-80: The tensile splitting strength of ternary concretes ($w/b = 0.40$)

4.4.2.3 Durability

- **Electrical resistivity**

Figures 4-81 shows results of electrical resistivity of ternary mixtures at 28, 56 and 91 days. At 28 days all mixtures were in very low penetration class except of Ter-GP, Ter-FAF and Ter-Slag which were in low penetration class. The reason of relatively low electrical resistivity of ternary concrete incorporating glass powder (GP), Fly ash (FAF) and Ground granulate blast furnace slag (GGBS) is relatively low fineness of these three SCMs compared with Metakaolin (MK) silica fume (SF). As explained before SCMs with higher fineness generate more impermeable matrix in concrete. At 56 and 91 days all mixtures were in very low penetration class. The control#1, control#2, Ter-SF and ter-MK showed significantly high electrical resistivity compared to Ter-GP, Ter-FAF and Ter-Slag.

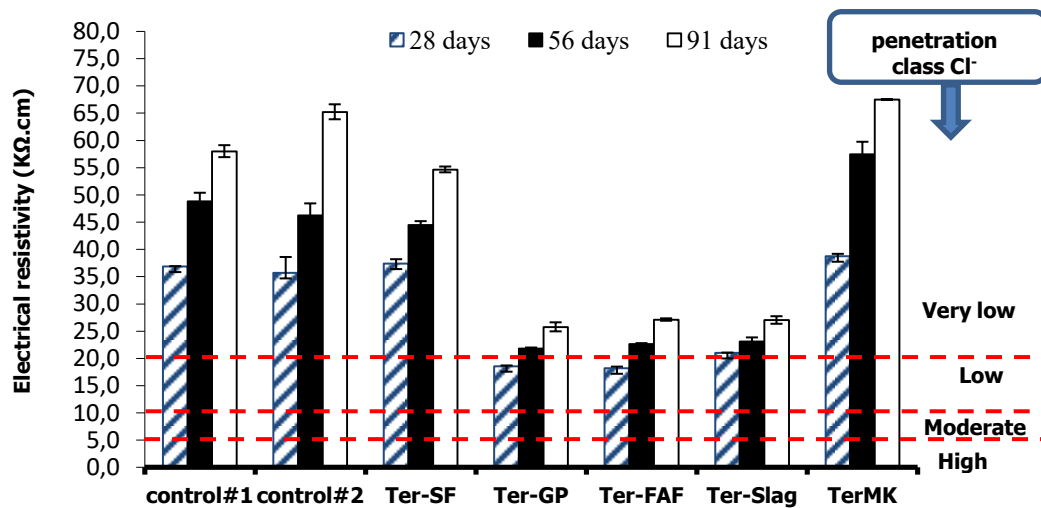


Figure 4-81: The electrical resistivity of ternary concretes ($w/b = 0.40$)

- **Chloride-ions penetrations**

Figure 4-82 presents chloride ions penetrations of ternary mixtures at 28 and 91 days. As observed before, for concrete binary systems, the results of chloride ions penetration of ternary concrete were in agreement with their electrical resistivity results. Similar to electrical resistivity

results, At 28 days all mixtures were in very low penetration class except Ter-GP, Ter-FAF and Ter-Slag which were in low penetration class. At 91 days all mixtures were in very low class of penetrations. The reduction of chloride ions penetration in presence of SCMs is widely reported (Papadakis, 2000; Zidol, 2014). According to Tinnea, because of pozzolanic properties of SCMS, concrete incorporating SCMs provides a less permeable matrix, and high electrical resistivity (Tinnea et al, 2009). As seen in binary concrete, replacing cement by AmSR generates less impermeable matrix and increased electrical resistivity. Therefore ternary concrete incorporating AmSR and SCMs showed high electrical resistivity and less chloride ions penetration.

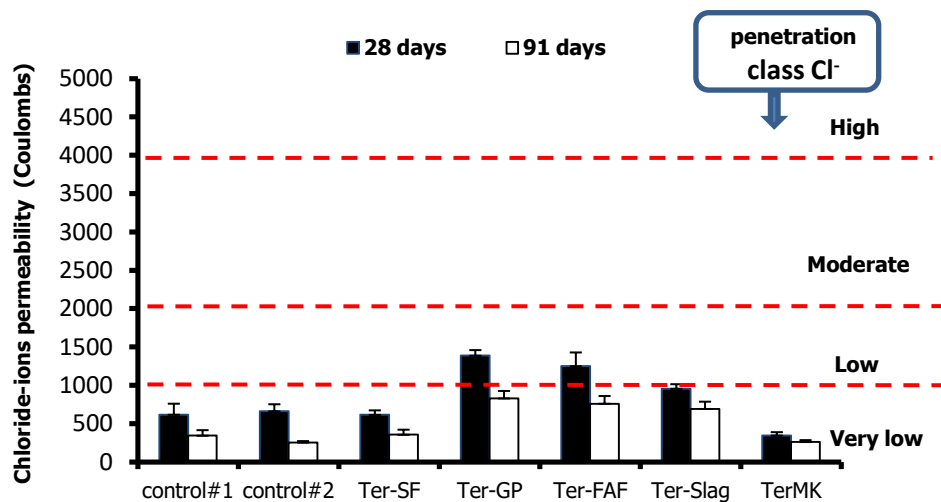


Figure 4-82: The chloride-ions penetration of ternary concretes ($w/b = 0.40$)

- **Drying shrinkage**

Figure 4-83 shows the results of drying shrinkage of ternary concretes with 0.40 of w/b during 140 days. It was observed that the expansion of Ter-Slag during first 28 days was significantly more than other ternary mixtures, and expansion of Ter-MK during first 28 days was less than other ternary mixtures. Ter-Slag showed less shrinkage compared to other ternary mixtures. The reason is high expansion of Ter-Slag during 28 days. It seen the shrinkage of Ter-SF, Ter-Gp and control#2 mixtures was approximately same at 140 days. The Ter-MK, Ter-FAF and control#1 mixtures showed same shrinkage at 140 days.

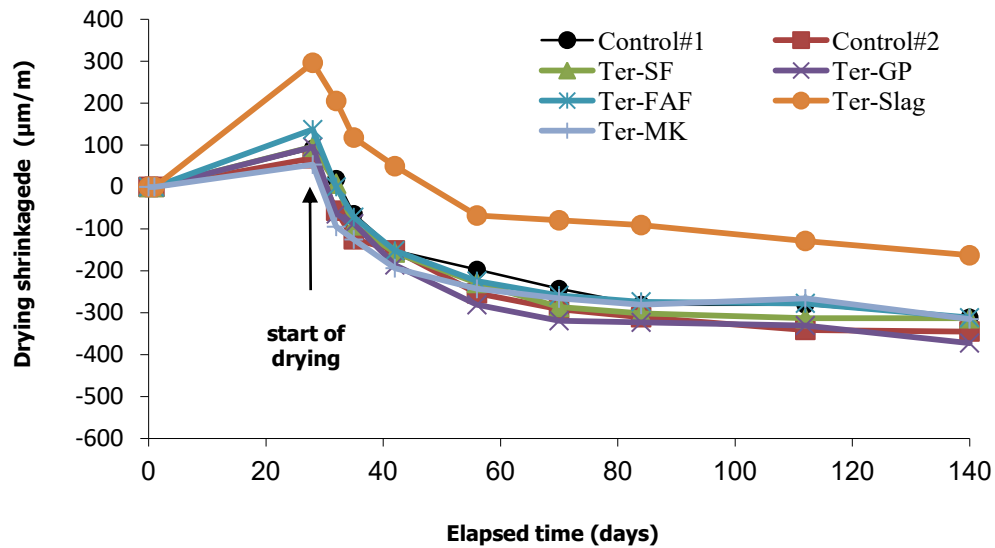


Figure 4-83: Drying shrinkage of ternary concretes ($w/b = 0.40$)

- **De-icing scaling**

Figure 4-84 shows results of scaling of ternary concretes with 0.40 of w/b at 28 days. As mentioned before according to BNQ 2621-900 standard, a concrete is considered resistant to scaling when the average scaled residue mass measured on two slabs does not surpassed 500 g/m^2 during 56 cycles of freezing and thawing. The sufficient air in concrete can improve concrete resistance against of freezing and thawing cycles, but it can not prevent scaling of the concrete surface due to the combined effect of freezing-thawing and the action of de-icing salt. It seen that the Ter-Slag, Ter-FAF, Ter-GP and control#1 had low scaling residue. Their scaling residues satisfied the limit of de-icing scaling resistance. The Ter-SF, Ter-Mk and control#2 mixtures showed high scaling residue. Their scaling residue surpassed BNQ 261-900 specification limit. It expects that the amount of scaling residues significantly decrease after 91 days curing. As explained before the finishing surface of the slabs can significantly change the air-void system, and therefore it affects freezing and thawing resistance in presence of de-icing salt.

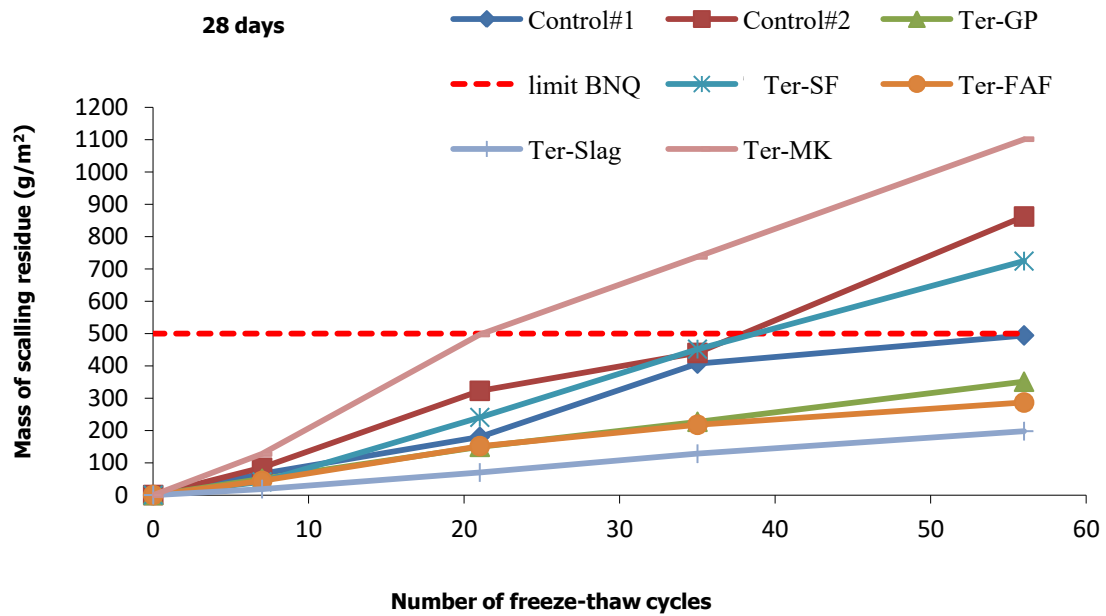


Figure 4-84: The de-icing scaling of ternary concretes ($w/b = 0.40$)

- Freezing-thawing resistance

Freezing-thawing tests were started after 14 days of curing. Table 4-23 shows durability coefficient of ternary concretes with 0.40 of w/b . All of mixtures showed excellent durability after 300 freezing and thawing cycles. The durability coefficient of all mixtures is surpassed 60% set by ASTM C 666 specification.

Table 4-23: The durability coefficient of ternary concretes

Durability coefficient (%)							
Mixtures	Control#1	Control#2	Ter-SF	Ter-GP	Ter-FAF	Ter-Slag	Ter-MK
Ternary concrete $w/b = 0.40$	100	99	103	96	99	97	100

5. Conclusions and recommendations

5.1. Conclusions

In this project two industrial by-products are investigated as alternative supplementary cementitious materials (ACMs), wastepaper sludge ash (WSA) and non-toxic amorphous Silica Residue (AmSR). Wastepaper sludge ash is by-product of combustion of de-inking sludge, bark and residues of woods in fluidized-bed system from Brompton mill located near Sherbrooke city and AmSR is by-product of production of magnesium from Alliance Magnesium near of Asbestos and Thetford Mines Cities Quebec, Canada. During decade wastepaper sludge ash had been studied as ASCMs in concrete group of university of Sherbrooke. Utilization of WSA as cementitious material in concrete manufacturing leads to reduce the quality of concretes. These problems are caused by disruptive hydration products of biomass fly ash once these ashes partially blended with cement in concrete manufacturing. The pre-wetting process of these biomass fly ashes enabled us to reduce disruptive hydration products. Moreover, in this project the AmSR as new industrial by-product is investigated for its valorization in cementitious system. This study aimed to develop an economic and ecological concrete containing the partial replacement of cement by WSA or AmSR. The following conclusions are drawn from the study of characterizations and performance of mortar and concrete incorporating WSA or AmSR in this thesis:

a) WSA

- ✚ The specific surface Blaine of pre-wetted WSA is $360 \text{ m}^2/\text{kg}$, which is near to Portland cement;
- ✚ The D_{50} of Portland cement, regular and pre-wetted WSA are 16.2, 47.6 and $89.41 \mu\text{m}$;
- ✚ The regular and pre-wetted WSA have relatively higher carbon content (indicated as LOI), thus leading to absorbing water and requiring more admixtures for concrete manufacturing;
- ✚ The WSA is rich in CaO , SiO_2 and Al_2O_3 contents, also it has high content of SO_3 (more than limit (5%) of ASTM C 618) ;

- ✚ The main crystalline phases of WSA are lime, anydrit, calcite, meyenite, portlandite and quartz and the main crystalline phases are ettringite, calcite, quartz, portlandite and Albite. In fact, lime converted to portlandite and also partially reacts with meyenite to create carboaluminate and carboaluminates reacts with anydrite to create ettringite;
- ✚ Replacement of cement by regular and pre-wetted WSA increased water demand. The water demand of pre-wetted WSA is more than regular WSA;
- ✚ Partial replacement of regular WSA as cement replacement, increase both initial and final setting time, and partial replacement of pre-wetted WSA as cement in concrete decrease initial and final setting time (decreased setting time is in range of CSA 3004);
- ✚ Replacement 20% of cement by pre-wetted WSA in mortar with 0.485 of w/b, increased 13% strength activity index (SAI) at 56 days compare with regular WSA;
- ✚ Replacement 20% of cement by pre-wetted WSA in concrete with 0.40 of w/b, improved 25% compressive strength compare with regular WSA at 91 days. The compressive strength of 20% pre-wetted WSA concrete was around 2% less than control;

b) AmSR

- ✚ The specific surface Blaine of AmSR is around $4907 \text{ m}^2/\text{kg}$, which is approximately ten times higher than Portland cement. It should be noted that the higher fineness significantly influence the kinetic of hydration reaction and increase the water demand;
- ✚ The D_{50} of Portland cement and AmSR are 16.2, 8.4 μm ;
- ✚ The AmSR is rich in SiO_2 (60%) and based XRD result their silica is amorphous;
- ✚ The strength activity (SAI) of mortar with 0.485 of w/b improved by replacement 10, 15, 20 and 25% of cement by AmSR. The SAI for all mortar mixtures except 30% AmSR were more than 100% since 7 days to 182 days;
- ✚ The strength activity (SAI) of mortar with w/b = 0.40 is improved by replacement 10%, 15% and 20% of cement by AmSR;
- ✚ The SAI of mortars incorporating 20% AmSR with 0.40 and 0.485 of w/b was respectively 125.6% and 126% which was more than other mortar mixtures. Hence, the optimum rate of replacement of cement by AmSR is suggested around 20%;

- ✚ The electrical resistivity of mortar significantly increased by increasing rate of replacement of cement from 10 to 30%;
- ✚ The HPC with 0.35 of w/b incorporating AmSR showed approximately same compressive strength compare with control at 91 days. Its compressive strength was 2.7% less than control at 91 days;
- ✚ The replacement of cement by AmSR improved compressive strength of OC mixtures with 0.40, 0.45, 0.50, 0.55 and 0.65 of w/b compare with their control mixtures. But the compressive strength of OC with 0.70 of w/b incorporating 20% AmSR was 3.9% less than control at 91 days;
- ✚ The rate of improvement of compressive strength of HPC with 0.35 of w/b and OC mixtures with 0.40, 0.45, 0.50, 0.55, 0.65 and 0.70 of w/b incorporating 20% AmSR compare with their control mixtures were -2.7%, +7.3%, +20%, +13.2%, +12.9%, +8.8%, -3.9%. Hence, the w/b affected the rate of improvement of concrete incorporating AmSR compare with control mixtures. The OC 20AmSR with 0.45 of w/b showed more compressive strength improvement;
- ✚ The trend of tensile and flexural strength and modulus of elasticity of HPC and OC mixtures were same as their compressive strength;
- ✚ The electrical resistivity of HPC and OC mixtures with presence of 20% AmSR significantly increased compare with their control. The concrete with high electrical resistivity shows low risk of corrosion;
- ✚ The chloride-ions penetration of all mixtures of HPC and OC incorporating 20% AmSR significantly decreased compare with their control. The concrete incorporating 20% AmSR shows good durability;
- ✚ The autogenous shrinkage for concrete with low w/b (less than 0.40) is important and could generate early age cracking. The autogenous shrinkage of HPC with 0.35 of w/b incorporating 20% AmSR was significantly less than control mixture during 30 days. The variation of temperature of HPC incorporating 20% AmSR and control with 0.35 of w/b was substantially same during 30 days;
- ✚ The HPC and OC mixtures incorporating 20% AmSR showed more expansion compare with their control during first 28 curing days. The HPC 20AmSR showed slightly more drying shrinkage compare with control. All OC mixtures incorporating 20 % AmSR

except of OC with 0.40 of w/b showed more drying shrinkage compare with their control mixtures;

- ✚ The scaling residue of HPC 20AmSR with 0.35 of w/b was very low. Its scaling residue was less than 170 g/m^2 after 56 cycles (the scaling residue less than 500 g/m^2 recommended by BNQ 2621-900);
- ✚ The OC mixtures with 0.40 and 0.45 incorporating 20% AmSR satisfied the demand of de-icing scaling resistance (less than 500 g/m^2). But, the scaling residue of OC with 0.50 and 0.55 surpassed limit of BNQ 2621-900 (more than 500 g/m^2) ;
- ✚ Based on freezing-thawing results of HPC with 0.35 of w/b and OC mixtures with 0.40, 0.45 and 0.50 of w/b incorporating 20% AmSR and control, the durability coefficient of all mixtures is surpassed 60% set by ASTM C 666 specification. The durability coefficient of all mixtures was between 94% and 104%;
- ✚ The SCC with 0.42 of w/b incorporating 10% and 20% AmSR showed acceptable fresh properties;
- ✚ The plastic viscosity and yield shear stress increased by increasing rate of replacement of cement by AmSR from 0 to 20 %;
- ✚ The compressive strength of SCC increased by replacement of cement by 10 and 20% AmSR at long term, the improvement rate of compressive strength for SCC 10AmSR and 20 AmSR at 56 days was 11.3 and 6.3% respectively. The compressive strength of all SCC mixtures surpassed 40 MPa at 56 days;
- ✚ The trend of tensile, flexural strength and modulus of elasticity of All SCC mixtures was same as compressive strength;
- ✚ Increasing rate of replacement of cement by AmSR in SCC, increased significantly electrical resistivity and decreased chloride ions penetrations ;
- ✚ The SCC incorporating 10% AmSR showed less drying shrinkage compare with control and the SCC incorporating 20 % AmSR showed more drying shrinkage compare with control during 140 days;
- ✚ The AmSR provides good resistance of freezing-thawing after 300 cycles for SCC as well as HPC and OC mixtures;

- ✚ Finally it can concluded that formulate a stable and homogenous SCC with 0.42 of w/b and with good mechanical and durability performance, containing up to 20% AmSR in a binary matrix is possible;
- ✚ Dosage of SP for achieving same slump of all ternary mixtures was more than control#1 and control#2, the required SP of Ter SF and Ter-MK was more than other ternary mixtures ;
- ✚ The compressive strength of all ternary mixtures with 0.40 of w/b surpassed 50 MPa except Ter-GP. The compressive strength of Ter-SF (20% AmSR and 5% SF) was near to control#1 and control#2 at 91 days and the compressive strength of Ter-MK (15% AmSR and 10% MK) was more than control#1 and control#2 at 91 days. The compressive strength of other mixtures were less than control#1 and control#2;
- ✚ All ternary mixtures showed high electrical resistivity. At 56 and 91 days all mixtures were in very low penetration class. The control#1, control#2, Ter-SF and ter-MK showed significantly high electrical resistivity compare to Ter-GP, Ter-FAF and Ter-Slag;
- ✚ All ternary mixtures showed low chloride-ions penetration. At 28 days all mixtures were in very low penetration class except Ter-GP, Ter-FAF and Ter-Slag which were in low penetration class. At 91 days all mixtures were in very low class of penetrations;
- ✚ The expansion of Ter-Slag during first 28 days was significantly more than other ternary mixtures and expansion of Ter-MK during first 28 days was less than other ternary mixtures. Ter-Slag showed less shrinkage compare with other ternary mixtures. The shrinkage of Ter-SF, Ter-Gp and control#2 mixtures was approximately same at 140 days. The Ter-MK, Ter-FAF and control#1 mixtures showed same shrinkage at 140 days;
- ✚ The Ter-Slag, Ter-FAF, Ter-GP and control#1 had low scaling residue. Their scaling residues satisfied the limit of de-icing scaling resistance(less than 500 g/m^2).ButtheTer-SF, Ter-Mk and control#2 mixtures showed high scaling residue. Their scaling residue surpassed BNQ 261-900 specification limit(more than 500 g/m^2);
- ✚ All of ternary mixtures showed excellent durability after 300 freezing and thawing cycles. The durability coefficient of all mixtures is surpassed 60% set by ASTM C 666 specification. The durability coefficient of all mixtures was between 96% and 103%;

Conclusion (en français)

a) Cendres volantes de biomasse (CVB)

- ✚ La surface spécifique Blaine du CVB pré-mouillé est de $360 \text{ m}^2 / \text{kg}$, soit sensiblement similaire a celle du ciment Portland type GU ;
- ✚ Le D50 de ciment Portland, CVB régulier et pré-mouillé sont de 16,2, 47,6 et $89.41 \text{ }\mu\text{m}$;
- ✚ Le CVB régulier et pré-mouillé ont une teneur en carbone relativement plus élevée (comme reflétée par LOI), conduisant ainsi à l'absorption importante de l'eau et l'utilisation d'un fort dosage des adjuvants chimiques ;
- ✚ Le CVB est riche en CaO , SiO_2 et Al_2O_3 et il a aussi une teneur élevée en SO_3 (plus que la limite (5%) de la norme ASTM C 618) ;
- ✚ Les principales phases cristallines de CVB sont la chaux, l'anhydrite, le calcite, le meyenite, la portlandite et le quartz et les principales phases cristallines de CVB pré-humidifiée sont l'ettringite, le calcite, le quartz, la portlandite et l'albite ;
- ✚ Le remplacement du ciment par le CVB régulier et pré-mouillé augmente la demande en eau. La demande en eau du CVB mouillé est plus importante que celle du CVB régulier;
- ✚ Le remplacement partiel du ciment par le CVB régulier augmente à la fois le temps de prise initial et final alors que le remplacement partiel du ciment par CVB pré-mouillé dans le béton diminue le temps de prise initial et final. La finesse et la composition chimique sont deux paramètres principaux pour expliquer l'hydratation des matériaux cimentaires et donc le temps de prise. La lenteur du temps de prise du béton incorporant le CVB pourrait être attribué à une teneur relativement élevée de soufre (7,8%). Le SO_3 provoque directement la génération d'ettringite. La formation de cristaux d'ettringite crée une mince couche autour des grains de ciment non hydraté, ralentissant ainsi la réaction rapide des aluminates de calcium avec de l'eau (Tzouvalas et al, 2004) ;
- ✚ Le remplacement de 20% du ciment par le CVB pré-mouillé dans le mortier avec $E/L = 0,485$, augmente de 13% la résistance à 56 jours par rapport au CVB régulier ;
- ✚ Le remplacement de 20% du ciment par le CVB pré-mouillé dans le béton avec $E/L = 0,40$ améliore de 25% la résistance à la compression en comparaison avec le CVB régulier ;

b) Des résidus de silice Amorphe (RSA)

- ✚ La surface spécifique Blaine de RSA est d'environ $4907 \text{ m}^2/\text{kg}$, soit plus de dix fois celle du ciment Portland type GU. La RSA accélère la cinétique d'hydratation et augmente la demande en eau.
- ✚ La D_{50} du ciment Portland type GU et RSA sont respectivement de 16.2, 8.4 μm ;
- ✚ Le RSA est riche en SiO_2 (60%) et le résultat du DRX montre la présence de silice amorphe;
- ✚ Le RSA présente un très bon indice de pouzzolanité dans les matrices ayant $E/L = 0,485$ ou $E/l = 0,40$;
- ✚ Un indice de pouzzolanité maximum est observé avec un taux d'incorporant de 20% RSA. Par conséquent, 20% RSA est suggéré comme taux optimal ;
- ✚ La résistivité électrique du mortier augmente significativement avec un taux de remplacement du ciment par RSA;
- ✚ Le BHP avec $E/L = 0,35$ incorporant 20% RSA montre approximativement la même résistance à la compression que le BHP témoin à 91 jours;
- ✚ Le remplacement du ciment par RSA améliore la résistance à la compression des BO ayant différents rapports E/L comparativement à leurs témoins. Mais la résistance à la compression du BO ayant $E/L = 0,70$ incorporant 20% RSA était 3,9% moins que celle du témoin le témoin à 91 jours;
- ✚ Les taux d'amélioration de la résistance à la compression du BHP ayant $E/L = 0,35$ et les BO ayant $E/L = 0,40, 0,45, 0,50, 0,55, 0,65$ et $0,70$ incorporant 20% RSA en comparaison avec leurs bétons témoins sont de -2,7%, +7.3%, +20%, +13,2%, +12,9%, +8,8% et -3,9% respectivement. Par conséquent, le E/L affecte le taux d'amélioration de la résistance à la compression du béton ordinaire incorporant RSA ;
- ✚ Les effets du RSA sur la résistance à la traction, la résistance à la flexion et module d'élasticité du BHP ou des BO sont similaires à ceux observé sur les résistances à la compression ;
- ✚ La résistivité électrique du BHP et BO incorporant 20% RSA augmente significativement comparativement au témoin. Un béton à haute résistivité électrique présente un faible risque de corrosion;

- ✚ La pénétration des ions chlorure de tous les BHP et BO incorporant 20% RSA diminue significativement. Le béton incorporant 20% RSA montre une bonne durabilité;
- ✚ Le retrait endogène du BHP avec $E/L = 0,35$ incorporant 20% RSA est nettement inférieur à celle du béton témoin pendant 30 jours. Les variations de la température du BHP incorporant 20% RSA et à celles du témoin ayant $E/L = 0,35$ sont sensiblement similaires;
- ✚ Les BHP et BO incorporant 20% RSA montrent une plus grande expansion en comparaison avec leur témoin pendant 28 premiers jours de cure humide. Le BHP incorporant 20% RSA montre un peu plus le retrait de séchage en comparaison avec le témoin. Tous les mélanges de BO incorporant 20% RSA sauf BO ayant $E/L = 0,40$ montre plus le retrait de séchage en comparaison avec leurs témoins;
- ✚ La perte de masse à l'écaillage du BHP contenant 20% RSA ayant $E/L = 0,35$ est très faible. Cette perte de masse à l'écaillage est inférieure à 170 g/m^2 après 56 cycles (soit nettement inférieure à la limite de 500 g/m^2 recommandée par la norme BNQ 2621-900);
- ✚ Le BO ayant $E/L = 0,40$ et $0,45$ incorporant 20% RSA satisfont la limite de perte de masse à l'écaillage (moins de 500 g/m^2). Cependant la perte de masse à l'écaillage des BO ayant $E/L = 0,50$ et $0,55$ dépassent la limite de BNQ 2621-900 (plus de 500 g/m^2);
- ✚ Le coefficient de durabilité de tous les bétons se situaient entre 94 et 104%, ils montrent que les bétons sont résistants au gel-dégel;
- ✚ Les BAP ayant $E/L = 0,42$ incorporant 10% et 20% RSA montrent des propriétés à l'état frais acceptables;
- ✚ Les propriétés rhéologiques comme la viscosité plastique et le seuil de cisaillement augmentent avec le taux de remplacement du ciment par RSA;
- ✚ Les résistances à la compression du BAP incorporant 10 et 20% RSA augmentent à long terme. Le taux d'amélioration de résistance à la compression des BAP 10% RSA et 20% RSA à 56 jours sont de 11,3 et 6,3% respectivement. La résistance à la compression de tous les BAP dépasse 40 MPa à 56 jours;
- ✚ Les effets du RSA sur la résistance à la traction, la résistance à la flexion et le module d'élasticité de tous les BAP sont le même que ceux observé sur la résistance à la compression;

- ✚ L'augmentation du taux de remplacement du ciment par RSA dans le BAP augmente la résistivité électrique et diminue la pénétration des ions chlorures;
- ✚ Le BAP incorporant 10% RSA montre moins de retrait de séchage en comparaison avec le témoin et le BAP incorporant 20% RSA montre plus de retrait de séchage en comparaison avec le témoin;
- ✚ Les bétons incorporant RSA présentent d'une bonne résistance au gel-dégel ;
- ✚ Il est alors possible de formuler un BAP stable et homogène ayant $E/L = 0,42$ et incorporant jusqu'à 20% RSA et développer d'excellentes performances mécaniques et de bonne durabilité ;
- ✚ En visant le même affaissement pour tous les bétons ternaires, les ternaires incorporant RSA requièrent du dosage en SP plus élevé que le témoin#1 ou témoin#2 ;
- ✚ La résistance à la compression de tous les bétons ternaires ayant $E/L = 0.40$ dépassent 50 MPa sauf Ter-GP. La résistance à la compression de Ter-SF (20% RSA et 5% SF) est presque équivalente à celle du témoin#1 et témoin#2 à 91 jours et la résistance à la compression de Ter-MK (15% RSA et 10% MK) est plus élevée que du celle témoin#1 et témoin#2 à 91 jours ;
- ✚ Tous les bétons ternaires montrent de la résistivité électrique élevée. À 56 et 91 jours, tous les bétons présentant de la résistivité se situent en classe de pénétration très faible. Le témoin#1, témoin#2, Ter-SF et Ter-MK montrent une résistivité électrique élevée considérablement en comparaison à celle des bétons Ter-GP, Ter-FAF et Ter-Slag ;
- ✚ Tous les bétons ternaires montrent une pénétration des ions chlorure faible ;
- ✚ L'expansion de Ter-Slag au cours des premiers 28 jours est significativement plus élevée que celle des autres mélanges ternaires. L'expansion de Ter-MK au cours des 28 premiers jours était inférieure à celle des autres bétons ternaires. Le Ter-Slag montre moins de retrait de séchage par rapport aux autres bétons ternaires. Le retrait de Ter-SF, Ter-Gp et de témoin#2 sont approximativement similaires à 140 jours. Le Ter-MK, Ter-FAF et le témoin#1 montrent quasiment même le retrait à 40 jours.
- ✚ Le Ter-Slag, Ter-FAF, Ter-GP et témoin#1 présentent une faible perte de masse à l'écaillage. Leurs résidus d'écaillage satisfont la limite recommandée par la norme BNQ. Ter-SF, Ter-Mk et témoin#2 présentent de pertes de masse à l'écaillage plus important et ils dépassent la limite de la norme BNQ 261-900 spécification (plus que 500 g/m^2) ;

- ✚ Tous les bétons ternaires montrent une excellente durabilité au gel-dégel après 300 cycles. Le coefficient de durabilité de tous les bétons ternaires dépassent 60%, recommandée par la norme ASTM C 666 ;
- ✚ Le RSA montre une très bonne synergie avec d'autres matériaux cimentaire ;

5.2. Recommendations for future research

This research has demonstrated that AmSR has great potential to use as Alternative cementitious materials in binary and ternary combinations in different type of concrete. This research also showed the pre-wetting of WSA is feasible approach to improve performance of concrete incorporating WSA. The following recommendations can be proposed for future research about WSA and AmSR:

- optimization of pre-wetting procedure of WSA and microstructure study of past and concrete incorporating optimized pre-wetted WSA
- Comprehensive study of self-consolidating concrete (SCC) incorporating AmSR in binary and ternary
- Microstructure study of AmSR in cementitious system

6. Reference

ASTM C39, (2012), Standard Test Method for Compressive Strength of Cylindrical Concrete Specimens.

ASTM C666, (2003), Standard Test Method for Resistance of Concrete to Rapid Freezing and Thawing.

ASTM C78, (2002), Standard Test Method for Flexural Strength of Concrete (Using Simple Beam with Third-Point Loading).

ASTM C143, (2012), Standard Test Method for Slump of Hydraulic-Cement Concrete.

ASTM C157, (2008), Standard Test Method for Length Change of Hardened Hydraulic-Cement Mortar and Concrete.

ASTM C138, (2001), Standard Test Method for Density (Unit Weight), and Air content (Geravimetric).

ASTM C231.(2010), Standard Test Method for Air Content of Freshly Mixed Concrete by the Pressure Method.

ASTM C497, (2010), Standard Test Method for Static Modulus of Elasticity and Poisson' s Ratio of Concrete in Compression.

ASTM C403, (2013), Standard Test Method for Time of Setting of Concrete Mixtures by Penetration Resistance.

ASTM C496, (2014), Standard Test Method for Splitting Tensile Strength of Cylindrical Concrete Specimens.

ASTM C1202, (1997), Standard Test Method for Electrical indication of Concretes Ability to Resist Chloride ion penetration, chloride content, corrosion,

ASTM D7348, (2015), Standard Test Methods for Loss on Ignition (LOI) of Solid Combustion Residues.

ASTM C1611, (2010), Standard Test Method forSlump Flow of Self-Consolidating Concrete

ASTM C1621, (2010), Standard Test Method for Passing Ability of Self-Consolidating Concrete by J-Ring

ASTM C618, (2002), Standard specification for Coal Fly Ash and Raw or Calcined Natural Pozzolan for Use in Concrete.

Aubert, J. E., Husson, B., &Vaquier, a. (2004). Metallic aluminum in MSWI fly ash: “quantification and influence on the properties of cement-based products”. Waste Management (New York, N.Y.), P 589-96.

Ahmaruzzaman, M. (2010) “A review on the utilization of fly ash” Progress in Energy and Combustion Science, P 327–363

Aranda Usón, A., López-Sabirón, A. M., Ferreira, G., &LleraSastresa, E. (2013). “Uses of alternative fuels and raw materials in the cement industry as sustainable waste management options”. Renewable and Sustainable Energy Reviews, P 242–260.

Ahmad, S, Malik, M. I., Wani, M. B., & Ahmad, R. (2013).“Study of Concrete Involving Use of Waste Paper Sludge Ash as Partial Replacement of Cement”,P 6–15.

Archie G. (1942) “The electrical resistivity log as an aid in determining some reservoir characteristics”. Transaction of the American of Mining and Metallurgical Engineers, p. 54 – 62.

Barbara. L, Karen. S, R. Hooton “Supplementary cementitious materials” Cement and Concrete Research, P 1244–1256

Bilodeau, A., Sivasundaram, V., Painter, K. E., and Malhotra, V M. (1994). “Durability of Concrete Incorporating High Volumes of Fly Ash From Sources in the U.S”. ACI material journal, p. 3-12.

Bai, J., Chaipanich, a, Kinuthia, J., O’Farrell, M., Sabir, B., Wild, S., & Lewis, M., (2003). “Compressive strength and hydration of wastepaper sludge ash–ground granulated blastfurnace slag blended pastes”. Cement and Concrete Research, P 1189–1202.

Banfill, P., & Frias, M. (2007).“Rheology and conduction calorimetric of cement modified with calcined paper sludge”.Cement and Concrete Research, P 184–190.

Benhelal, E., Zahedi, G., Shamsaei, E., &Bahadori, A. (2013).“Global strategies and potentials to curb CO₂ emissions in cement industry”.Journal of Cleaner Production, P 142–161.

Byars, E.A., Morales-Hernandez B., H.Y. Zhu. (2004).“Waste Glass as Concrete Aggregate and Pozzolan”. Laboratory and Industrial Concrete Projects, P 41-4.

Bouzoubaa, N., Fournier B., (2004). “Current Situation with the Production and Use of Supplementary Cementing Materials (SCMs) in Concrete Construction in Canada”, Canadian Journal of Civil Engineering, P 129-43

Bentz, D. P. (2008). “A review of early-age properties of cement-based materials”. Cement and Concrete Research, P 196–204.

Bentz, D. P., Geiker, M. R., & Hansen, K. K. (2001). “Shrinkage-reducing admixtures and early-age desiccation in cement pastes and mortars”. Cement and Concrete Research, P 1075–1085.

Bentz, D. P., & Jensen, O. M. (2004). “Mitigation strategies for autogenous shrinkage cracking”. Cement and Concrete Composites, P 677–685.

Cheah, C. B., & Ramli, M. (2011). “The implementation of wood waste ash as a partial cement replacement material in the production of structural grade concrete and mortar: An overview”. Resources, Conservation and Recycling, P 669–685.

Davidenko, T., Xie, A., Mikanovic, N., & Tagnit-hamou, A. (2012). “Effect of wastepaper sludge ash on cement blends”, proceeding in 12th International Conference on Recent Advances in Concrete Technology and Sustainability issues, Prague, P 709-727.

Davidenko, T. (2014). “Hydratation d’un system cimentaire binaire contenant des cendres volantes de biomasse” Phd theses, Sherbrooke university.

Ding, J.T., and Li, Z.J. (2002). “Effects of metakaolin and silica fume on properties of concrete”. ACI Materials Journal, p.393-398

Elvis M. Mbadike, N. N. Osadebe. (2013) “The effect of amorphous silica residue in the production of concrete” International Journal of Sustainable Construction Engineering & Technology.

Frias, M., Garcia, R., Vigil, R., & Ferreiro, S. (2008). “Calcination of art paper sludge waste for the use as a supplementary cementing material”. Applied Clay Science, P 189–193.

Feys, D., Verhoeven, R. et De Schutter, G. (2007). “Evaluation of time independent rheological models applicable to fresh self-compacting concrete”. Applied Rheology, P 1-10.

Gavrilescu, D. (2008). “Energy from biomass in pulp and paper”, P 537–546.

Gluth, G. J. G., Lehmann, C., Rübner, K., & Kühne, H.-C. (2014). “Reaction products and strength development of wastepaper sludge ash and the influence of alkalis”. Cement and Concrete Composites, P 82–88.

Glenn, J.(1997). “Paper mill sludge; Feedstock for tomorrow”.Biocycle, p 30.

Huang, C.-H., Lin, S.-K., Chang, C.-S., & Chen, H.-J.(2013). “Mix proportions and mechanical properties of concrete containing very high-volume of Class F fly ash”.Construction and Building Materials, P 71–78.

Hewlett, Peter C. (2004). “Lea's chemistry of cement and concrete”.4th edition, Butterworth-Heinemann, P 1092.

Holt, E. E. (2001). Early age autogenous shrinkage of concrete. Technical research of Finland.VTT publication, P 184–446.

Hwang, S., Khayat, K. H. et Bonneau, O. (2006). Performance-Based Specifications of Self-Consolidating Concrete Used in Structural Applications, 103(2), 121-129.

Javellana M.P, Jawed I. (1982). “Extraction of Free Lime in Portland cement and Clinker by Ethylene Glycol”.Cement and Concrete Research, P 399–403.

Kosmatka, S.H., Kerkhoff, B., Panarese, W.C., Macleod, N.F., and Mcgrath, R.J. (2002).“Design and Control of Concrete Mixtures”.7th edition, Cement Association of Canada, Ottawa, Ontario, Canada, P 368.

Khayat, K. H. (1999). Workability , Testing , and Performance of Self-Consolidating Concrete. ACI Materials Journal, P 346-354.

Mozaffari, E., Kinuthia, J. M., Bai, J., & Wild, S. (2009). “An investigation into the strength development of Wastepaper Sludge Ash blended with Ground Granulated Blastfurnace Slag”. Cement and Concrete Research, P 942–949.

Mozaffari, E., O’Farrell, M., Kinuthia, J. M., & Wild, S. (2006). “Improving strength development of wastepaper sludge ash by wet-milling”. Cement and Concrete Composites, P 144–152.

Mathumathi .S, G. C. (2000).“A glass ceramics from pulp and paper.Master theses”.

Malhorta, V. M, Ramezaniapour,A.A. (1994). “Fly ash in concrete”, second edition, p 307.

Nehdi,M, Mindess, S. Aïtcin, P. (1998) “Rheology of High-Performance Concrete” Effect of Ultrafine Particles, P 687–697.

Nemerow, Nelson Leonard (1983).“Industrial solid wastes”, Ballinger publishing company, P 356.

Neville, Adam M. (1996). “Properties of Concrete” 4th edition, John Wiley & Sons, New York, P 844.

Pattengil, M., Shutt T.C. (1973). “Use of ground glass as a pozzolan, Symp. on Utilisation of Waste Glass in Secondary Products”, Albuquerque, New Mexico, U.S.A., P 137–53.

Papadakis, V. G. (2000). “Effect of supplementary cementing materials on concrete resistance against carbonation and chloride ingress”. Cement and Concrete Research, P 291–299.

Shayan, A, Xu, A. (2006). “Performance of glass powder as a pozzolanic material in concrete: A field trial on concrete slabs”. Cement and Concrete Research, P 457-68.

Segui, P., Aubert, J. E., Husson, B., & Measson, M. (2012). “Characterization of wastepaper sludge ash for its valorization as a component of hydraulic binders”. Applied Clay Science, P 79–85.

Sotomayor Cruz, C. D. (2012). “Développement des bétons semi autoplacants à rhéologie adaptée pour des infrastructures”.

Shi, C., Wu, Y. Riefler, C., Wang H., (2005) “Characteristics and pozzolanic reactivity of glass powders”, Cement and Concrete Research, P 987-93.

Shayan, A. Xu, A. (2004). “Value added utilization of waste glass in concrete”. Cement and Concrete Research, P 81-9.

Tinnea, R.; Tinnea, J.; Kuder, K.; Daudistel, R.; Hassane, B.; Stoll, C. et Tomosada, K. A. (2009) Testing of high-resistivity concrete. International Corrosion Conference Series, P 22-26.

Wild, S., Kinuthia, J. M., Jones, G. I., & Higgins, D. D. (1999). “Suppression of swelling associated with ettringite formation in lime stabilized sulphate bearing clay soils by partial substitution of lime with ground granulated blastfurnace slag (GGBS) ”. Engineering Geology, P 257–277.

Whiting, D. (1988). “Permeability of selected concretes”, American Concrete Institute, Detroit, p. 195-222.

Wallevik, O. H. (2006). “Rheology of Cementitious Materials”. The Icelandic Building Research Institute.

Xie, A. (2009) “Characteristics of wastepaper sludge ash and its potential application in concrete” Master theses, Sherbrook University.

Xie, A., Tagnit-Hamou, A. (2011) “Wastepaper Sludge Ash; A new type of supplementary cementitious material used in concrete”, 13th int. Congre. chem of cement, Madrid, Spain.

Yan, S., Sagoe-Crentsil, K., & Shapiro, G. (2011). “Reuse of de-inking sludge from wastepaper recycling in cement mortar products”. *Journal of Environmental Management*, 92(8), 2085–90.

Zidol, A. (2009). “Optimisation de la finesse de la poudre de verre dans les systèmes cimentaires binaires”, Master's thesis, University of Sherbrooke, Québec, P 156.

Zidol, A., Pavoine, A., Tagnit-Hamou, A. (2012) “Effect of glass powder on concrete durability”. *International Congress on Durability of Concrete*, Trondheim, Norway.